

**Production in *Pichia pastoris* and
characterization of genetically engineered
hepatitis B surface antigen virus-like particles**

Von der Naturwissenschaftlichen Fakultät
der Gottfried Wilhelm Leibniz Universität Hannover

zur Erlangung des Grades
Doktorin der Naturwissenschaften

Dr. rer. nat.

genehmigte Dissertation

von

M.Sc. Maria Zahid

geboren am 04.01.1984 in Lahore, Pakistan

2013

Referent

Prof. Dr. Thomas Scheper
Institut für Technische Chemie
Gottfried Wilhelm Leibniz Universität Hannover

Korreferentin

Prof. Dr. Ursula Rinas
Institut für Technische Chemie
Gottfried Wilhelm Leibniz Universität Hannover

Tag der Promotion

17th December, 2012

Erklärung zur Dissertation

gemäß §6(1) der Promotionsordnung der Naturwissenschaftlichen Fakultät der Gottfried Wilhelm Leibniz Universität Hannover für die Promotion zum Dr. rer. nat.

Hierdurch erkläre ich, dass ich meine Dissertation mit dem Titel selbständig verfasst und die benutzten Hilfsmittel und Quellen sowie gegebenenfalls die zu Hilfeleistungen herangezogenen Institutionen vollständig angegeben habe. Die Dissertation wurde nicht schon als Masterarbeit, Diplomarbeit oder andere Prüfungsarbeit verwendet.

Maria Zahid

17th October, 2012

Declaration

The work described in this thesis was carried out in the period from April 2009 to October 2012 at Leibniz University of Hannover, Germany, under the supervision of Prof. Dr. Thomas Scheper and Prof. Dr. Ursula Rinas at the Institute of Technical Chemistry, Hannover. I hereby declare that this submission is my own work and that, to the best of my knowledge and belief, it contains no material previously published or written by another person nor material which has been accepted for the award of any other degree or diploma of the university or other institute of higher learning, except where due acknowledgment has been made in the text.

Maria Zahid

17th October, 2012

Perplexity is the beginning of knowledge.

Khalil Gibran

Table of Contents

Abstract.....	x
Zusammenfassung	xi
1. Theoretical background	1
1.1. Epidemiology of HBV.....	2
1.2. HBV genomic organization.....	3
1.3. Hepatitis B virus morphology	3
1.4. Mechanism of virus-mediated immune response.....	5
1.5. HBV replication cycle	6
1.6. Vaccines for hepatitis B	7
1.6.1. Plasma-derived vaccines.....	7
1.6.2. DNA vaccines	8
1.6.3. Subunits vaccines.....	8
1.6.4. VLP-based vaccines.....	8
1.7. Expression systems used for HBV vaccine production.....	9
1.8. <i>Pichia pastoris</i> as expression host.....	10
1.9. VLPs as vaccines.....	10
1.10. Immunogenic properties of VLPs	12
1.11. VLP assembly.....	13
1.12. Physicochemical features of HBsAg.....	14
2. Objectives of the thesis	16
3. Experimental methods.....	18
3.1. Strain and vector for HBsAg expression.....	18
3.2. Preliminary expression of HBsAg in <i>Pichia pastoris</i>	18
3.3. High cell density cultivation of <i>P. pastoris</i> GS115 Mut ⁺	20
3.3.1. Online and offline measurement.....	20

3.3.2.	Cell harvesting	21
3.3.3.	Cell lysis	21
3.3.4.	<i>P. pastoris</i> GS115 control cell culture	21
3.4.	Downstream processing of HBsAg	21
3.4.1.	Preparation	23
3.4.2.	Capturing and intermediate purification	23
3.4.3.	Polishing	24
3.5.	General analytical methods for HBsAg estimation	24
3.5.1.	SDS-PAGE analysis	24
3.5.2.	Western blot	25
3.5.3.	ELISA analysis	25
3.5.4.	Protein concentration estimation	25
3.5.5.	RP-HPLC analysis	26
3.6.	Electron microscopic analysis	26
3.6.1.	Scanning electron microscopy (SEM) protocol	26
3.6.2.	Transmission electron microscopy (TEM) protocol	26
3.6.3.	Image processing for TEM	28
3.7.	Fluorescence spectroscopy for stability experiments	29
3.7.1.	Intrinsic fluorescence measurements	29
3.7.2.	Extrinsic fluorescence measurements	29
3.7.3.	Defolding studies via fluorescence spectroscopy	29
3.7.4.	Data analysis	30
3.8.	VLP determination using Virus counter	30
3.8.1.	Sample preparation	31
3.8.2.	Measurement protocol for the Virus counter	31
3.9.	VLP analysis using dynamic light scattering	31
3.9.1.	Sample preparation	32

3.9.2.	Measurement protocol for DLS	32
4.	Results and discussion	33
4.1.	Production in <i>Pichia pastoris</i> GS115 and downstream process of recombinant hepatitis B surface antigen virus-like particles.....	33
4.1.1.	Shake flask cultivation.....	33
4.1.2.	Bioreactor cultivation	35
4.1.2.1.	RP-HPLC.....	37
4.1.2.2.	Western blot.....	37
4.1.2.3.	ELISA analysis.....	38
4.1.3.	Downstream processing of HBsAg.....	39
4.1.3.1.	PEG precipitation	39
4.1.3.2.	Adsorption on Aerosil 380	39
4.1.3.3.	Ion exchange chromatography	40
4.1.3.4.	Size exclusion chromatography.....	40
4.1.3.5.	KSCN treatment	41
4.1.4.	Protein concentration	43
4.1.5.	Electron microscopy of HBsAg.....	44
4.1.6.	Conclusion	44
4.2.	Insight into the <i>in vitro</i> assembly process during downstream processing via TEM using HBsAg virus-like particles as a model case.....	45
4.2.1.	TEM analysis of purified product.....	45
4.2.2.	Probing through downstream process via TEM	46
4.2.2.1.	VLP size	48
4.2.2.2.	VLP morphology	48
4.2.3.	Control experiments for TEM background.....	49
4.2.4.	Effect of host cell components on VLPs	50
4.2.5.	Effect of solvent system on VLPs.....	51
4.2.6.	VLP count during the downstream process and control experiments .	54
4.2.7.	Effect of Tween 20 and EDTA on VLPs.....	56
4.2.8.	Conclusion	65

4.3. Monitoring of conformational changes in HBsAg VLPs in the presence of chaotropic agents via steady-state fluorescence spectroscopy	67
4.3.1. Fluorescence spectroscopic studies of HBsAg VLPs	68
4.3.1.1. HBsAg intrinsic fluorescence measurements	68
4.3.1.2. Extrinsic fluorescence measurements.....	68
4.3.2. Denaturation studies of HBsAg	70
4.3.3. Stern-Volmer relation	75
4.3.4. HBsAg VP count determination using Virus counter.....	76
4.3.5. Dynamic light scattering measurements	78
4.3.5.1. Preliminary DLS studies.....	78
4.3.5.2. Discrepancy in VLP size via DLS.....	78
4.3.5.3. Effect of SMW species.....	79
4.3.5.4. Effect of aggregates	80
4.3.5.5. Optimized DLS measurement	80
4.3.6. Conclusion	82
5. Summary and perspectives	84
6. References.....	88
7. Appendix.....	98
Acknowledgements	117
Curriculum Vitae.....	118

Abstract

Vaccine production is one of the most important applications of biotechnology. Virus-like particles (VLP) serve well the purpose of a safe and effective vaccine. Yet till now many aspects of this biological tool have been under discovered. In present work, an effort has been made to characterize the structural aspects of genetically modified VLPs. As a model system, hepatitis B surface antigen (HBsAg) VLPs have been produced in methylotrophic yeast, *Pichia pastoris*. In the initial part of the work, downstream processing has been probed to discover the crucial points in gradual development of VLP formation. In later part, the purified VLPs have been subjected to chaotropic conditions to observe the type and extent of molecular forces holding these tiny particles together.

Self-assembly, from subunits to a well defined symmetry, is the most prominent characteristic of VLPs, however, little is known about when and how they appear in the process. It has been observed in previous studies that no VLPs are observed during the cultivation in *Pichia pastoris* cells. In order to pinpoint the most crucial steps for VLP assembly, samples were collected during the downstream process. Transmission electron microscopy was used to examine samples from multi-step purification and the data was analyzed to draw a quantitative relation. During initial steps of the purification process, no VLPs were observed despite the presence of enough amount of HBsAg protein. Adequate VLP count was observed only after adsorption on the hydrophobic resin. Control experiments using non-HBsAg-producing *Pichia pastoris* cells were carried out to observe the background structures and their influence. These control experiments, containing VLPs, in presence and absence of suspected agents clearly prove that host cell components as well as buffer system are decisive factors in the *in vitro* assembly process of HBsAg.

The stability tests were performed in the presence of denaturants and changes in VLP structure and size were ascertained via fluorescence spectroscopy (intrinsic and extrinsic) and dynamic light scattering (DLS). The trend in structural changes as a function of molarity of the salts indicates that VLPs undergo denaturation process by several intermediates, which may occur as a cascade of reactions involving gradual detachment of subunits.

Key words: Hepatitis B surface antigen, Virus-like particle, Self-assembly, Transmission electron microscopy, Steady-state fluorescence spectroscopy, Dynamic light scattering

Zusammenfassung

Die Herstellung von Vakzinen ist eine der wichtigsten Anwendungen in der Biotechnologie. Virusartige Partikel (VLPs) werden als ungefährliche und effektive Impfstoffe eingesetzt. Dennoch sind viele Aspekte dieser biologischen Werkzeuge bis heute immer noch nicht genügend erforscht. In dieser Arbeit werden die strukturellen Aspekte von genetisch veränderten VLPs charakterisiert. Als ein Modellsystem diente Hepatitis B Oberflächenantigen (HBsAg) Protein, das in der methylotrophen Hefe, *Pichia pastoris*, produziert wurde. Im ersten Teil dieser Arbeit wurde der Aufreinigungsprozess untersucht, um die entscheidenden Schritte während der allmählichen Entwicklung der VLP Bildung zu erforschen. Im späteren Teil dieser Arbeit wurden die aufgereinigten VLPs unter chaotropen Bedingungen untersucht, um die Art und das Ausmaß der molekularen Kräfte, die diese Partikel zusammenhalten, zu analysieren.

Selbstassemblierung von Monomeren zu gut definierter Symmetrie ist die bekannteste Eigenschaft der VLPs, aber es ist wenig bekannt darüber, wie und wann die VLPs während der Aufreinigung gebildet werden. Es wurde in den letzten Studien beobachtet, dass keine VLPs in *Pichia pastoris* Zellen während der Kultivierung auftreten. Um den wichtigsten Punkt der Selbstassemblierung der VLPs genau bestimmen zu können, wurden Proben während der Aufreinigung entnommen. Mithilfe der Transmissionselektronenmikroskopie wurden die Proben der mehrstufigen Aufreinigung charakterisiert und die ermittelten Daten zur Quantifizierung der VLP Bildung eingesetzt. Während der Anfangsschritte der Aufreinigung wurden keine VLPs trotz der Anwesenheit von genügend HBsAg gefunden. Eine ausreichende Anzahl an VLPs wurde jedoch nach dem Aufreinigungsschritt mittels hydrophobem Harz festgestellt. Es wurden Kontrollversuche mit nicht produzierenden HBsAg *Pichia pastoris* Zellen durchgeführt, um die Strukturen des Hintergrunds und deren Einfluss auf die VLP Bildung zu beobachten. Diese Kontrollproben, die VLPs enthalten, zeigen in An- und Abwesenheit der vermuteten Wirkstoffe deutlich, dass die Wirtszellkomponenten sowie das Puffersystem entscheidende Faktoren für den *in vitro* Selbstassemblierungsprozess des HBsAg darstellen.

Die Stabilitätstests wurden in Anwesenheit von Denaturierungsmitteln durchgeführt und die Veränderungen der VLP-Struktur und -Größe mithilfe der Fluoreszenzspektroskopie (intrinsisch und extrinsisch) und Lichtstreuungsmessungen

nachgewiesen. Der Trend der strukturellen Veränderungen als Funktion der Molarität der Denaturierungsmittel zeigt, dass VLPs einen Denaturierungsprozess mit vielen Zwischenprodukten durchlaufen, der eine Art Kaskadenreaktion mit schrittweiser Abtrennung von Monomeren darstellt.

Stichwörter: Hepatitis B Oberflächenantigen, Virusähnliche Partikel, Selbstassemblierung, Transmissionselektronenmikroskopie, Steady-state Fluoreszenzspektroskopie, Dynamische Lichtstreuungsmessung

1. Theoretical background

Hepatitis B is a viral infection that attacks the liver and can cause both acute and chronic disease. According to the WHO (World Health Organization), an estimated two billion people, about one third of the world's population, have been infected with the hepatitis B virus (HBV), and more than 350 million have chronic (long-term) liver infections [1]. HBV belongs to the hepadnaviridae family and has a DNA genome (3.2 kb) that is replicated via an RNA intermediate. Depending on the patient's immune response, infection by HBV can be asymptomatic, chronic or acute [2]. In acute illness, the infection lasts for 2-3 weeks and patient's liver needs about 6 months to recover completely. In chronic hepatitis B, the infection leads to chronic liver inflammation including liver cirrhosis and ultimately hepatocellular carcinoma.

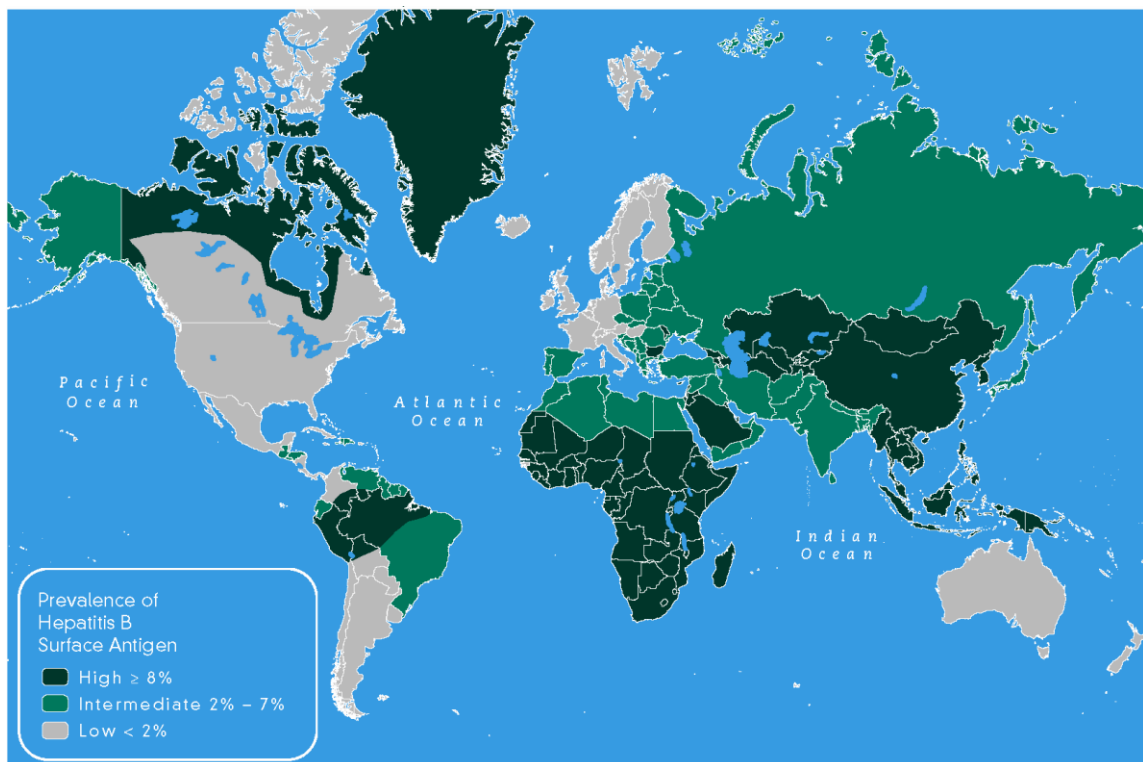


Figure 1.1. Geographic prevalence of chronic infection with hepatitis virus surveyed until 2006; Courtesy WHO [3].

1.1. Epidemiology of HBV

The environmental factors such as healthy life style and safe health care system play the major role to prevent the spread of disease. The common means of spreading HBV are through sexual contact with infected person, percutaneous or mucosal exposure to infectious blood and vertical (perinatal) transmission [4]. Despite the fact that there exists a vaccine against hepatitis B since 1980s, its incidence has been increasing. Due to recommendations by WHO, the prevalence of disease has been decreased in several countries e.g., in Korea, where more than 98.9% infants have been vaccinated since 1990, the prevalence of HBV carriage has declined greatly [5]. Similarly in Europe, the reported HBV cases per 100,000 have declined from 6.7 to 1.5 during 1995-2007 [6]. However weak immunization strategies in other countries and limited domestic funding in many more create challenges to achieving regional targets.

The major endemic regions facing the problem of hepatitis B are China and central and southern parts of Africa [7]. The disease is relatively rare in western countries and is usually observed in adults. On the other hand, in Asia and Africa, hepatitis B is acquired during the childhood, mostly via perinatal transmission [7]. Apart from endemic regions, southern parts of east and central Europe, the Middle East, the Amazon and the Indian subcontinent show quite high occurrence of hepatitis B. Most of the cancer cases, not only in parts of Africa and Asia but also in developed countries, are due to primary liver cancer caused by hepatitis B [8, 9].

WHO has recommended that each child should get their vaccine dose against hepatitis B as soon as possible, preferably within 24 hours after the birth. The first dosage is followed by 2 or 3 more doses depending on the pattern adopted for vaccination. Two further doses are enough if they are given simultaneously with first and third dose of DPT vaccine (diphtheria-pertussis-tetanus vaccine). The younger cohorts should be given priority for catch-up vaccination as they face a higher risk of chronic illness. Additionally, people who are under medical treatment where they require blood-related therapy or other blood exchange activity, face a high risk and therefore should be given a booster dose [10]. In more than 90 % of the adult patients, the infection clears spontaneously and the immune protection lasts for the life time [11].

1.2. HBV genomic organization

The hepatitis B virus has a partially double stranded circular DNA of approximately 3200 base pairs. HBV has four overlapping open reading frames (ORFs) which encode seven polypeptides [12]. The seven polypeptides constitute the surface- and coat-proteins, transcriptional transactivator, polymerase, reverse transcriptase and RNase. The envelope protein genes i.e., pre-S1 (large), pre-S2 (middle), and S (small or surface) overlap with the polymerase ORF [13].

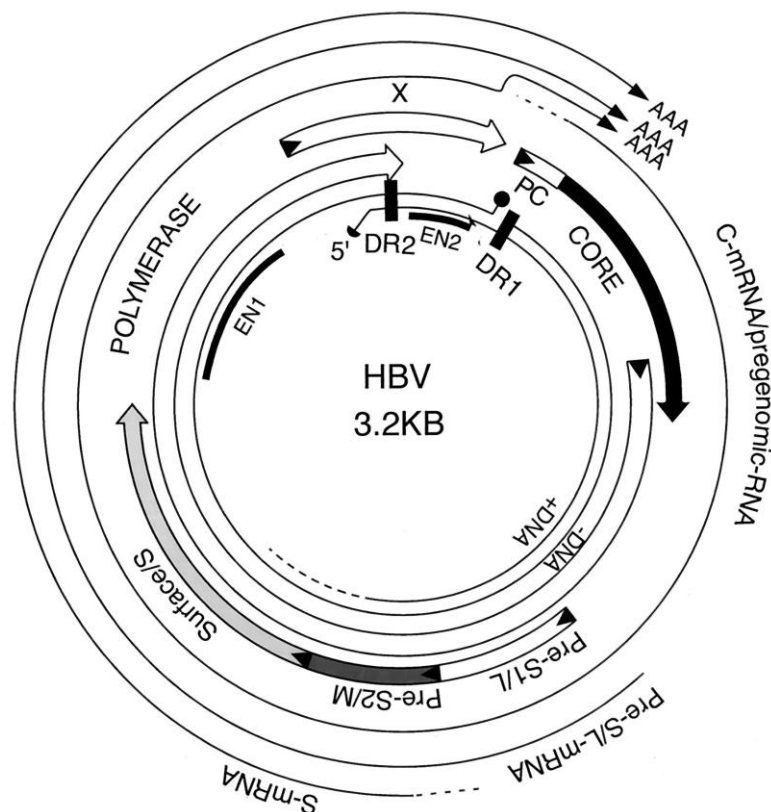


Figure 1.2. The physical map of hepatitis B genomic organization [13].

The viral polymerase is covalently attached to the 5' end of the minus strand which is the longest and contains an ORF that encodes for viral proteins and the cis-elements responsible for regulation of HBV gene expression and replication. A plus strand of variable length maintains the circular structure of the cohesive hybridization that straddles the 5' and 3' ends of the minus strand [14].

1.3. Hepatitis B virus morphology

The hepatitis B virus has an icosahedral shape with an outer coat. Electron microscopy shows three morphological forms of HBV in serum. The most abundant form is the

spherical one with 22 nm diameter. The second most common is the filamentous or tubular form also with 22 nm diameter but in length may reach up to 200 nm. These both forms are devoid of DNA. The third and least observed form is the 42 nm spherical virus, originally referred to as Dane particle.

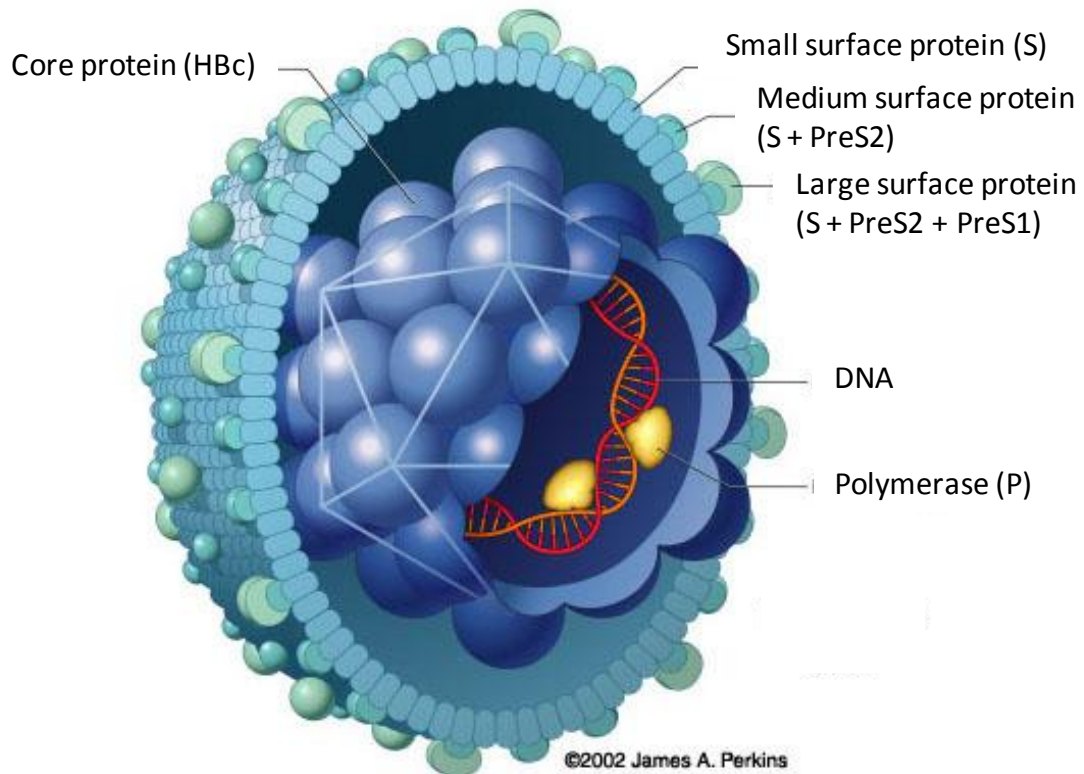


Figure 1.3. Illustration of a HBV-particle, also known as the Dane particle. The outer surface (coat) of the virus consists of three types of HBV surface antigens. In addition to the icosahedral core, made up of core protein (HBc), the virus contains viral DNA and the polymerase enzyme inside the inner core. With permission, adapted from © 2002 James A. Perkins, Medical and Scientific illustrations.

Structurally, HBV consists of three major components, surface proteins, core proteins and the genetic material (Figure 1.3). The surface coat itself comprises three proteins i.e., large protein (L-protein), medium protein (M-protein) and small protein (S-protein). There have been continuous efforts since decades to develop a recombinant vaccine against hepatitis B inspired by different immunogenic domains of the original virus, for example, VLP vaccines made up of only core protein. [15]. Out of all three components, the most attractive and popular candidate, with respect to efficacy, is the surface antigen, known as hepatitis B surface antigen (HBsAg).

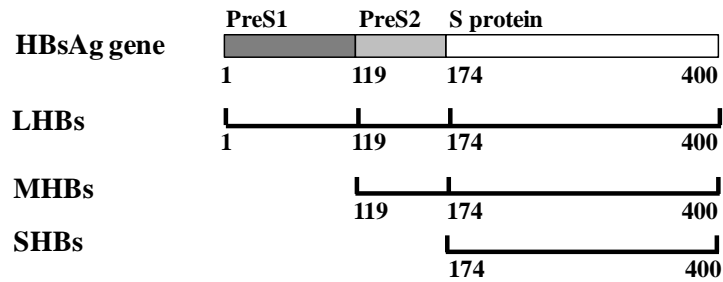


Figure 1.4. A schematic representation of surface proteins of HBV. The S-region is common in all of the surface antigens, which comprises 226 amino acids.

All of the envelope proteins contain the sequence of the small protein i.e. S-region, whereas the two other proteins have additional amino acid sequence namely preS1 and preS2 (Figure 1.4). All three domains contain regions which are targets for neutralizing antibodies. The preS1 region directly binds to the cellular receptor whereas the preS2 sequence binds to the albumin receptor. The small protein is not directly involved in binding to the liver cell membrane, however, antibodies against this protein have a good neutralizing effect [16].

1.4. Mechanism of virus-mediated immune response

In general pathogens are averted from entering the human body in the first place via innate immunity which comprises of first and (partially) second line of defense. First line of defense of the immune system consists of various physical (e.g., skin) and chemical barriers (mucous, saliva, vaginal fluid etc) to prevent the virus from entering the body. Still if the virus manages to enter inside the human body, it has to deal with immune system at further levels [17]. When HBV enters the body via body fluids, it passes through blood and here the second line of defense comes in action. This is characterized by production of type 1 interferon (IFN)- α/β cytokines and the activation of natural killer (NK) cells [18, 19]. If HBV is able to pass through the innate immune system, it enters the hepatic cells where it undergoes multiple cycles of replication and the shredding occurs into the blood [20].

Depending on the stage of infection, various markers can be observed in the blood. Four major serological markers are i. hepatitis B surface antigen, ii. hepatitis B surface antibody (anti-HBs), iii. total hepatitis B core antibody (anti-HBc) and iv. IgM antibody to hepatitis B core antigen (IgM anti-HBc). HBsAg is one of the initial markers appearing in third week after exposure and persists by the sixth month. From

second month of infection, high levels of IgM anti-HBc are detectable. Anti-HBs is observed variably from sixth month, after the disappearance of HBsAg [2].

By definition, hepatitis is inflammation of the liver but none of the hepatitis-inducing viruses, including HBV, are typically cytopathogenic. The HBV DNA integrates into host genome and the cellular damage observed in hepatitis is supposedly a result of immune response against infected hepatocytes [20].

1.5. HBV replication cycle

The life cycle of the HBV inside the human body is similar as that of other viral cycles. After entering, first the capsid gets attached to the hepatocytic surface via specific receptors [21] and double stranded DNA is released inside the hepatocyte [22]. Within the host nucleus, this viral DNA is converted into cccDNA (covalently closed circular DNA) which replicates to create several transcript copies including pregenome RNA [23].

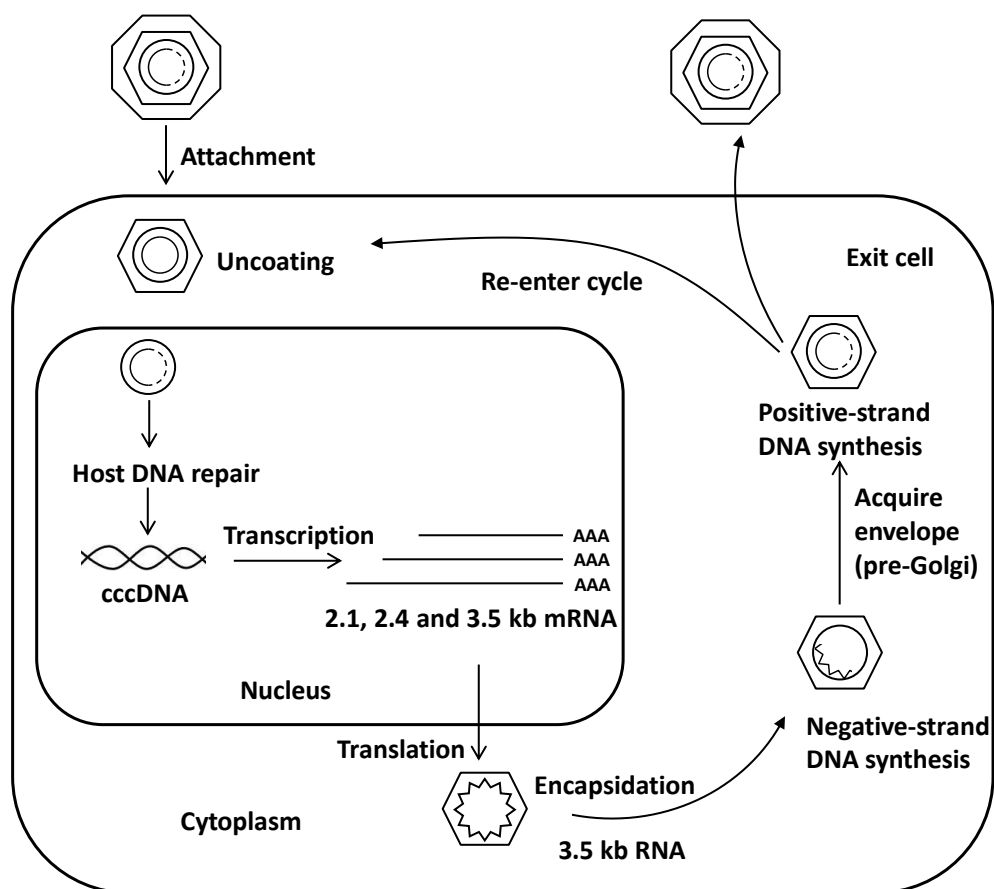


Figure 1.5. HBV replication cycle: HBV gets attached to a receptor on the surface of the cell. The capsid enters the cell, cccDNA replicates inside the host nucleus to produce several copies of pregenome RNA which is encapsidated and continues the cycle either in the same or in another cell. Adapted from Butel *et al.* [24].

Pregenome RNA is encapsidated with core protein and single-strand DNA is synthesized by viral polymerase within the core. Core particles bud from pre-Golgi compartment, acquire surface protein and exit the hepatocyte or enter another cycle of intracellular replication [23].

1.6. Vaccines for hepatitis B

The vaccines against hepatitis B exist since a while but the death toll caused by it is still increasing. Among many other reasons, it is because of absence of a suitable-for-all vaccine. In general, about 1-10% of healthy adults show non-response to vaccine because of one or the other reason. Therefore there is still a dire need of hepatitis B vaccine candidates with better immunogenic response and simpler delivery system.

HBsAg, originally known as Australia antigen, was first discovered by Blumberg *et al.* in 1965 in sera of leukemia patients [25]. Soon it was adapted to be exploited as vaccine against hepatitis B. Presently, various types of vaccines against hepatitis B are available.

1.6.1. Plasma-derived vaccines

The early efforts to propagate HBV in cell cultures were unsuccessful therefore it has not been fruitful to develop vaccine based on virus expressed in cell cultures [26, 27]. When infected with HBV, cell cultures produce low yield due to poor viral replication [28]. Other option was isolation of HBV particles (22 nm) from plasma of asymptomatic human carriers. The first generation of hepatitis B vaccine was developed from the formalin- or heat-inactivated virions from plasma of carrier patients [29].

The first plasma-derived vaccines were licensed in USA and France in 1981-1982. In addition to inadequacy of plasma, there have been many safety issues associated with plasma-derived vaccine. The risk of presence of active virus or viral DNA makes them unfavorable as a vaccine candidate. Occurrence of some undetected infectious agents in vaccine, despite the careful procedure of isolation from human plasma, has been a matter of concern [30]. Although plasma-derived vaccines are no longer produced in North America or Western Europe, they are still in use in many countries in Asia.

1.6.2. DNA vaccines

The naked DNA can be injected as expression plasmid which is taken up by the cells. This results in the expression of respective antigen which triggers the immune response [31]. In case of hepatitis B, this approach has been applied so far in mice using pDNA encoding HBsAg and has been reported to produce significant humoral and cellular response [32].

In general, in plasma- and DNA-derived vaccines, the results are less promising due to their tendency to contamination. Particularly in developing countries, where there is always a risk of contamination because of backward health care system, plasma derived vaccines are less successful.

1.6.3. Subunits vaccines

Subunit vaccines, as the name suggests, are the vaccines based on antigenic domains of the viral coat. In case of hepatitis B, polypeptide subunits have been tested in non-human primates and clinical tests have been carried out [29]. A trial of synthetic peptide vaccine comprising 19 amino acid residues from the pre-S2 protein (residues 14-32 from the N terminus) has been proven successful to produce immunological efficacy in chimpanzees [33]. The subunit has been stated to be expressed in *E. coli* in a number of reports [34, 35].

1.6.4. VLP-based vaccines

The HBsAg VLP-based vaccine has been one of the most significant success stories in biotechnology. The vaccine in common use today was approved in 1986 by US FDA and is considered as world's first genetically engineered vaccine [36]. It is also considered as the first vaccine against any cancer i.e. hepatocellular carcinoma. This vaccine comprises small virus-like particles (VLPs) which resemble the virus actually causing the disease with the major difference being that they lack genetic material i.e., they are non-infectious.

During infection, two types of viral particles are frequently produced. The infectious types, Dane particles, are about 44 nm in size. During chronic infection, HBsAg is expressed also as another non-infectious quasi-spherical form, with 22 nm of size. Both particles have octahedral symmetry [37].

1.7. Expression systems used for HBV vaccine production

The most common antigen used against hepatitis B as vaccine is the surface antigen. HBsAg has been successfully synthesized in a number of microbial systems. Like any other biopharmaceutical product, each system offers its advantages and disadvantages.

In case of *E. coli*, the expression of HBsAg polypeptide was successful but the activity could not be verified by radioimmunoassay [38]. The VLP formation ability has been very poor either because of lack of glycosylation of HBsAg derivatives [35] or because of inefficient transcription [34]; although the HBV genome does not contain ‘introns’ which *E. coli* is believed to be unable of transcribing [39].

Subsequently, *Saccharomyces cerevisiae* was employed as an alternative host system for the expression of HBsAg. The first successful commercial vaccine invented against hepatitis B virus (HBV) in 1984 was expressed in *S. cerevisiae* [40-42]. Till now, only two FDA approved vaccines, Engerix-B® (GlaxoSmithKline) and Recombivax HB® (Merck and Co. Inc.), are produced in *S. cerevisiae*.

Apart from *S. cerevisiae*, HBsAg has been expressed in other fungal systems such as *Pichia pastoris*, *Hansenula polymorpha* [43] and *Aspergillus niger* [44]. Commercially available *H. polymorpha*-derived vaccines are Hepavax-Gene (KGCC, Korea) and AgB (LPC, Argentina) [45]. In general, *A. niger* serves many inherent advantages such as glycosylation more similar to that of in humans and higher product yield but the cultivation process is rather tricky due to the danger of spore dust formation [46].

HBV antigens have been reported to be expressed also in viral expression systems. Both surface and core antigens were co-expressed in Vaccinia virus which resulted in formation of either HBsAg or HBcAg viral particles [47]. Further alternatives include adenovirus and baculovirus expression system.

Other successful expression systems in trial comprise Plant cell cultures [48-50], Chinese hamster ovary (CHO) cells [51, 52] and insect cell-based systems [53].

1.8. *Pichia pastoris* as expression host

As mentioned earlier, initially there have been efforts to express HBsAg in *E. coli* but there had been problems with the retention of the plasmid. Also, the immunogenic response was relatively less effective as compared to that generated by yeast-derived HBsAg [38, 54]. The isolation of a yeast specie capable of methanol assimilation as sole source of carbon and energy was reported for the first time in 1969 [55].

Pichia pastoris has been an attractive host system for the heterologous protein production due to many evident reasons. It is possible to produce large amount of recombinant protein by inserting multiple copies of target genes. *P. pastoris* has a strong, inducible promoter that can be used for protein production [56]. By and large the yields are good, final cell density of cultivation is high and post-translational modifications are correctly oriented [57-59]. In general, it is practicable to obtain the protein in active form in the medium. It is easy to grow to high cell density and being a eukaryote, *P. pastoris* is able to carry out the post-translational modifications.

Certainly, there are also some bottlenecks for *P. pastoris* as expression host system, especially with higher gene dosage. It is well known that expression can be increased significantly by increasing the gene dosage [60, 61] although in case of certain proteins, this may cause cellular stress [62]. The burden due to increased gene dosage causes protein folding stress which can lead to product accumulation in the ER [63].

1.9. VLPs as vaccines

VLPs are the nonreplicating virus capsids made by using recombinant DNA technology that mimic the structure of native virions. They are effective inducers of neutralizing antibodies as well as T-cell response. VLPs contain typically viral structural units, capsid or envelope, with absence of some elements required for assembly and viral genome and still capable of triggering immunologic effect. According to a view, the assembly pathway is difficult to establish because the polymerization is rapid and it is not always a single high-order reaction [64]. Usually VLP derived vaccines consist of one or more antigenic regions of original virus, which are allowed to self-assemble. Recombinant hepatitis B surface antigen (HBsAg) polypeptides assemble to form VLPs, which mimic the structure and hence

immunogenic effect of native virus. One subunit of HBsAg is 25 kDa and consists of 226 amino acids.

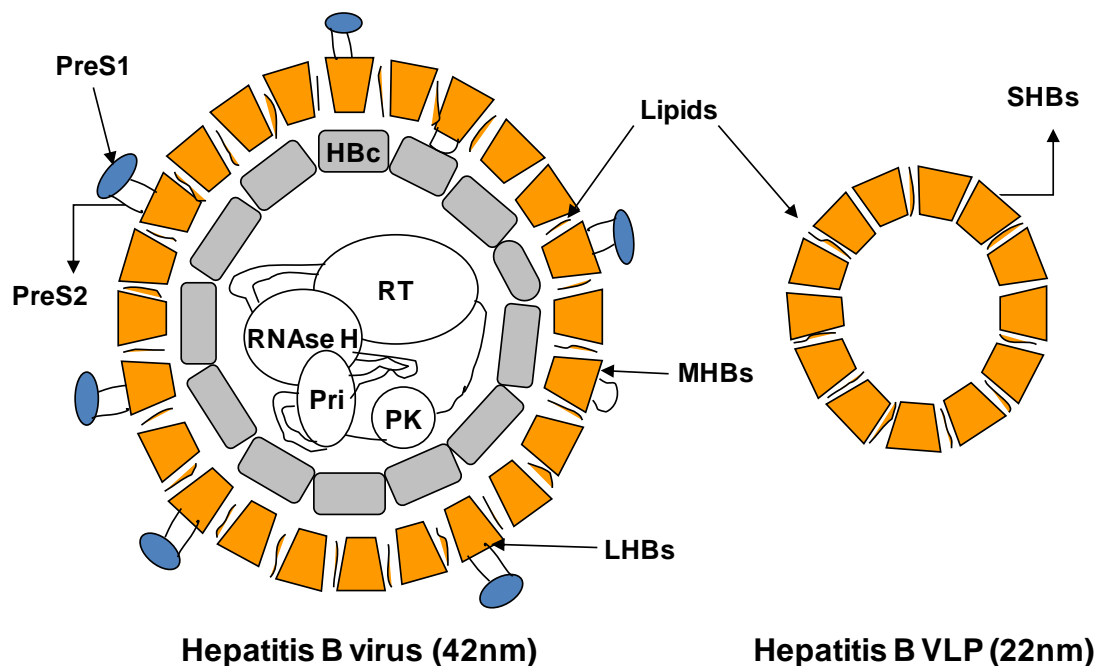


Figure 1.6. A cartoon of HBV (left) in comparison with HBsAg VLP (right). Three surface antigens are large surface protein (LHBs), middle surface protein (MHBs) and small surface protein (SHBs). HBV core is made up of core protein (HBc). In addition to that, HBV contains reverse transcriptase (RT), RNA primer (Pri) and protein kinase (PK). The small surface antigen gene is expressed heterologously and has the property to self-assemble into VLPs (right).

VLP vaccines offer many lucrative advantages over the parallel alternatives. Their prime advantage is the absence of genetic material which promises absence of mutations and infection. Many deleterious effects of attenuated vaccine can be avoided by adapting the VLP approach. In general, the immunogenic stimulus is strong which triggers both humoral and cellular responses. Depending on the expression system, the production costs can be cut to many folds low as compared to the conventional (attenuated and inactivated) vaccines. In case of microbial expression systems, large production scale and good yields guarantee the high profitability.

VLPs formed by the structural elements of viruses have received considerable attention over the past two decades and are considered as potential approach for future. Apart from hepatitis B, this technology can be proven useful in preparation of vaccines against many other viruses such as Dengue virus [65], Human papilloma virus (HPV) [66], Norwalk virus [49], Simian-Human Immunodeficiency virus [67] etc. More than

30 VLP based vaccine for humans and other animals have been developed till date [68].

1.10. Immunogenic properties of VLPs

In general, VLPs are more immunogenic as compared to the corresponding single subunits [69]. VLPs have potency to stimulate both cellular and humoral arms of the immune system. The repeated and ordered organization of subunits link with the specific immunoglobulins (Igs) which makes VLP ideal for triggering B-cell response [70].

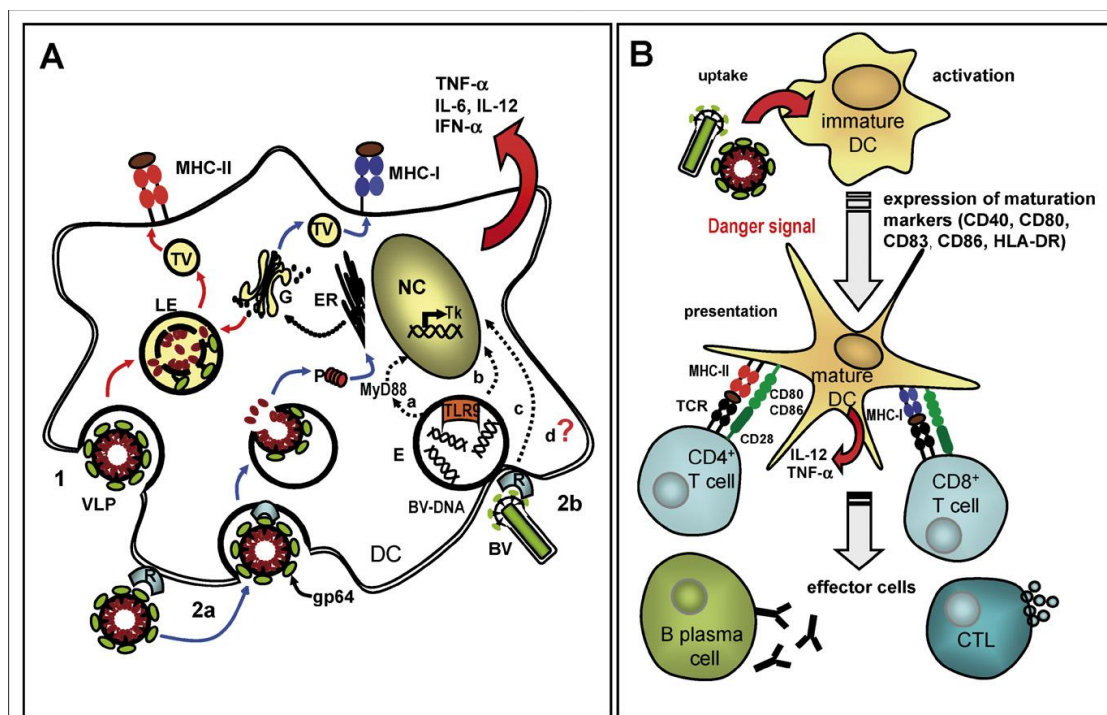


Figure 1.7. Supposed mechanism of Immunogenic interaction of a VLP inside the body; adapted from Ludwig *et al.* [71] (reproduced with permission).

Due to their relatively smaller size, it is easy for dendritic cells to uptake VLPs. The mechanism of VLP-mediated immune response involves the uptake of VLPs by dendritic cells (DCs) which result in the appearance of signals on the surface of these cells (Figure 1.7). These DCs are later transported to the lymphatic nodes to be presented to the T-cells [71].

1.11. VLP assembly

Despite the availability of HBsAg vaccine since 25 years, its structure at molecular level and the mechanism of self-assembly of the VLPs is not fully known. There have been some efforts to understand this mechanism in real viruses but in the field of VLPs, this area is still under-explored. The mechanism by which HBsAg undergoes VLP formation is of special interest as it may open prospects to other VLP based vaccines. As far as the mechanism of VLP formation in mammalian cells is concerned, it is relatively straightforward. For example in case of human hepatocytes, the particles are formed in ER (endoplasmic reticulum). They are retained in the ER lumen for some time and later excreted out to the intercellular space [72, 73].

In simpler expression systems, the process of secretion of HBsAg VLPs is rather tricky. In CHO cells, electron micrographs show the HBsAg accumulation in dilated areas of ER. Here the HBsAg resides in form of collection of filamentous structures with half time for secretion of about 5 h [74]. No HBsAg particles could be observed in the plant cell culture. Their failure to progress further than ER (or the Golgi) has been described as a result of presence of the cell wall [48]. In case of yeast, it has already been described that the assembly does not take place *in vivo* during the expression, [75] which leads to the conclusion that this process occurs during the downstream process.

Apart from protein physical properties, other decisive factors involved are environment components of protein solution. Physiochemical conditions like pH, ionic strength and temperature play important role in correct assembly process [76]. Moreover, the influence of stoichiometric ratio of structural (subunit) proteins on the concentration of assembled particles has been intensively studied [77].

It was considered in the past that there are no intermediates present in the HBsAg assembly process [78] however recently it has been reported that intermediates were trapped by phenylpropanamide assembly accelerators [79]. Theoretically, a capsid can undergo assembly via exponential folds of intermediates. For hepatitis B capsid, taking into account 120 dimers, a least magnitude of the order of 10^{26} is possible, where as for *in vitro* process, this number decreases to 10^{14} [80].

1.12. Physicochemical features of HBsAg

HBsAg subunits are the building blocks of hepatitis B VLP, with one subunit being 25 kDa in size. About 100 subunits, along with host cell lipids, assemble together to constitute one VLP. To understand the assembly mechanism, one needs to understand the structural aspects of single subunit protein. HBsAg is a hydrophobic protein which consists of mostly hydrophobic amino acids, as it is obvious from its hydrophathy plot (Figure 1.8).

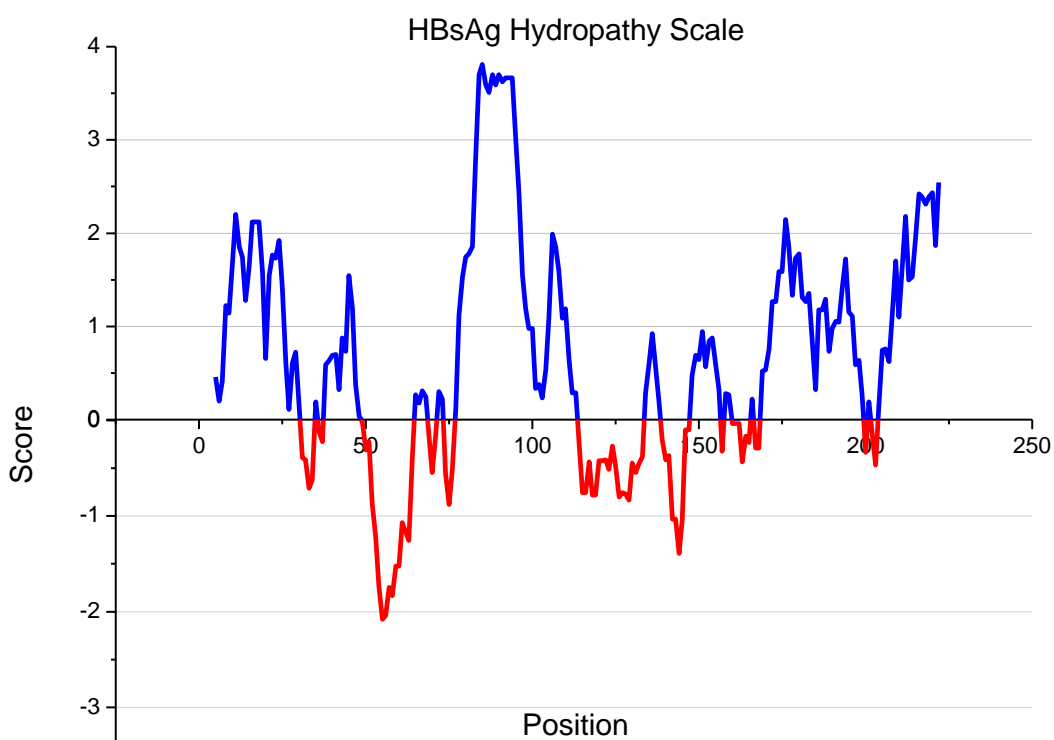


Figure 1.8. Kyte and Doolittle plot of the HBsAg amino acid sequence. The X-axis plots the 226 amino acids of the protein, whereas the Y-axis plots the respective hydrophathy scale (<http://web.expasy.org/protscale/>).

Chemically, HBsAg VLPs are composed of protein and lipid contents in a ratio of 60:40 respectively [52, 81]. Unlike typical (membrane) lipoproteins, HBsAg VLPs exhibit peculiar spatial arrangement of lipids. Instead of a lipid bilayer arranged around the protein layer, HBsAg particles have lipid layer embedded towards the inner region constituting hydrophobic core whereas the hydrophilic protein part faces towards the outside [82]. The lipids help to maintain the native conformation [83] and hence have an important influence on the immunogenic prosperities. This is evident from dissimilarity in immunogenic properties of HBsAg particles obtained from different sources. It is observed that when the same HBsAg encoded by the same DNA

sequence is expressed in different heterologous systems, exhibit different immunologic behavior [84].

In addition to lipids, plasma-derived HBsAg is reported to contain carbohydrate moiety. Peterson *et al.* have been suggested that the amino acid region 122-150 of the subunit protein (named as p-25) and its glycosylated form (named as gp-30) in HBsAg particle, isolated from the plasma of chronic carrier, exhibits an attachment site for carbohydrates [85]. Both proteins, p-25 and gp-30, contain 226 amino acids.

The antigenicity of HBsAg particles is dependent upon the correct disulfide bonds among the amino acids present in region aa101-172, the so-called a-determinant [86]. Several immunologic assays exploit this property to detect the presence of antigen in the serum [87]. The correct disulfide bonding in HBsAg dimers facilitates the correct conformation required for the *in vitro* VLP formation (Figure 1.9-B).

The cryomicroscopic studies of truncated form of HBV core protein (aa 1-149) suggest hydrophobic domains and disulfide bond between the monomers, as shown in figure 1.9 [88].

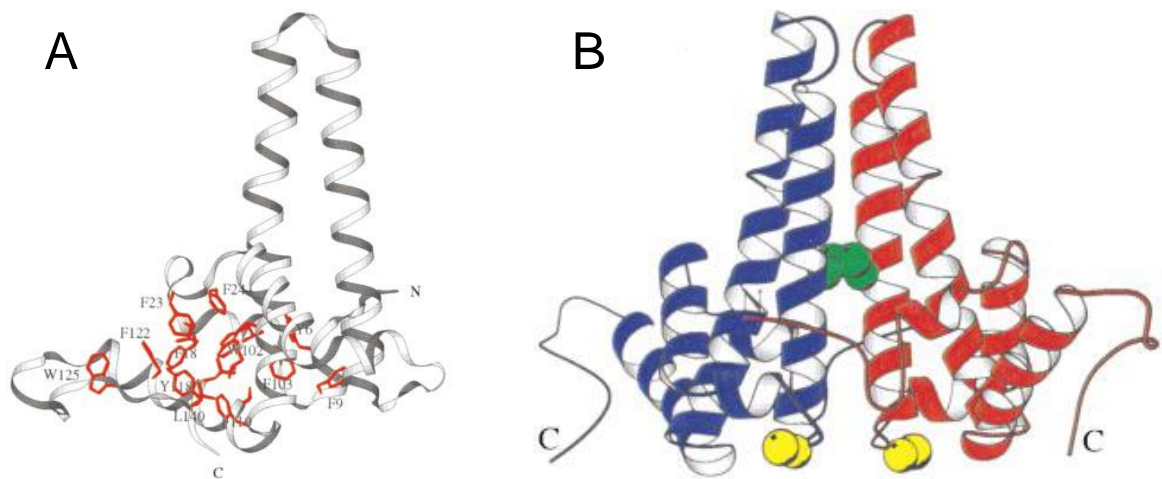


Figure 1.9. Structure of HBV capsid monomer: (A): The lower region of protein with aromatic amino acid residues (highlighted in red) constitutes the hydrophobic core. (B): HBsAg dimeric form. The disulfide bond between two monomers (shown in green) arises from Cys-61. With permission, reprinted from Wynne *et al.* [88].

CD spectroscopy shows that α -helix is the most abundant secondary structure found in HBsAg, constituting about 50% of the total protein structure. Some of these α -helices are believed to turn into γ -turns during the aggregation process in the purified protein [89].

2. Objectives of the thesis

Virus-like particles (VLPs) as vaccines have proven to be a promising option against several diseases. However despite of being an important mean to prevent millions of casualties worldwide, there has been an imperative need to investigate the process of self-assembly from protein subunits into the VLPs. In this thesis, HBsAg was taken as a model system to study the *in vitro* assembly process of VLPs. HBsAg VLP-based vaccine has been one of the most important success stories in biotechnology [36]. It is considered as the first vaccine against a cancer i.e., hepatocellular carcinoma.

Insight into the assembly process is important because (a) It will facilitate to develop new vaccines based on VLP technology, (b) It will be convenient to administer product homogeneity and quality, and (c) It will help to produce the VLPs with better immunogenicity. Moreover, *in vitro* investigation provides the possibility to manipulate the original process, e.g., disassembly and reassembly, leading to the resulting product which is more stable and effective.

It is known that the VLPs are not present intracellularly during HBsAg production in the yeast cells [75]. Therefore it was concluded that the assembly process takes place *in vitro* during the downstream process. Until now, there has not been any report about the monitoring of assembly process in HBsAg during downstream processing, which brings it to the aims of this thesis. The explicit purpose of this thesis was to answer the following questions:

How to obtain high quality HBsAg VLPs during downstream process?

How to probe the downstream process to monitor the VLP production?

How to provide better insight into assembly process using electron microscopic study?

How stable is the VLP structure and what happens when it is defolded?

The primary objective of this study is to apprehend the key aspects of *in vitro* VLP assembly. This report mainly focuses on the factors affecting the self-assembly of HBsAg VLPs during the downstream process. The suggested factors influencing the assembly being stated here are main constituents of the microenvironment such as host cell components (HCCs) and the buffer system. Hence the focus is given to examine

these factors together and individually with respect to their influence on VLPs. Several control experiments have been carried out to investigate the effect of above stated factors, together as well as individually.

The second aim of this work is to better understand the stability and structural aspects of VLPs and the changes induced therein by the addition of denaturing agents. The purified VLPs have been subjected to defolding process by addition of chaotropic salts. These changes have been observed via analytical tools like fluorescence spectroscopy and dynamic light scattering technique. Based on these observations, mechanism of defolding of the VLPs has been proposed.

3. Experimental methods

In this chapter, procedures of the major experiments performed will be stated. Their outcome will be discussed in the coming chapter, section-wise.

3.1. Strain and vector for HBsAg expression

The *Pichia pastoris* host strain used in this study to generate the HBsAg expressing transformants has been described previously [90]. Briefly, it is GS115 (HIS4), a histidine requiring auxotroph strain. The parent plasmid is pAO815 which contains the *AOXI* promoter with 8-copy HBsAg expression cassette inserted in it. The HBsAg producing strain was initially classified as Mut^S phenotype [90] but in a recent study in our group, the presence of *AOXI* gene has been reported, referring it to as a Mut⁺ phenotype [91]. It has been proposed earlier that expression of HBsAg makes the strain relatively slow as it takes more time to grow biomass and to express the recombinant protein, but this slower growth rate is considered to improve the percentage of HBsAg polypeptides which are later assembled into VLPs [92].

3.2. Preliminary expression of HBsAg in *Pichia pastoris*

To test the HBsAg expression, shake flask cultures of *P. pastoris* harboring HBsAg gene as well as *P. pastoris* GS115 (wild type) were grown and different media were used in growth of the cultures before and after induction under different conditions. The recipes of these media are given in the Appendix. For preliminary shake flask tests, the temperature and agitation were kept constant at 30°C and 250 rpm respectively. All the cultivations were done at least in duplicate. Initially, the expression of HBsAg was analyzed by SDS-PAGE.

A- Buffered Media

Different kinds of buffered media were chosen with minimal and complex composition. One of the media used was BMG (Buffered Minimal Glycerol) which is composed of 100 mM potassium phosphate, pH 6.0; 1.34% (w/v) yeast nitrogen base (YNB); 4 x 10⁻⁵% (w/v) biotin; 1% (v/v) glycerol. For induction phase of same

cultivations, BMM (Buffered Minimal Methanol) was used which has the same composition with exception of 0.5% methanol instead of 1% glycerol.

Another parallel expression was performed using BMGY (Buffered Glycerol-complex Medium), which included 1% (w/v) yeast extract and 2% (w/v) peptone in addition to 100 mM potassium phosphate, pH 6.0, 1.34% (w/v) YNB, 4×10^{-5} % (w/v) biotin and 1% (v/v) glycerol. As the biomass reached to the desired OD, the cells were introduced with BMMY (Buffered Methanol-complex Medium) which has same composition as that of BMGY except having 0.5% (v/v) methanol instead of 1% (v/v) glycerol.

Media BMG and BMGY were used to raise a biomass followed by media BMGY and BMMY induced with regular addition of MeOH i.e., 0.5% volume after every 24 hours, according to manufacturer's instructions [Pichia expression Kit, Catalog no. K1710-01, Invitrogen USA].

B- Defined Media

Defined medium A (DM A) has composition per liter as follows; 95.2 g (as well as 60 g, as DM-B) glycerol, 15.7 g $(\text{NH}_4)_2\text{SO}_4$, 9.4 g KH_2PO_4 , 1.83 g $\text{MgSO}_4 \cdot 7\text{H}_2\text{O}$, 0.28 g $\text{CaCl}_2 \cdot 2\text{H}_2\text{O}$, 0.4 mg biotin and 1.14 g yeast trace metal (YTM) solution.

The YTM solution (1 L) contains 760.6 mg $\text{MnSO}_4 \cdot \text{H}_2\text{O}$, 484 mg Na_2MoO_4 , 46.3 mg H_3BO_3 , 5.032 g $\text{ZnSO}_4 \cdot 7\text{H}_2\text{O}$, 12.0 g $\text{FeCl}_3 \cdot 6\text{H}_2\text{O}$, 207.5 mg KI and 9.2 g H_2SO_4 .

C- Semi Defined Media

The semi-defined media used include casein 1% to total volume as the complex ingredient. Semi-defined medium (Semi-DM) comprises of (per liter) 60 g Glycerol, 10 g Casein hydrolysate, 9 g $(\text{NH}_4)_2\text{SO}_4$, 4.3 g KH_2PO_4 , 3.2 g $\text{MgSO}_4 \cdot 7\text{H}_2\text{O}$, 0.22 g $\text{CaCl}_2 \cdot 2\text{H}_2\text{O}$ and 5 mL Pichia trace metal solution (PTM1) solution.

The recipe of PTM1 is 6.0 g/L $\text{CuSO}_4 \cdot 5\text{H}_2\text{O}$, 0.08 g/L NaI, 3.0 g/L $\text{MnSO}_4 \cdot \text{H}_2\text{O}$, 0.2 g/L $\text{Na}_2\text{MoO}_4 \cdot 2\text{H}_2\text{O}$, 0.02 g/L H_3BO_3 , 0.5 g/L CoCl_2 (/CoCl₃), 20.0 g/L ZnCl_2 , 65.0 g/l $\text{FeSO}_4 \cdot 7\text{H}_2\text{O}$, 5.0 ml H_2SO_4 and 0.2 g/L biotin [Pichia fermentation process guidelines, Invitrogen USA].

All the media were sterilized by autoclaving at 121°C for 20 min. The fine components, for example biotin and YTM solution, were filter sterilized. In all the initial shake flask cultivations, 100 µL of glycerol stock solution which contained $\approx 2.6 \times 10^9$ cell/mL ($OD_{600} = 52$) was introduced to 50 mL media. Subsequently, cells were grown in shake flasks at one liter scale to monitor the production yield of the strain and the medium.

3.3. High cell density cultivation of *P. pastoris* GS115 Mut⁺

As a next step, cultivation was upscaled to bioreactor level. To start the pre-inoculum, 100 µL of the HBsAg producing *P. pastoris* glycerol stock was introduced in 100 mL of BMGY (buffered media with glycerol) and incubated for 12-16 h until the OD_{600} reached 15. 10 mL of this pre-inoculum was introduced in 1 L BMGY to start the inoculum, which was incubated until $OD_{600} = 8$. After almost 14 h, the inoculum (1 L) was added in 9 L simple defined media to start the main culture [93].

The cultivation was carried out in a 10 L bioreactor (BiostatC, B.Braun Biotech International, Germany) using basal salt medium (for recipe, see Appendix). The temperature and pH were kept constant at 30°C and 5.6 respectively. The pH was maintained by using 12.5% (v/v) NH_4OH . The cells were grown in batch phase on glycerol as sole carbon source. A fed-batch production phase was started, 38 h after glycerol phase, when a sudden increase of dissolved oxygen (DO) was observed, indicating the decrease of respiratory activity and hence total consumption of glycerol in the media. During the fed-batch production phase, cells were grown on methanol and the feed was added manually to maintain a level of 6 g/L methanol. Trace elements were also added in methanol feed [93]. All on-line data was obtained via an in-house software, RISP (Real time integrating software platform, Institute of Technical Chemistry, Leibniz University Hannover). To avoid the froth formation, anti-foam (TEGO® Antifoam KS911, Evonik) was added, when necessary.

3.3.1. Online and offline measurement

During the course of cultivation, aeration rate, oxygen transfer and CO_2 evolution were measured by the off-gas analyzer. The dissolved oxygen (DO) regulation was obtained

with a cascade of agitation, air flow and finally enrichment of air with oxygen. The pH regulation was performed with 12.5% (v/v) NH_4OH and 2 N phosphoric acid addition.

Samples were collected, at different time points during the cultivation, to check the biomass and amount of expression. For optical density measurement, samples were collected from the cultures regularly and diluted to suitable extent (between $\text{OD}_{600\text{nm}}$ 1-8) with 0.9% (w/v) saline solution. The optical density was measured at 600 nm wavelength via spectrophotometer (Uvikon, Kontron Instruments). For each sample three readings were observed and the mean was taken.

3.3.2. Cell harvesting

In shake flask experiments, induction phase spanned from 120 to 190 h after induction. During bioreactor cultivation, cells were harvested 136 hours after induction, at $\text{OD}_{600} = 320$. The culture was connected via tubing to the continuous-flow centrifuge unit (Centrifuge Stratus, Continuous flow rotars, Heraeus) to obtain the biomass in the form of pellet. For about one week, samples were stored at -20°C and for longer terms at -80°C .

3.3.3. Cell lysis

For different purposes, different lysis techniques were adopted. To observe the product formation during the cultivation, glass beads (0.45 mm; Sigma G-8772) were used to lyse the cells. For purification at pilot scale, lysis was carried out using Microfluidizer (M110L, Microfluidics). Detailed protocols of the lysis are described in the Appendix.

3.3.4. *P. pastoris* GS115 control cell culture

As a control, *P. pastoris* GS115 cells without plasmid were grown in the defined medium in shake flask. The cells were harvested and the lysate was treated for the purification process likewise as that of the producing cell culture. The samples were collected at various points of this purification-like process to use as a background control for transmission electron microscopy analysis.

3.4. Downstream processing of HBsAg

After the successful production of HBsAg in *P. pastoris* under previously optimized conditions, the biomass was subjected to downstream processing. In general, the

purification protocol from Pointek *et al.* [94] and Lünsdorf *et al.* [75] was followed; however some modifications were made, where necessary. The Purification was done by using different chromatographic techniques. The complete process is summarized in the figure 3.1.

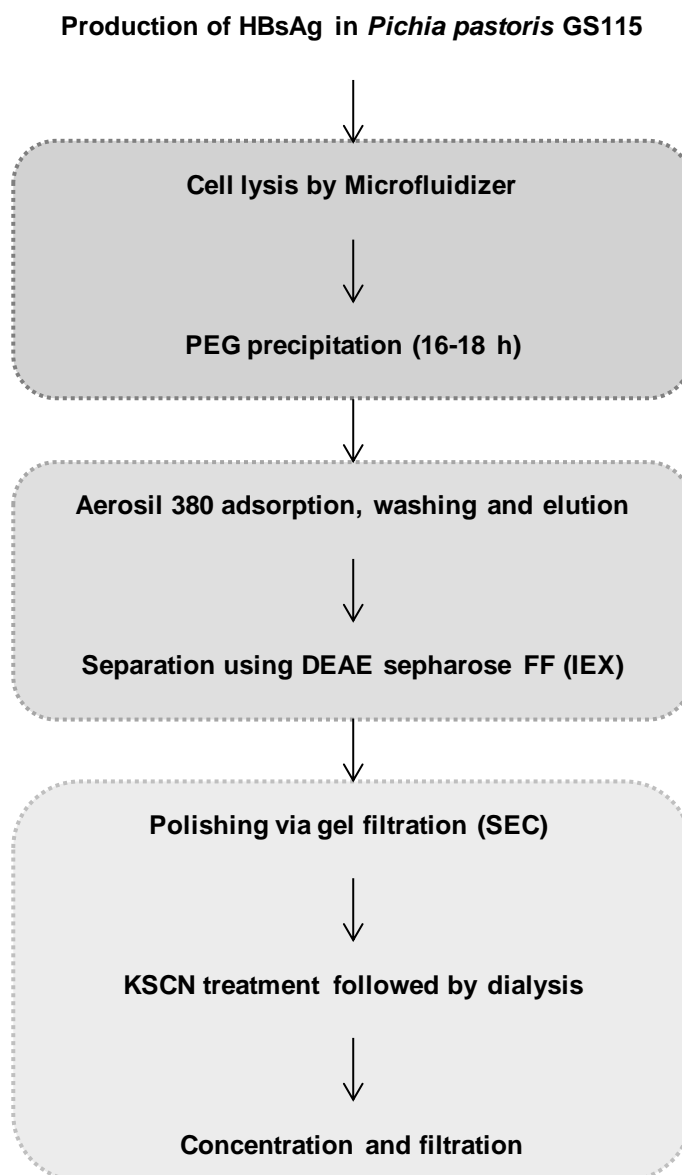


Figure 3.1. Flow-sheet illustration of HBsAg purification. The three blocks represent three stages of purification i.e. preparation, capturing and intermediate purification and ultimately, polishing. After salt mediated PEG precipitation, the cell lysate is subjected to capturing based on hydrophobic interaction using fumed silica. The Aerosil eluate is proceeded with ion exchange chromatography (IEX) to remove further contaminants. The semi-purified product is polished via size exclusion chromatography (SEC) and treated with KSCN. Final product is filtered and stored at 4°C till further analysis.

3.4.1. Preparation

The biomass from the cultivation (100 g) was resuspended in the lysis buffer [25 mM sodium phosphate buffer, pH 8, 5 mM EDTA] to adjust $OD_{600} \approx 200$. Afterwards, Tween 20 was added to adjust a final concentration of 0.6 % (v/v) and the pH was readjusted to 8.0. The mixture was passed through Microfluidizer at a pressure of 12,000 psi and $\sim 4^{\circ}\text{C}$, 12-14 times. Complete lysis was confirmed by viewing the cell lysate under the microscope.

Polyethylene glycol 6000 (PEG 6000) was slowly added to the cell lysate to a final concentration of 5% (w/v) followed by the addition of 5 M NaCl to obtain a final concentration of 500 mM, in about half an hour keeping the mixture at 4°C . The mixture was stirred for 2 h and the precipitation was allowed to occur for 12-16 h at 4°C . This suspension was clarified by centrifuging at 4°C and 4,000 rpm ($3,345 \times g$) for 25 min.

3.4.2. Capturing and intermediate purification

The PEG supernatant was added to pre-equilibrated slurry of Aerosil 380 (Evonik, Hanau, Germany) in the binding buffer [25 mM sodium phosphate buffer, pH 7.2, 500 mM NaCl]. To pre-equilibrate, the Aerosil was gently mixed in the binding buffer [0.13 g Aerosil per 1 g wet biomass] and centrifuged at 4,000 rpm ($3,345 \times g$). The supernatant was discarded and the Aerosil pellet was resuspended in the binding buffer (e.g. 10 g + 500 mL buffer). The suspension obtained by mixing the PEG supernatant and the Aerosil pellet was stirred at 4°C and 300 rpm. After 4 hours, the Aerosil suspension was centrifuged at 4°C and 4000 rpm ($3,345 \times g$) for 25 min. The pellet was washed twice using the wash buffer [25 mM phosphate buffer, pH 7.2], resuspended in the elution buffer [50 mM sodium carbonate-bi-carbonate buffer, pH 10.8, 1.2 M urea] and incubated for 12 h at 37°C and 120 rpm. Aerosil eluate (supernatant fraction) was separated from the pellet after centrifugation for 150 min at 25°C and 10,000 rpm ($8664.5 \times g$) and clarified by vacuum-filtration (0.2 μm pore size).

The filtered eluate was stored at 4°C for 24 h to improve stability of HBsAg, a phenomenon often referred to as the aging. Later this eluate was loaded on anionic exchange resin, DEAE Sepharose FF, 20 mL, which was prewashed with 1 M NaOH,

ddH₂O and 25 mM sodium carbonate-bicarbonate buffer, pH 8.0. The self-packed column was washed with and the HBsAg was eluted with elution buffer [50 mM Tris-HCl buffer, pH 8.0, 500 mM NaCl]. The fractions containing HBsAg were pooled and concentrated using ultrafiltration concentrator of 10 kDa cut off (Vivaspin membrane 10,000 MWCO, Sartorius Stedium Biotech GmbH, Germany). The protocol for ion exchange chromatography is reported in the Appendix.

3.4.3. Polishing

The HBsAg concentrate was loaded on pre-equilibrated gel filtration (GF) column [Sephacryl-S300, 26/60, GE healthcare] and eluted with the phosphate buffered saline, pH 7.2 [137 mM NaCl, 2.7 mM KCl, 10 mM Na₂HPO₄, 1.76 mM KH₂PO₄, pH 7.2] at 1 mL/min flow rate. The protocol for size exclusion is described in the Appendix. The fractions containing HBsAg were pooled and treated with KSCN, to a final molarity of 1.2 M, for partial defolding. This mixture was incubated at 100 rpm and 37°C for 5 h in an orbital shaker.

The KSCN treated HBsAg was dialyzed against phosphate buffered saline, pH 7.2 (PBS, pH 7.2) using a membrane of cut-off size of 14 kDa (Cellulose acetate membrane, Visking, Carl-Roth, Karlsruhe). The purified VLPs were filter-sterilized (0.2 µm pore size) and stored at 4°C.

3.5. General analytical methods for HBsAg estimation

In this part of the experimental work, several analytical techniques were used to evaluate the purified HBsAg VLPs. Later, different steps during the downstream processing were probed to find out the crucial stages for VLP assembly and this was performed by electron microscopy.

3.5.1. SDS-PAGE analysis

Samples collected during the time points of cultivation were lysed with glass beads (0.45 mm; Sigma G-8772) by vortexing 8 times and incubating on ice successively. The lysates were boiled with equal volume of the sample buffer [10 mM Tris-HCl, pH 6.8, 1 mM EDTA, 2.5% (w/v) SDS, 0.2% Bromophenol blue, 45% (v/v) β-mercaptoethanol, 5% (v/v) glycerol], vortexed for 1 min and boiled for 10 min at 95°C. 10 µL of each sample was loaded per well on a 12% SDS-polyacrylamide gel.

The gel was stained overnight with the colloidal coomassie [95]. Silver staining was performed to examine the purity of final product.

3.5.2. Western blot

The cell lysate was analyzed via Western blot to verify the presence of HBsAg. The sample was electro-transferred from SDS-PAGE to equilibrated PVDF membrane for 30 minutes. The transfer was verified by the prestained kaleidoscope marker. The membrane was fixed in the blocking buffer and incubated with the primary antibody for 1 h. A mouse monoclonal anti-HBsAg antibody was used which is linear epitope specific. This blot was incubated for 1 h with goat-anti mouse secondary antibody and later developed using insoluble TMB substrate (Sigma-Aldrich, Germany). The reaction was stopped after visualization of bands by washing the membrane in ddH₂O, for two to four times.

3.5.3. ELISA analysis

The samples taken from different time points during the cultivation and after the purification were analyzed for the estimation of soluble HBsAg by ELISA kit (Hepanostika micro ELISA, bioMérieux France). Cell pellets of the samples collected at time points during the cultivation with OD₆₀₀ = 100 were lysed using a lysis buffer containing Tween 20 (Polysorbate) to a final concentration of 0.6% (v/v). All the samples were diluted appropriately with PBS, pH 7.2 and the antibody specific for an epitope between the amino acids 175-186 of S protein (present outside the so called a-determinant region) was used to bind the antigen [96]. According to the manufacturer's instruction, 100 µL of each controls, positive and negative, and samples at appropriate dilutions were loaded on the ELISA plate and incubated at 37°C for 1 h. 50 µL of the conjugate was added to the above and incubated at 37°C for 1 h. Washed the wells 6 times with PBS, added 100 µL of substrate (Urea Peroxide + H₂O₂) and incubated at RT for 30 min. An HRP labeled anti-HBs conjugate was used to develop the signal. 100 µL of 1 M H₂SO₄ was added as stopper and the plate was scanned at 450 nm.

3.5.4. Protein concentration estimation

Total protein contents were estimated by Pierce bicinchoninic acid (BCA) method (Pierce BCA protein Assay kit, Thermo Fisher Scientific). For pure HBsAg samples, as indicated by the SDS-PAGE, the concentration was estimated by measuring the

absorbance at 280 nm by using $\epsilon = 3.2 \text{ M}^{-1} \text{ cm}^{-1}$ (<http://web.expasy.org/protparam/>). All protein determinations were performed in triplicates.

3.5.5. RP-HPLC analysis

The HBsAg in crude cell lysate was quantitatively measured via reverse phase-High performance liquid chromatography (RP-HPLC). The lysate was treated with the solubilizing buffer, 8% (w/v) SDS, 50% (v/v) β -mercaptoethanol, 1 M DTT [97]. The RP-HPLC protocol is given in the Appendix.

3.6. Electron microscopic analysis

In order to confirm the presence of VLPs, initially, and later for the characterization, electron microscope techniques were used.

3.6.1. Scanning electron microscopy (SEM) protocol

Scanning electron microscopy (FEI Quanta 200, EDAX XL 30) was used to obtain images of purified HBsAg. Pure HBsAg (0.8 mg/mL) in PBS, pH 7.2, was used to prepare the grids. The grid was allowed to dry out overnight at room temperature and at next day was observed by SEM.

3.6.2. Transmission electron microscopy (TEM) protocol

The samples after downstream processing were analyzed using the energy-filtered transmission electron microscope Libra 120 (Zeiss, Oberkochen, Germany). Purified HBsAg VLPs were diluted with PBS, pH 7.2 to an appropriate protein concentration (0.2 mg/mL), adsorbed for 1 minute to a glow-discharged CFormvar foil and negatively stained with 2% (w/v) uranylacetate, pH 4.5. The zero-loss images, under the surveyance of realtime FFT (iTEM software, OSIS, Münster, Germany), were taken with a 2048 \times 2048 CCD camera (Tröndle, Moorenweis, Germany) using a slit-width of 15 eV and an objective aperture of 60 μm . The samples collected during the downstream processing were diluted to a suitable dilution (0.2 – 0.5 mg/mL) and images were recorded as described above.

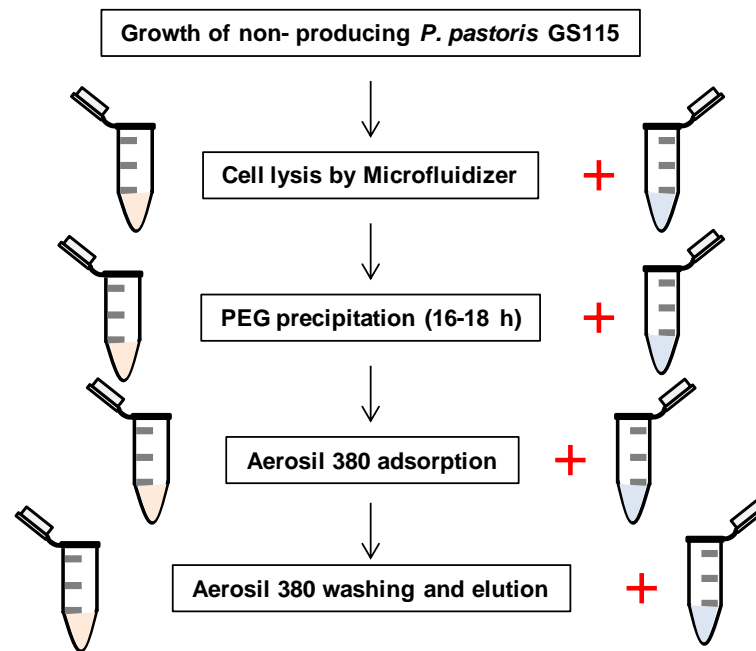


Figure 3.2. The scheme for control experiments to monitor the effect of collective background on HBsAg VLP assembly. In control-1 (left hand side), *P. pastoris* GS115 cells were lysed via Microfluidizer and the lysate was treated for purification process in same way as the routine purification procedure. In control-2 (right hand side), the *P. pastoris* GS115 samples collected at each step during control-2 were supplemented with HBsAg VLPs and allowed to stand overnight at 4°C.

For monitoring the background structures and effect of the milieu on VLP morphology, five control experiments were carried out. *P. pastoris* GS115 cells (non-producing) were grown in defined media and the lysate was treated in the same way as the purification process of HBsAg-producing *P. pastoris* cell lysate. The samples collected at each point were named as control-1 (Figure 3.2, left hand side). In a parallel control, the purified VLPs were added in samples from *P. pastoris* GS115 lysate during control-1 and were incubated at 4°C for 24 h (Figure 3.2, right hand side). These samples were taken as control-2 and the TEM images were captured. The samples in control-2 experiment were supplemented with purified VLPs according to the percent contents of HBsAg in initial four steps of routine downstream process. For example in the producing cell lysate, 11 % of the total protein contents is HBsAg, so in the corresponding control-1 sample, purified VLPs were added to obtain 11 % HBsAg concentration. Finally, all the samples (control-1 and control-2) were diluted to get the total protein concentration of 0.2 mg/mL.

Same procedure was applied to investigate the effect of purification buffers pertaining to initial four steps (control-3), with a parallel control in storage buffer, PBS, pH 7.2

(control-4). Before acquiring the TEM images, the samples were diluted to appropriate concentration (ranging from 0.2 mg/mL to 0.5 mg/mL).

For the concluding control experiments, the cells were lysed in the routine lysis buffer as well as in the absence of all constituents one by one. Lysis buffer contains 25 mM PB, pH 8.0; 5 mM EDTA and 0.6% Tween 20. The resulting control lysate samples were used in TEM analysis, with a final protein concentration of 0.5 mg/mL. These control lysis (CL) samples are denoted as CL-1, CL-2, CL-3 and CL-4, hereafter. The outline of control-5 is explained in the figure 3.3.

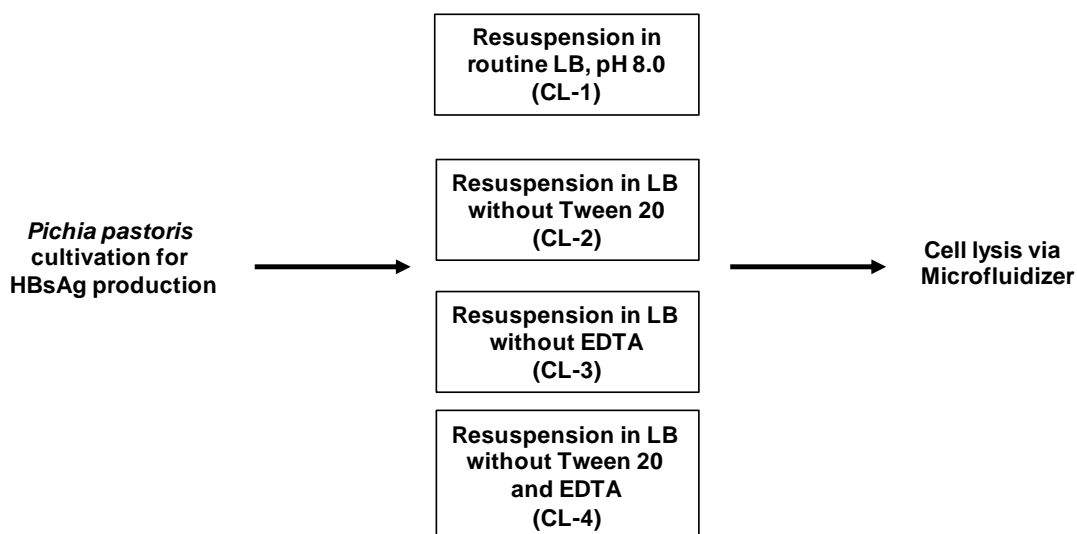


Figure 3.3. Outline of the control experiment for the effect of Tween 20 and EDTA. Here, LB stands for the lysis buffer. The control lysate samples are referred to as CL-1, CL-2, CL-3 and CL-4.

For all the TEM analyses, samples were stored at 4°C, and analyzed not later than one week.

3.6.3. Image processing for TEM

TEM images were analyzed to measure average VLP size (diameter) and VLP count. An in-house software (Graphic analyzer, Patrick Lindner, TCI, Leibniz University of Hannover), was used to measure the average diameter and count of purified HBsAg VLPs. The detailed protocol is described in the Appendix. For more complicated samples, containing host cell components or VLP agglomerates, the VLP count was estimated via ImageJ [98]. The detailed protocol can be found in the Appendix.

3.7. Fluorescence spectroscopy for stability experiments

The structural stability of HBsAg VLPs as a function of the concentration of denaturing agent was monitored by observing the fluorescence properties, both intrinsic as well as extrinsic.

3.7.1. Intrinsic fluorescence measurements

The fluorescence emission spectra were obtained employing LS 50B Luminescence spectrophotometer with Xenon discharge lamp as light source (PerkinElmer Ltd., United Kingdom). The samples were diluted to a concentration of 2 μM HBsAg VLP and excited at 280 nm. The resulting intrinsic extrinsic spectra were recorded using single scan mode (a cumulative average of 10 measurements) between 300-450 nm. The slit width for both excitation and emission measurements was kept at 5 nm. Temperature was kept constant at 25°C by using circulating water bath (Frigomix R, B. Braun Biotech International, Germany).

3.7.2. Extrinsic fluorescence measurements

The extrinsic fluorescence measurements were performed similar to the intrinsic fluorescence. The samples were excited at 400 nm and spectra were scanned between 430-550 nm. The rest of parameters were kept the same. Bis-ANS (4,4'-Dianilino-1,1'-binaphthyl-5,5'-disulfonic acid, Sigma-Aldrich) was used to bind with hydrophobic sites of HBsAg VLPs. Following concentration of HBsAg (with respect to VLP) was used for the formation of complex.

2 μM HBsAg : 20 μM Bis-ANS

A stock solution of 1 mM bis-ANS in DMSO was prepared and stored in dark at room temperature. The final concentration of bis-ANS was determined by measuring the extinction coefficient $\epsilon_{360\text{nm}}=23,000 \text{ cm}^{-1}\text{M}^{-1}$.

3.7.3. Defolding studies via fluorescence spectroscopy

Defolding series was performed with three denaturing salts, namely, guanidine thiocyanate (GdnSCN), potassium thiocyanate (KSCN) and guanidine hydrochloride (GdnHCl). For intrinsic denaturing measurements, stock solution of pure HBsAg VLPs

[0.8 mg/mL i.e., 30 μ M] was treated with series of chaotropic salts (GdnSCN, KSCN and GdnHCl) to obtain a final concentration of 0.2 μ M and allowed to stand at 25°C for 3 min. The sample were excited at 280 nm and then scanned for the fluorescence.

For denaturing measurements using extrinsic fluorescence properties, the purified HBsAg (2 μ M) was mixed with bis-ANS (20 μ M) and left for at least 10 min. The complex (HBsAg.bis-ANS) was then mixed with chaotropic salts (series of GdnSCN, KSCN and GdnHCl), allowed to stand for incubation and scanned after being excited at 400 nm. The preliminary experiments showed that the trend in defolding curve remains the same after 3 min and 24 h, therefore rest of the measurements were done with 3 min incubation time.

3.7.4. Data analysis

All the measurements were normalized before being processed for graphical form. For normalization, the fluorescence intensity in absence of any chaotropic agent was taken as the standard and the rest of readings were taken as a ratio with respect to it.

In order to characterize the hydrophobic regions, Stern-Volmer equation was used.

$$F_0/F = 1 + K_{SV} [Q]$$

Equation 3.1: Stern-Volmer relation

Here, F_0 and F are the fluorescence intensities in the absence and presence of quenchers, K_{SV} is the Stern-Volmer quenching constant (M^{-1}) and $[Q]$ is the concentration of the quencher.

All the fluorescence data obtained was normalized by taking a ratio between intrinsic fluorescence value in the absence (F°) and presence (F) of any chaotropic agent.

3.8. VLP determination using the Virus counter

To verify the defolding curves obtained via fluorescence spectroscopy, HBsAg VLPs were analyzed using the virus counter, ViroCyt 2100 (InDevR Inc. USA). Virocyt is a specialized flow cytometer designed specifically for viruses. It works on the same principle as that of flow cytometer and has two photomultiplier tubes (PMT), one for the protein signal and the other for the nucleic acid signal.

One unique feature of flow cytometry is that it measures fluorescence per cell or particle. This contrasts with spectrophotometry in which the percent absorption and transmission of specific wavelengths of light is measured for a bulk volume of sample.

3.8.1. Sample preparation

For the sample preparation, the dye kit from instrument's manufacturer was used. The composition of most of the components of the kit is confidential. The stock solution of HBsAg VLPs consists of 30 μM [0.8 mg/mL] from which a further dilution of 2 μM is being prepared. From initial experiment, it was concluded that a dilution of 1:100 was optimal for measuring the samples. Since for the normal fluorescence measurements, the dilution factor is roughly 15 times, a further dilution of ≈ 6 times is required to get a final dilution of a factor 100.

The HBsAg VLP stock solution was mixed with the denaturant solution (GdnSCN, KSCN) to get a total volume of 60 μL and left for 3 min at 25°C. This mixture was further diluted with 240 μL of SDB (sample dilution buffer) to make the total volume 300 μL and a final concentration of 2 μM HBsAg VLPs. 150 μL of combo dye was added in this final mixture [a 2:1 sample to dye ratio]. The samples were incubated at ambient temperature for at least 30 min in dark prior to analysis.

3.8.2. Measurement protocol for Virus counter

Before starting the measurements, the instrument was validated for cleanliness and performance. First the inter sample wash [ISW] was run followed by cleanliness verification fluid [CVF]. Then the performance validation standard was run to check the performance status. After validation, samples were analyzed using the standard settings i.e., flow rate: $\sim 3700\text{-}6500$ nL/min; Pressure: 15 psi; Threshold for nucleic acid: 0.34 - 0.75 [PMT signal (V)] and for protein 0.57 – 1.76 [PMT signal (V)]

3.9. VLP analysis using dynamic light scattering

The stability of HBsAg VLPs was studied by monitoring of their size as a function of concentration of the chaotropic salts via dynamic light scattering (DLS). The instrument used for this purpose was DynaPro Titan with software Dynamics V6 (Wyatt Technology, Europe). The source of light for illumination is a semiconductor laser beam of ~ 830 nm wavelength.

3.9.1. Sample preparation

The samples were prepared in a similar manner as that for fluorescence studies. The VLP stock solution consists of 10 μM HBsAg VLPs. The stock solution was mixed with dilution series of chaotropic agents (GdnSCN, KSCN, GdnHCl) to give a final concentration of 2 μM HBsAg VLP, allowed to stand for 3 minutes at 25°C and analyzed via the DLS instrument.

3.9.2. Measurement protocol for DLS

The parameters for the DLS measurements are given in the table 1.

Variables	Specification
Acquisition time	5 sec
Acquisition number	30
Cut offs	5,150
Laser intensity	Adjusted accordingly
Model:	Rayleigh sphere
Sample (model)	Globular protein
Temperature	25°C

Table 3.1. The instrument settings applied for DLS measurement of the HBsAg VLPs for the purpose of stability studies.

All the measurements were done in duplicates. During the whole set up, temperature was kept constant at 25°C.

4. Results and discussion

Vaccines, whether prophylactic or therapeutic play an important role in preventing several diseases and hence to enhance the general quality of the living. VLP vaccines being non-infectious and relatively economical are candidate against many illnesses. In this thesis, hepatitis B surface antigen (HBsAg) VLPs are used as the model system to study the *in vitro* self-assembly process. The main goal of this study is to elucidate the mechanism of VLP assembly and to characterize the structure of assembled particles.

In previous sections, the theoretical aspects of the project and experimental methods were described. In this chapter, the final results of performed experiments will be reported. Alongside, these findings will be discussed in details and ultimately concluded in the end. For convenience, the work has been divided into three main sections, namely,

- Production and purification of HBsAg
- TEM analysis during downstream procedure to monitor *in vitro* assembly process
- Stability studies of HBsAg via different analytical techniques

4.1. Production in *Pichia pastoris* GS115 and downstream process of recombinant hepatitis B surface antigen virus-like particles

In the first stage of experimental work, cultivation parameters were optimized to generate HBsAg in the methylotrophic yeast, *Pichia pastoris*. The *P. pastoris* cells were cultivated at different scales to monitor the reproducibility of the system. The cells were lysed and the downstream process was carried out to obtain pure HBsAg VLPs.

4.1.1. Shake flask cultivation

For the preliminary expression tests of HBsAg in *P. pastoris*, defined, semi-defined and complex media were tested at shake flask scale. During all the cultivations, temperature and agitation were kept constant at 30°C and 250 rpm respectively. The

cells were allowed to grow till $OD_{600} = 2-6$ on glycerol as the sole carbon source. The cultures were induced with 0.5% methanol when the stationary phase started. Several samples were collected during the cultivation at regular intervals (e.g., 0 h, 24 h, 48 h, 92 h, and 120 h). During the initial shake flask cultivations, no significant increase in the product yield was observed after 120 h post-induction period. Therefore the later cultures were harvested 120 h after inducing with methanol.

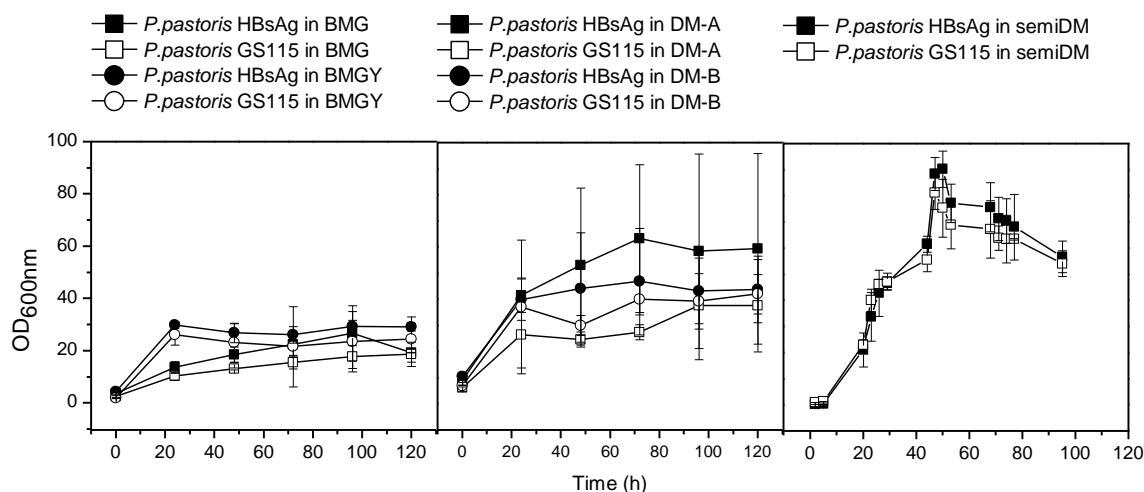


Figure 4.1. Growth curves of the shake flask cultivations for optimization of the HBsAg production. All the cultivations were done at least in triplicate at 30°C and 250 rpm. Left box represents growth curves in complex buffered media, BMG and BMGY. Middle and right box shows growth trend in defined (DM) and semi-defined media (semi-DM), respectively.

A higher growth rate was observed in the semi-defined media as compared to in the defined media, despite of less product expression. The basal salt media (defined media A) showed medium cell density with a growth rate of 0.08 h^{-1} during the exponential phase. In the defined medium, a common problem to cope with was lower pH value. This problem was observed in defined as well as in semi-defined media i.e., from pH 6.0 in the beginning to pH 3-4 towards the end of cultivation. This situation was tried to overcome by adding 25% (v/v) NH_4OH every 24 h, to readjust the pH 6.0, measured by pH strips. On the other hand the complex media, due to presence of a buffer system, maintained pH 6.0 till the harvest.

Surprisingly, the semi-defined media which showed a growth rate of 0.034 h^{-1} during the exponential phase demonstrated least amount of HBsAg expression. In context of expression level, the buffered-minimal glycerol media (BMG) was observed to be most efficient. This may be due to the fact that complex media contain rich nutrient

supplements like peptone and yeast extract which ensure a higher expression of the product.

	BMG	BMGY	DM-A	DM-B	Semi-DM
<i>P. Pastoris</i> HBsAg	0.01	0.01	0.01	0.01	0.04
<i>P. pastoris</i> GS115	0.01	0.01	0.01	0.01	0.03

Table 4.1. Growth rates of *P. pastoris* in different media after the onset of methanol phase.

As a comparison, growth rates during the whole methanol phase are being summarized in table 4.1.

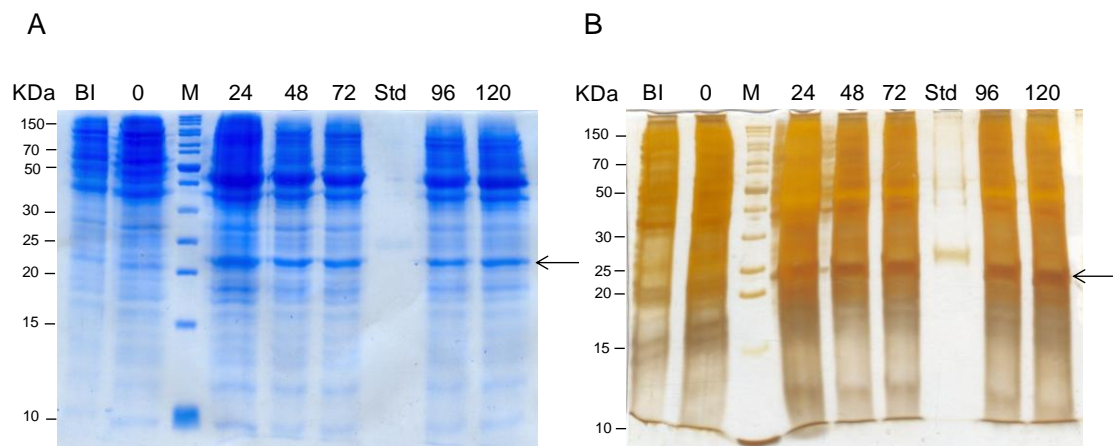


Figure 4.2. SDS-PAGE analysis of HBsAg expression in 1 L cultivation in BMG. The culture was induced with 0.5% MeOH, after every 24 h. Box A and B contain images of the two gels developed with colloidal coomassie and silver staining respectively. Arrows show the HBsAg monomer band.

After comparing all the media for expression, basal salt media (defined media A) was chosen to continue to produce HBsAg in *P. pastoris* at bioreactor level. Basal salt media was chosen because of its reproducibility and in spite being simple its ability to produce HBsAg, under controlled pH. Moreover it contains specific components such as, $\text{MgSO}_4 \cdot 7\text{H}_2\text{O}$ and Yeast Trace Metal elements (YTM), which are important for growth of *P. pastoris* culture.

4.1.2. Bioreactor cultivation

The cells were grown in batch phase using glycerol as the carbon source till $\text{OD}_{600} = 200$. The production phase was started when a sudden increase in dissolved oxygen was observed due to the fact that the cells consumed all the glycerol present in media. At this point, methanol was added to the cultivation as the carbon source. The

methanol concentration required per day for the HBsAg-producing *P. pastoris* cultivation was calculated according to the previous cultivations [93] and YTM containing methanol feed was added manually at each 8 h interval to maintain a level of 6 g/L. The biomass was measured by observing OD₆₀₀ every 2-3 hours before and every 8 h after induction.

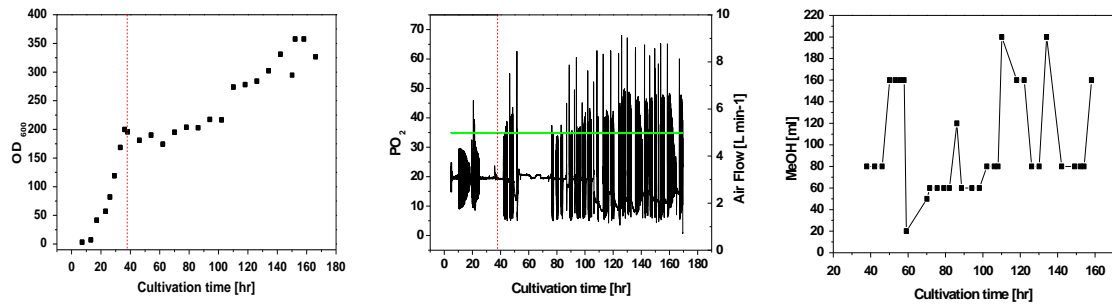


Figure 4.3. *P. pastoris* cultivation before and after induction (separated by the red dotted line) in a 10 L bioreactor. Cascade agitation and continuous air flow (green line) was used to keep the dissolved oxygen level constant. Here methanol was added manually at every 8 h to keep the level at 6 g/L.

The cells were harvested 136 h after induction at OD₆₀₀ \approx 330. The cells were spun down, washed with the phosphate buffer, pH 7.2 and resuspended in the lysis buffer (for recipes, refer to the Appendix). The growth rate (μ) during growth on glycerol and on methanol was recorded as 0.134 h⁻¹ and 0.006 h⁻¹, respectively.

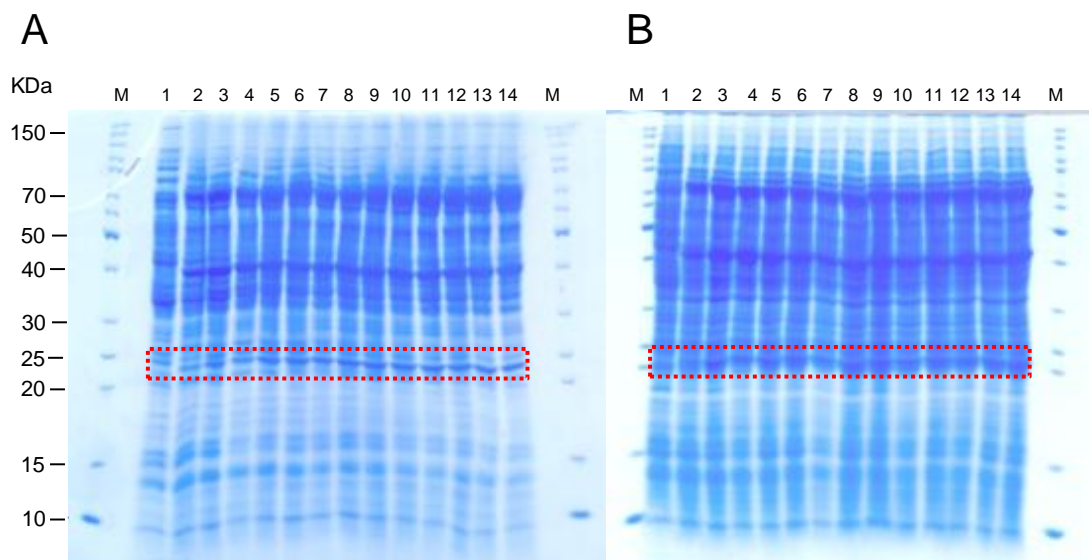


Figure 4.4. SDS-PAGE of the samples collected during the bioreactor cultivation time points. Gel A consists of the soluble fractions whereas gel B of the whole cell lysates. Lane 1 corresponds to the sample taken before induction. Starting from lane 2 to 14, each

sample was collected with 8 h difference. The dotted box indicates monomer band of HBsAg.

The high cell density cultivation of *P. pastoris* was evaluated by examining the samples collected at various time points for the HBsAg expression. The SDS-PAGE of cell lysates shows a significantly high expression of HBsAg, present in form of monomer of 25 kDa and dimer of 48 kDa size (figure 4.4).

4.1.2.1. RP-HPLC

The cell lysate from producing and non-producing cultivations was treated with the solubilizing buffer before analyzing via reverse phase-high performance liquid chromatography (RP-HPLC) to investigate the presence of HBsAg.

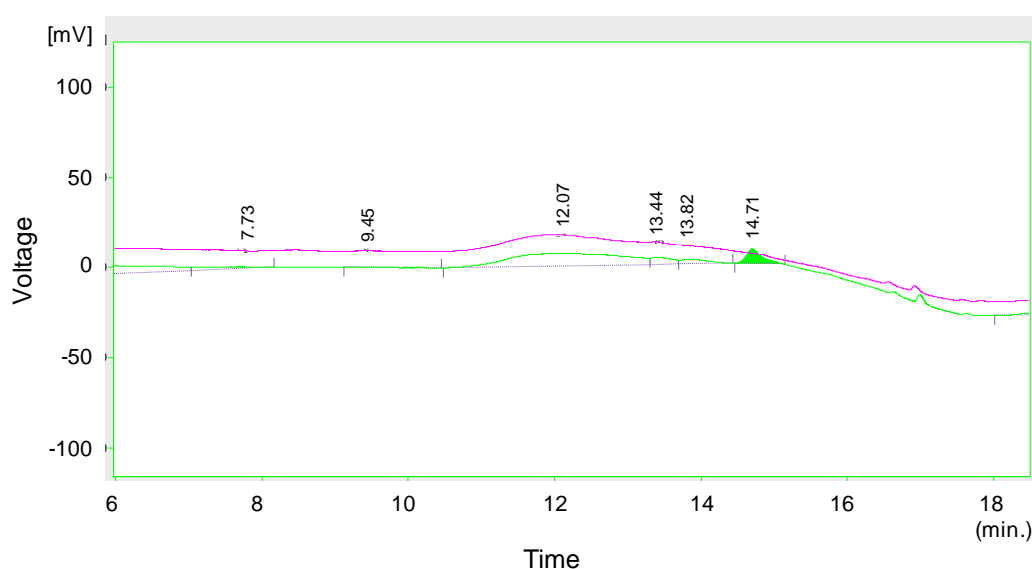


Figure 4.5. Reverse-phase HPLC analysis of HBsAg in the cell lysate, treated with the solubilizing buffer. The pink line represents cell lysate from the non-producing *P. pastoris* GS115 cultivation. The green line represents the HBsAg producing *P. pastoris* GS115 cultivation.

The RP-HPLC results represent total (soluble and insoluble) HBsAg, as the sample was solubilized under denaturing conditions. To analyze the soluble fraction, Western blot and ELISA test were performed.

4.1.2.2. Western blot

The Western blot under reducing conditions was performed to confirm the expression of HBsAg in *P. pastoris* cultivation. A mouse monoclonal anti-HBsAg antibody against HBsAg was used to reveal the respective band. This monoclonal antibody is linear epitope specific for HBsAg (a kind gift from Navin Khanna, ICGEB India).

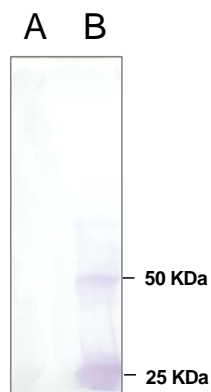


Figure 4.6. The Western blot analysis of *P. pastoris* total cell lysate: Well A consists of the whole cell lysate of non-producing *P. pastoris* GS115 whereas the well B shows lysate from HBsAg producing culture.

The Western blot analysis, of HBsAg-producing *P. pastoris* cell lysate (with non-producing *P. pastoris* cell lysate as a negative control), confirms the presence of HBsAg. The band for subunit dimer indicates the presence of disulfide bonds which are prerequisite for the VLP assembly.

4.1.2.3. ELISA analysis

The antigenicity of HBsAg was tested by ELISA. The soluble HBsAg in cell lysate (biomass = 100 OD₆₀₀) was analyzed by ELISA kit. All the samples were diluted by factor of 1000-2000 with PBS, pH 7.2.

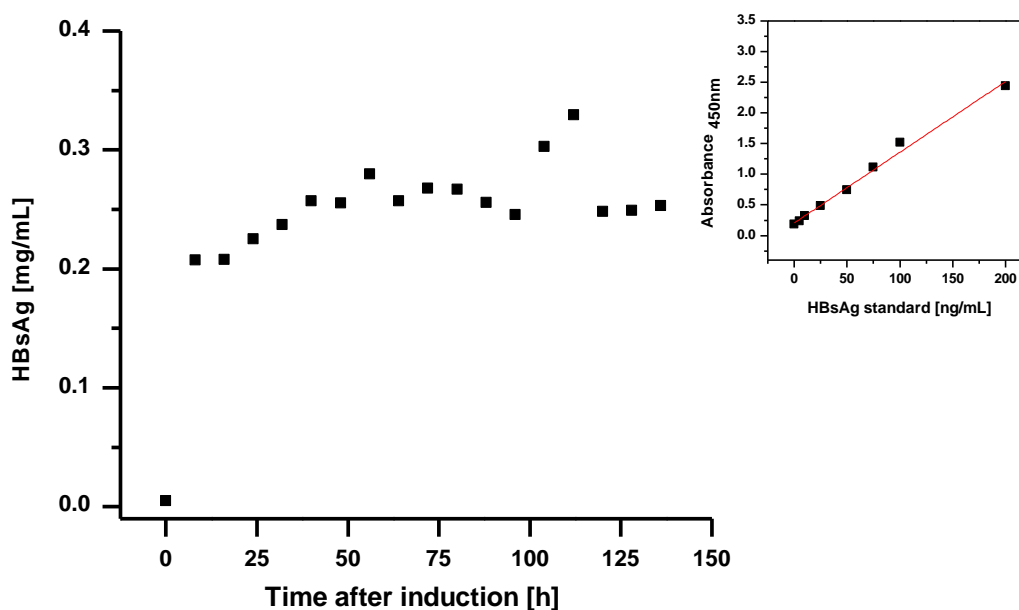


Figure 4.7. ELISA test of HBsAg in cell lysates. Soluble HBsAg contents from samples collected at cultivation time points after the induction phase are shown (OD_{600nm}=100). In the inset, HBsAg standard curve to quantify the soluble protein contents is shown.

According to ELISA result, the presence of HBsAg is observed from 8 hours after the induction phase of cultivation. The amount of HBsAg per 100 OD of cell pellet does not increase extensively (Figure 4.7), although, an effective increase in protein concentration is observed due to increase in total biomass (Figure 4.3).

4.1.3. Downstream processing of HBsAg

Downstream processing is arguably the most important part of a production method. Each step leads to higher purity of the desired product but at the same time a loss in the yield. A compromise ought to be made between the required purity and the obtained yield. In general, the downstream process for all the yeast derived HBsAg consists of similar procedure. The cells, after the lysis, are processed with multiple chromatographic steps and finally polished to proceed for the morphological analysis.

4.1.3.1. PEG precipitation

The cells after cultivation were spun down, washed with the phosphate buffer, pH 7.2 and 100 g biomass was resuspended in lysis buffer (for recipe, refer to the Appendix). The lysis was performed via Microfluidizer, using 12,000 psi pressure and 12-14 cycles. The crude whole cell lysate was subjected to PEG precipitation in the presence of high salt concentration. All the hydrophilic proteins were precipitated (a phenomenon known as salting out) as a result of PEG addition. Unlike typical PEG precipitation, here the supernatant contains the product of interest. The presence of at least 500 mM NaCl has been suggested as vital for the efficiency of sedimentation. About 5% (w/v) or more PEG helps also to get rid of DNA by co-precipitating it [99]. The mechanism of PEG precipitation is not fully understood. It has been proposed that the process of precipitation occurs as a result of displacement of precipitant from the solution and consequently salting out [100].

4.1.3.2. Adsorption on Aerosil 380

After PEG precipitation, the resulting supernatant was adsorbed on the fumed silica, Aerosil 380. The principle involved in the purification based on hydrophobic interaction forces is that hydrophobic part of a protein binds to the hydrophobic stationary phase. In this work, Aerosil 380 has been used as the capturing material onto which the proteins adsorb according to their hydrophobicity. The non-adsorbed contents, called as Aerosil flow through, were discarded. Further contaminants were

removed with washing steps and the proteins were desorbed from Aerosil in the urea containing elution buffer. The Aerosil eluate was filtered (0.2 μm pore size) to make sure the complete removal of silica particles. The eluate was stored at 4°C for 24 h for aging purpose which renders stability to HBsAg and was later loaded on DEAE resin.

4.1.3.3. Ion exchange chromatography

150 ml of the Aerosil eluate (0.88 mg/mL), after aging, was proceeded for the anionic exchange chromatography. Here a self-packed column of FF Sepharose resin (≈ 20 mL CV) was used for the chromatography. This step removed essentially the host system contaminants and the remaining silica particles, if any. For pooling, only those fractions were selected which contained bands corresponding to the HBsAg mono- and dimer. The protocol for size exclusion chromatography of HBsAg is described in the Appendix.

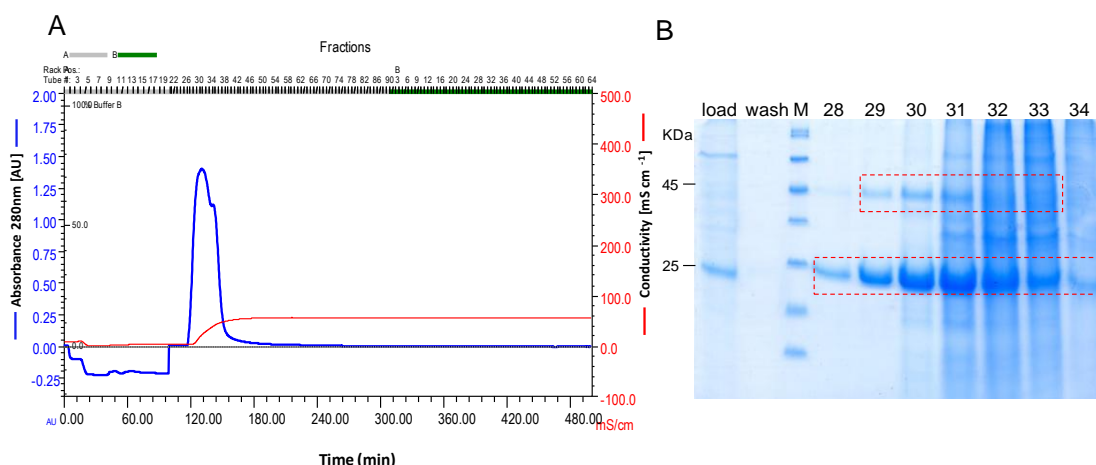


Figure 4.8. Ion exchange chromatography profile of Aerosil eluate using DEAE Sepharose FF ion exchange beads (A). SDS-PAGE of fractions corresponding to the peak is shown in the panel B. Here “load” correspond to the sample loaded on the IEX resin.

At the end of ion exchange chromatography, relatively concentrated protein sample is obtained because of binding on the anionic exchange resin and efficiently narrow elution with 500 mM NaCl. However pooling of all the fractions, belonging to the HBsAg peak, gives a low concentration of final sample (Figure 4.10, lane 8).

4.1.3.4. Size exclusion chromatography

Since size exclusion chromatography has a dilution effect on the protein fractions, the pooled sample from IEX was concentration using ultrafiltration concentrator column (Vivaspin membrane 10,000 MWCO). 15 mL of this concentrated pooled fraction

(4.26 mg/mL) obtained after anion exchange chromatography was loaded on the gel filtration (GF) column to separate well-defined VLPs from the aggregates. Phosphate buffered saline (PBS), pH 7.2 was used as the mobile phase. It is known that, due to their large size, the HBsAg VLPs appear within 20% of void volume whereas the aggregates, along with other host cell proteins, show up later as a second peak or as a tailing (Figure 4.9), depending essentially on the separation efficiency of stationary phase. The protocol for size exclusion chromatography is given in the Appendix.

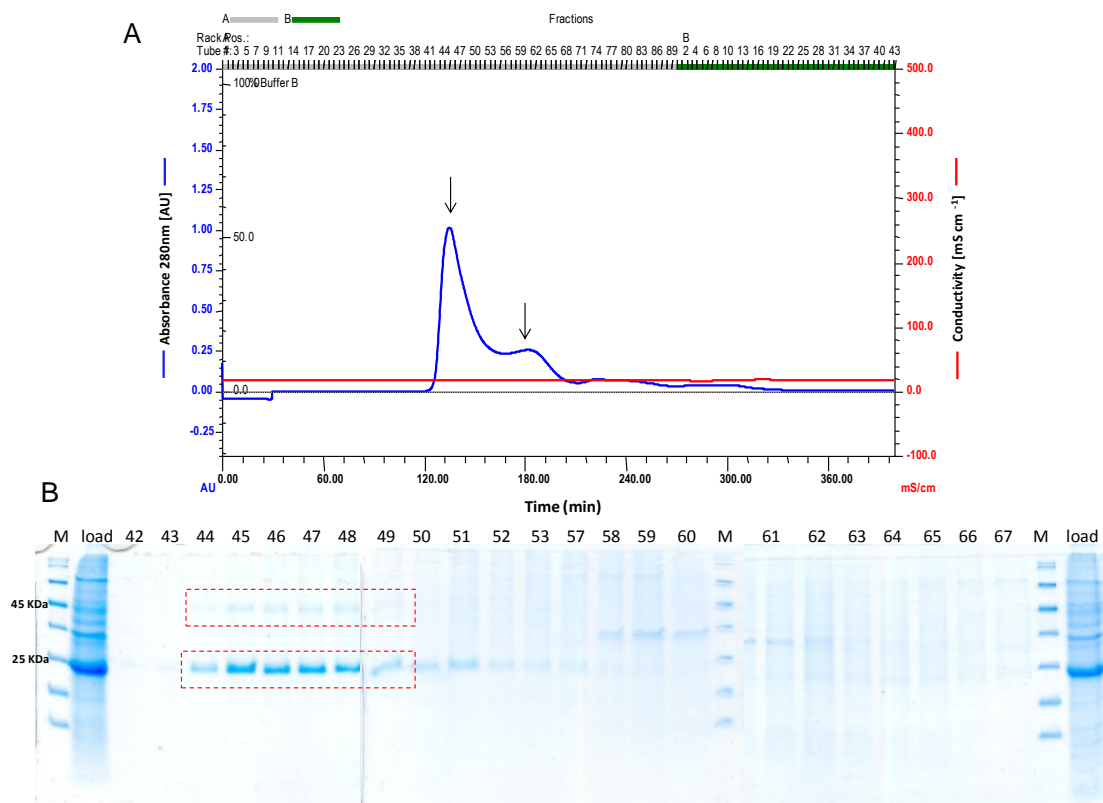


Figure 4.9. The purification step of HBsAg via size exclusion chromatography. (A) The peak appearing in 20 % void volume correlates to the HBsAg VLPs. The tailing of the peak belongs to non-VLP form and *P. pastoris* proteins. Lower panel (B) shows SDS-PAGE of corresponding fractions stained with the colloidal coomassie.

The GF fractions including mono- and dimer bands were pooled to process further. The pooled fractions were concentrated using the ultrafiltration concentrator column (Vivaspin membrane 10,000 MWCO, Sartorius Stedium Biotech GmbH, Germany). After the gel filtration step, a significantly pure protein is obtained (Figure 4.10).

4.1.3.5. KSCN treatment

The fractions corresponding to the HBsAg VLPs were collected and the pool was treated with KSCN to a final molarity of 1.2 M. Treatment of the purified protein with

KSCN is reported to improve the tertiary structure by increasing the disulfide bonding [101]. Zhao *et al.* has reported that an increase in the antigenicity of HBsAg VLPs, after the KSCN treatment, has been observed due to increased cross-linking, which is a result of the rearrangement in the mis-matched disulfide bonds [86].

To remove the KSCN and other salts, the purified HBsAg was dialyzed against PBS, pH 7.2 at least thrice with ≥ 900 times volume of the purified sample to be dialyzed. Finally the purified product was collected and further analyzed.

The presence of HBsAg was verified by the ELISA and purity by 12 % SDS-PAGE under the denaturing conditions (Figure 4.10-B). Two bands corresponding to the mono- and dimer were observed around 25 and 50 kDa respectively. Even the presence of SDS and β -Mercaptoethanol was not able to break all the disulfide bonds, explaining the presence of a dimer band around 50 kDa in SDS-PAGE analyses (Figure 4.10).

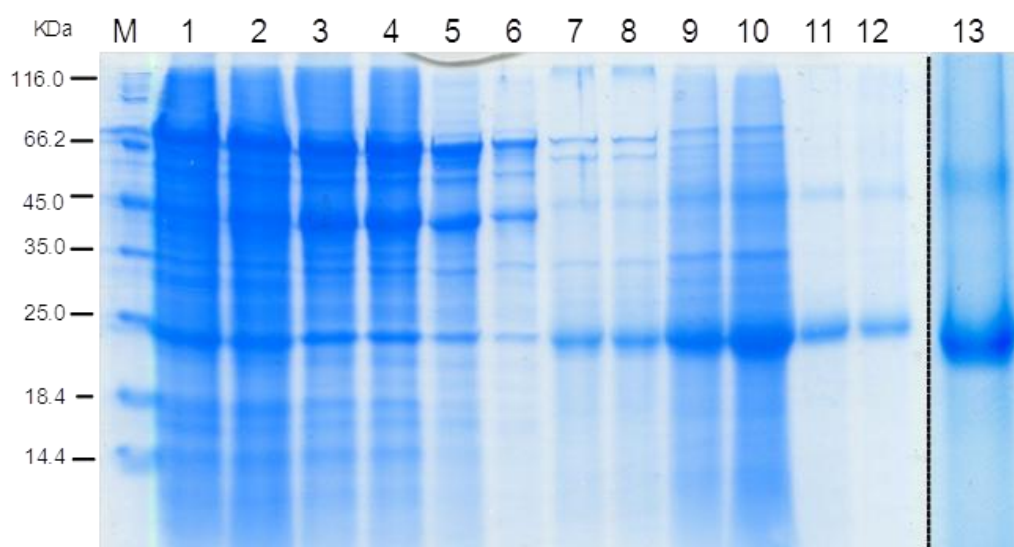


Figure 4.10. SDS-PAGE of the samples collected during the entire downstream procedure. 1: Whole cell lysate; 2: Soluble fraction of cell lysate; 3: PEG supernatant; 4: Aerosil flow through (unbound fraction); 5: Aerosil wash 1; 6: Aerosil wash 2; 7: Aerosil eluate; 8: DEAE load; 9: DEAE pool (collective fractions of HBsAg containing peak); 10: GF load; 11: GF pool (of HBsAg containing fractions); 12: purified HBsAg after KSCN treatment. Lane 13 shows the purified product 5X concentrated, showing bands for mono- and dimeric form. Note that the first sample was diluted 3X and next three 2X with the sample buffer. The gel was stained overnight with the colloidal coomassie dye.

The purity of product can be observed in the SDS-PAGE where 5 times concentrated sample was loaded (Figure 4.10, lane 13).

4.1.4. Protein concentration

The extent of HBsAg purity increases considerably after each step of the downstream process. The step by step proportion between the contaminants and the product was calculated via densitometry. These figures are shown in the percentage (Figure 4.11, panel A).

Protein estimation during the downstream process depicts in average 30% loss of the product during the initial steps i.e. PEG precipitation and treatment with Aerosil (Figure 4.8). Overall, 1-2 percent of the total HBsAg could be recovered by the end of the purification process (Figure 4.11, panel B).

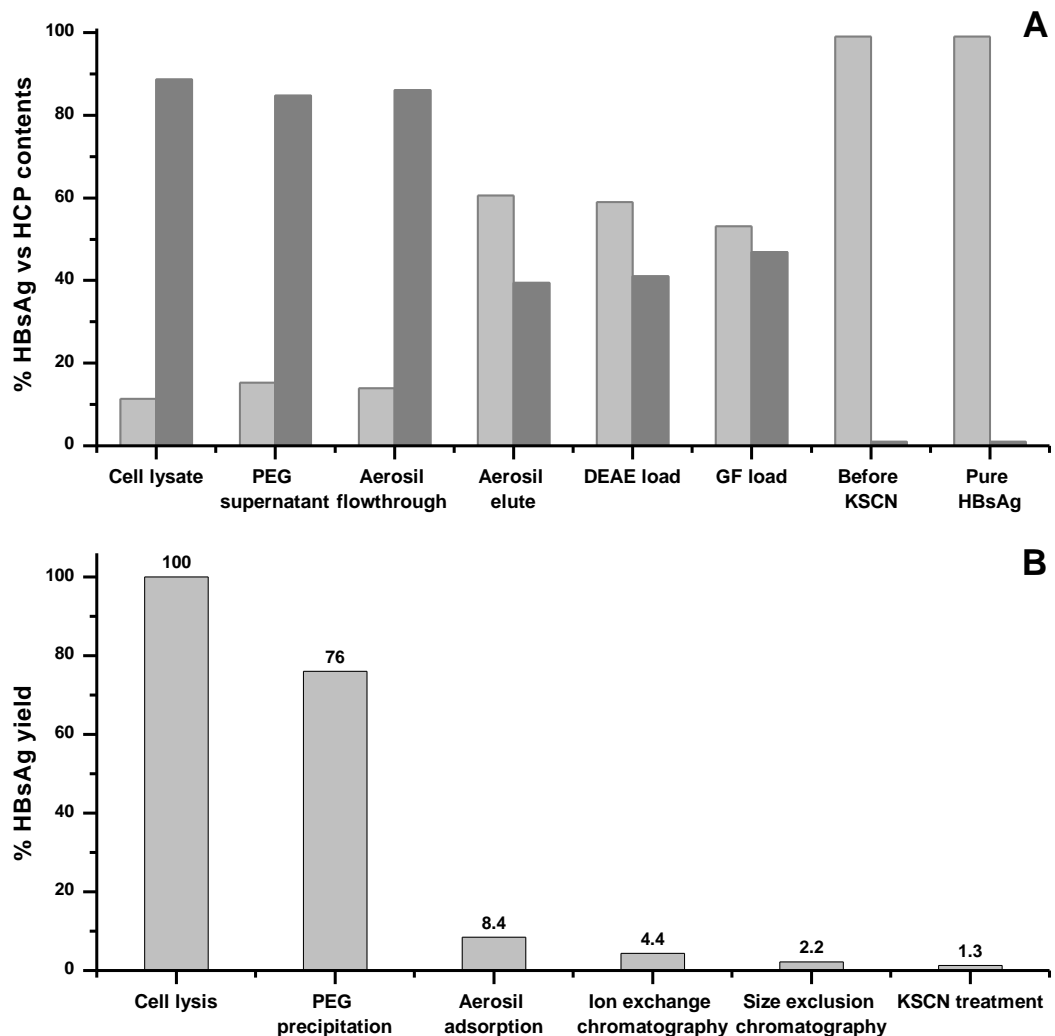


Figure 4.11: Summary of the downstream process in terms of protein contents and HBsAg purity. In upper panel (A), the graph corresponds to the percentage ratio between product and contaminants contents. The black bars represent host cell proteins (HCPs) and the grey bars stand for the total HBsAg. The last bars show the purity of final product. In lower panel (B), the percent yield of HBsAg after the major purification steps is shown. Notice the major loss during PEG precipitation and Aerosil adsorption.

The concentrations of purified HBsAg via BCA assay and ELISA are 0.25 mg/mL and 0.28 mg/mL respectively. The final yield of HBsAg per preparative process is 12.5 mg (per 100 g biomass as the starting material).

4.1.5. Electron microscopy of HBsAg

The purified product was analyzed via scanning as well as transmission electron microscopy. No VLPs could be visualized via scanning electron microscopy (data not shown). This could be due to the fact that during the drying process before mounting, the VLPs may lose their structure. The results from TEM measurement were more promising as they not only showed the presence of VLP but also paved a way for further analysis. The results from TEM studies of HBsAg VLPs are discussed comprehensively in the coming section of this chapter.

4.1.6. Conclusion

In this section, the production and purification of HBsAg was described. It was observed by the SDS-PAGE analysis that the expression increases many fold while upscaling from shake flask to the bioreactor scale. HBsAg was produced in *P. pastoris* in a 10 L bioreactor using the defined medium. In purification process, most of the host cell components were removed during Aerosil adsorption step and anion exchange chromatography. The final yield of pure HBsAg is 12.5 mg/100 g WCW.

The data from densitometry suggests that out of the total expressed proteins, 11 percent is HBsAg. From this HBsAg, the major part is lost during PEG precipitation and Aerosil adsorption. The greatest loss is observed during the Aerosil treatment where more than 60% product is lost.

The purified product was examined via SDS-PAGE, Western blot and ultimately TEM. SDS-PAGE shows the presence of HBsAg but not necessarily the VLPs. Western blot confirms the correct conformation of HBsAg but still does not prove the presence of VLP. The routine analytical techniques have a limitation to distinguish between single subunit and a VLP, therefore the most reliable method to verify the presence of VLPs is visualization by TEM. SEM could not examine the VLPS due to the nature of sample immobilization protocol.

4.2. Insight into the *in vitro* assembly process during downstream processing via TEM using HBsAg virus-like particles as a model case

In the field of virology, electron microscopy (EM) has been the most prominent and pivotal technique. Developed in 1931, it gained popularity quickly pertaining to its applicability and versatility. Formerly, it was not possible to view the viruses with conventional microscopes. Transmission electron microscope (TEM) was the initial type of electron microscopy where the electron beam is transmitted through the thin preparation of sample. On the other hand, in scanning electron microscopy (SEM), the secondary electrons are used to generate the image. These are actually the emitted electrons after the striking of electron beam on the surface of object.

With the magnification as high as 40,000 times, TEM provides the opportunity to actually visualize the viruses as well as proteins of the size up to 1 nm. There is no requirement of specialized or individualized staining techniques for each specimen. Usually the sample immobilized on the grid can be kept for years and is good to analyze even later. Apart from the diagnostics, TEM is also useful in the viral replication and assembly studies. In recent decades, EM has proved to be the key tool in the ultra-structural study of VLPs.

4.2.1. TEM analysis of purified product

In previous part, the cultivation of HBsAg producing *P. pastoris* GS115 cells and the downstream processing of biomass to obtain the purified product was described. The efficiency of purification was evaluated by analyzing the electron micrographs for the presence of VLPs. In general, the final purified product was observed to have no structures other than VLPs (Figure 4.12).

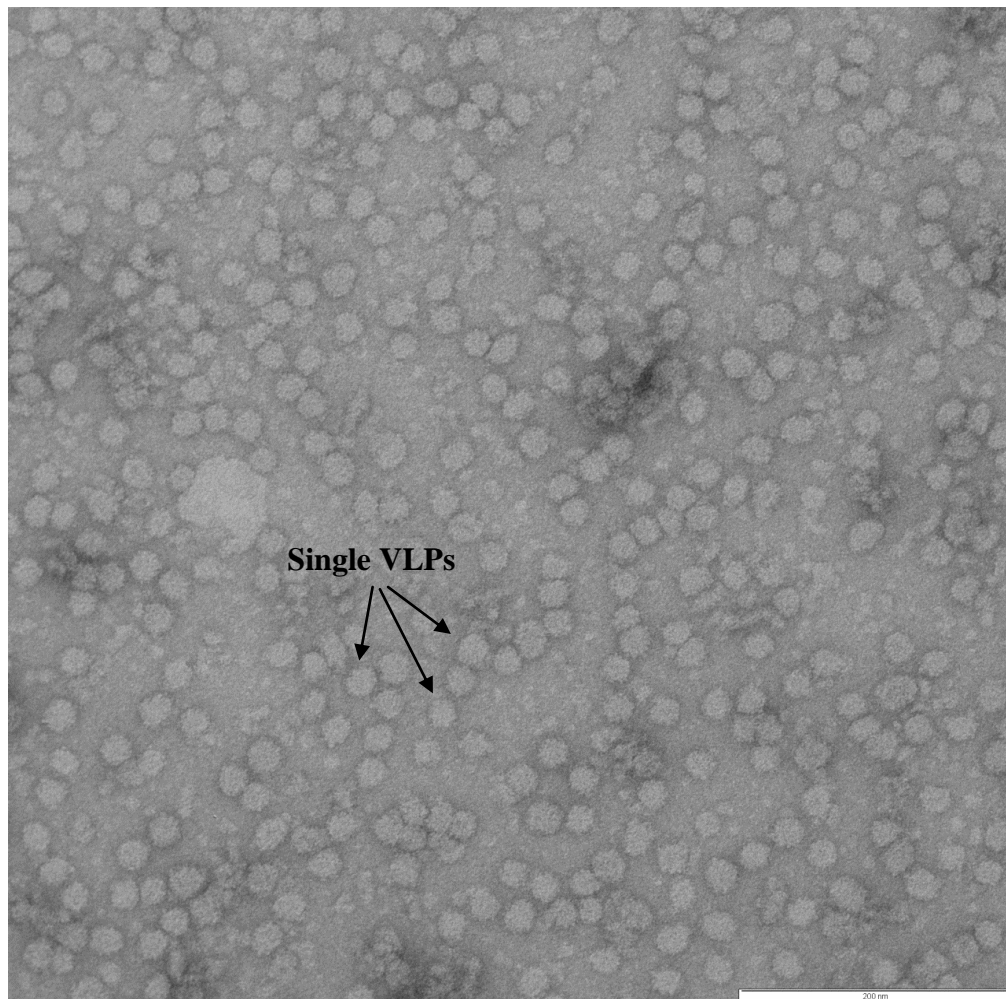


Figure 4.12. TEM image of the pure HBsAg VLPs after the downstream process. The VLPs were stored in PBS, pH 7.2 and later negatively stained with the 2% (w/v) uranyl acetate, pH 4.5.

HBsAg VLPs of an average size (diameter) of 22 nm were observed in the purified sample (Figure 4.12). In this part of the work, numerous samples were collected during the crucial steps of purification procedure and their TEM images were captured for the VLP size and count estimation.

4.2.2. Probing through downstream process via TEM

As reported by Lünsdorf *et al*, VLPs are not present during the production stage inside the *P. pastoris* cells [75]. In this part, several steps throughout the purification procedure were probed for the VLP presence. Samples were collected at each step and analyzed via TEM. The stepwise layout of the purification protocol and corresponding TEM images are shown in the figure 4.13. As observed in the images, the steps in red

box do not show VLPs, except the last step i.e. Aerosil elution. The steps encircled in green box do show VLP occurrence, with the quality being improved progressively.

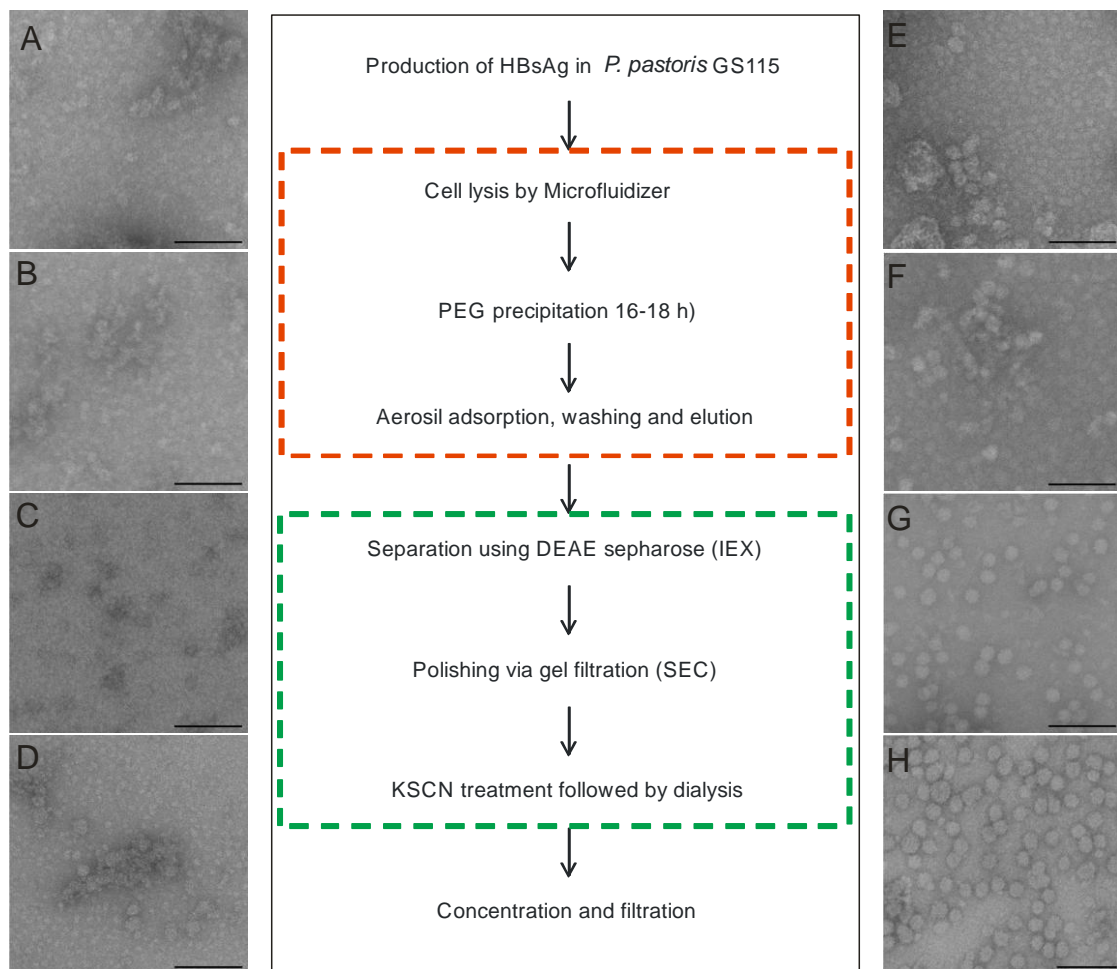


Figure 4.13. A flow-sheet illustration of the HBsAg purification. The steps encircled in the red exhibit no or very few VLPs while the ones in the green do. A: Crude cell lysate; B: PEG supernatant; C: PEG supernatant adsorbed on Aerosil; D: Aerosil eluate; E: DEAE load; F: GF load; G: GF pool before KSCN treatment; H: HBsAg VLPs after KSCN treatment. Scale bar = 100 nm

As described previously, there are no or negligible VLPs observed in the initial steps of purification (Figure 4.13, A-C). They appear for the first time in reasonable amount after the Aerosil elution step. Although the VLP count increases drastically after ion exchange chromatography, few contaminants are still observable until the size exclusion step.

It was observed that in the middle steps (during Aerosil elution and IEX chromatography), though present in significant number, the VLPs tended to stick together in the form of clumps rather than single independent particle which portrays the hydrophobicity of immature VLPs. Moreover the VLPs possess better structure

definition towards the end of purification, especially after the KSCN treatment (Figure 4.13, E-H).

4.2.2.1. VLP size

The size of VLPs during different steps of the downstream processing was investigated via Graphic analyzer. The average diameter (hydrodynamic) observed for the HBsAg VLPs was 22 nm \pm 2. The small deviation might be due to the fact that depending on the solvent, the hydrodynamic radius can differ from radius of gyration [84].

The size of VLPs remains more or less the same irrespective of their count during different steps. However, it is observed that the VLPs improve their uniformity in the size and geometry during the course of purification. In general, the VLPs observed in the initial stages, are less consistent in octahedral geometry. On the contrary, the VLPs obtained after the polishing step are more precise in their construction and their structure compactness, developed due to increased disulfide bonding, can be noticed in the TEM images.

4.2.2.2. VLP morphology

The shape and appearance of VLPs distinctly becomes improved and homogenous during the course of purification as the inter-subunit interactions are increased due to higher HBsAg purity and removal of detergent and denaturing components. The trend from clumping together to the single well-defined VLPs can be observed in the TEM images (Figure 4.13). The control experiment (Control 2 and 3) showed that even the good quality VLPs (from optimized purification protocol) tend to lose their structure when put under relevant milieu i.e. consisting of the HCCs and certain constituents in the buffer system such as Tween 20, EDTA and urea.

In coming lines, the effect of various milieu factors on the morphology as well as count of the VLPs will be discussed comprehensively. For monitoring these factors, control experiments were performed, whose details can be found in chapter 3, section TEM protocol. For convenience these control experiments are stated here shortly. As standard, the samples from routine downstream process were examined via TEM. For background structures, GS115 cell lysate was treated with same protocol as that of routine HBsAg purification and the samples from this process were introduced with

purified HBsAg VLPs. These experiments were denoted as control-1 and control-2, respectively. The experiments pertaining to incubation of purified VLPs in purification buffer (for initial four purification steps) and storage buffer (PBS, pH 7.2) were named as control-3 and control-4, respectively. Lysis tests in various combinations of the lysis buffer components were called control-5.

4.2.3. Control experiments for TEM background

Several peculiar membranous structures were observed in the samples taken during the initial steps of downstream processing. Mostly, these structures have a cup-shaped appearance with a double membrane (Figure 4.14). To investigate whether these structures are arriving from HBsAg or not, positive and negative control experiments were performed. In control-1 experiment, non-producing *P. pastoris* GS115 cells were lysed and handled according to the routine purification protocol of HBsAg.

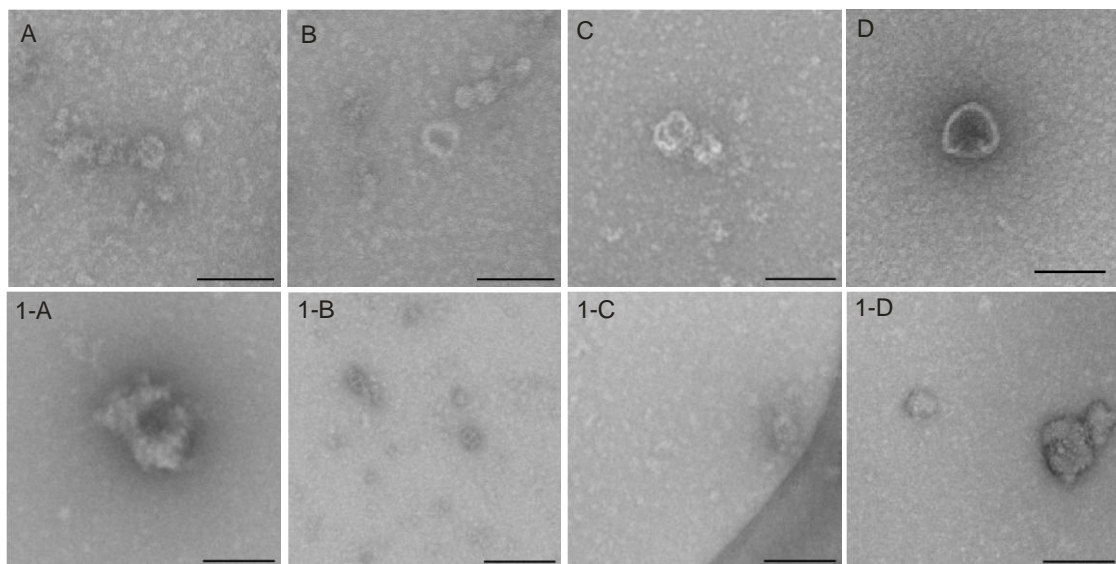


Figure 4.14. Electron micrographs of samples corresponding to background control. A-D: Cup-shaped membranous structures found in *P. pastoris* lysate during routine purification of expression culture; A: micrograph of HBsAg producing *P. pastoris* lysate; B: PEG supernatant; C: PEG supernatant bound on Aerosil; D: Aerosil eluate; 1-A – 1-D: Micrographs of corresponding samples from control-1 i.e. *P. pastoris* GS115 cell lysate treated with the same procedure as that of routine protocol. Scale bar = 100 nm.

The cup-shaped structures were observed also in the control samples irrespective of the presence or absence of HBsAg (Figure 4.14 1-A to 1-D). The TEM images of both of these controls are shown in figure 4.14. As these spherical structures exist also in non-producing *P. pastoris* cell lysate, it was concluded that they do not arrive from HBsAg. It may be concluded that these structures are outcome of cellular membranes of host

cell system; however, further investigation is required for the confirmation. The similar circular structures in *P. pastoris* lysate have been observed in previous studies as well [102].

4.2.4. Effect of host cell components on VLPs

In order to demonstrate the effects of host cell components (HCCs) present as contaminants in the lysate, control-2 was performed. In control-2, the *P. pastoris* GS115 lysate samples collected during the control-1 were supplemented with purified HBsAg VLPs and incubated for 24 h at 4°C. The study showed that the structure and compactness of intact VLPs is disturbed when they are added to corresponding samples from mock purification of *P. pastoris* GS115 lysate (control-1). Figure 4.15 shows the comparison of samples collected during control-1 and their corresponding samples from control-2.

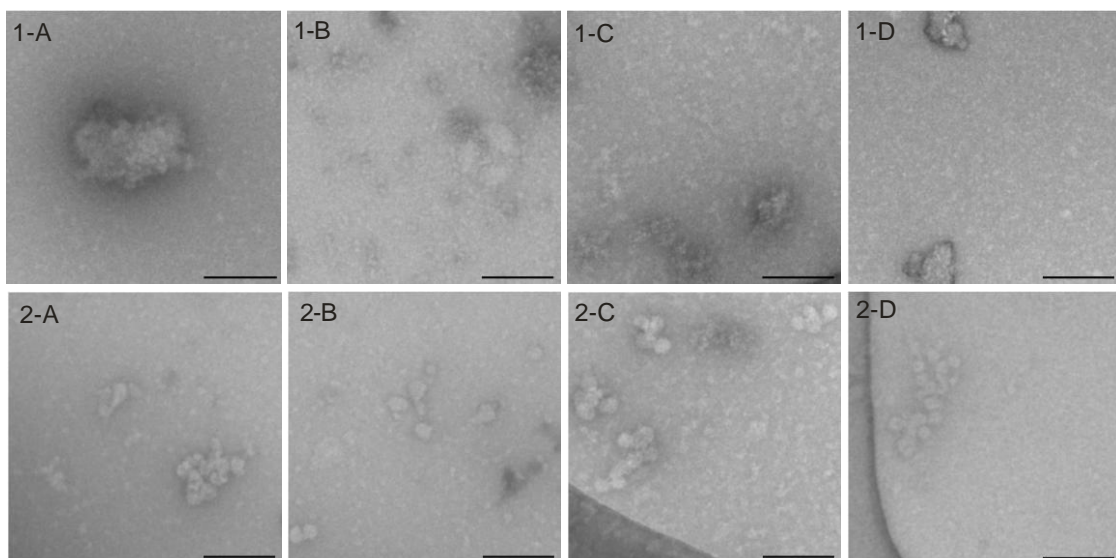


Figure 4.15. TEM micrographs of the samples collected from control-1 and control-2. In control-1 purification (above), non-producing cells were lysed and processed for purification. In control-2 (below), the samples were supplemented with purified HBsAg VLPs and incubated for 24 h at 4°C. A: *P. pastoris* GS115 lysate; B: PEG supernatant; C: PEG supernatant bound on Aerosil; D: Aerosil eluate. TEM analysis was done to observe the changes in structure. Scale bar = 100 nm.

There are two possibilities which explain this trend. Firstly, it can be due to the strong buffer system e.g., presence of detergents, high salt concentration and/or denaturants like urea. Second hypothesis involves the effect of protein-protein interaction. Many host cell components (HCCs) which are present as contaminants, at least in initial four steps, may result in an unfeasible atmosphere for building VLPs even though HBsAg

is present in amounts ranging from 1 mg/mL (crude cell lysate) to 0.5 mg/mL (Aerosil eluate). This may also be attributed to the negative effect of certain *P. pastoris* homologous proteins. However further experiments are required to investigate this effect in detail.

The condition of VLP is greatly dependent on the milieu they are in at any particular moment. The system at initial stages is composed of buffers with high salt concentration and detergents in addition to HCPs which act as contaminant and constitute a large part of total protein contents. It might be assumed that all these factors result in an unfavorable environment for VLP assemble to occur. Due to this same reason, the intact VLPs are also distorted when put in this milieu for 24 h (Figure 4.15).

4.2.5. Effect of solvent system on VLPs

To probe further the influence of native proteins and buffer system, next experiments were performed to study the effect caused by the buffer system in isolation from that of HCPs. To pin down the decisive factor, VLPs were introduced into the buffer system of the initial four steps (control-3). To have a comparison, the same amount of protein was added to PBS, pH 7.2 and incubated (control-4). The VLP count is observed to be higher in PBS than in its parallel purification buffer system (Figure 4.16). The buffer composition of each sample is given in table 4.2.

Sample	Purification step	Buffer composition	pH
3-A	lysis	25 mM PB, 8.0, 5 mM EDTA, 0.6% Tween 20	8.0
3-B	PEG precipitation	lysis buffer, 500 mM NaCl, 5% PEG 6000	8.0
3-C	Aerosil binding	25 mM PB, 500 mM NaCl	7.2
3-D	Aerosil elution	50 mM CBB, 1.2 M Urea	10.8

Table 4.2. The buffer composition of samples from control-3 experiment. In this control, the buffer systems from routine purification process were introduced by the purified HBsAg VLPs. The VLP containing samples were incubated at 4°C for 24 h and later analyzed via TEM. Here the abbreviations used are PB (phosphate buffer), CBB (carbonate-bicarbonate buffer).

The results in figure 4.16 illustrate that the intact VLPs are disassembled when added to the purification buffer corresponding to the initial purification step. The difference between VLP count in a certain buffer and its twin sample in PBS is considerably vivid (Figure 4.17). Moreover, the remaining VLPs appear to be less compact and sticking together (Figure 4.16, 3-A – 3-D). Hence it can be concluded that due to the presence of detergent like Tween 20 and denaturant like urea and EDTA, the initial downstream steps do not offer a feasible environment for the VLP assembly as HBsAg subunits are surrounded by high concentration of denaturing salts. The impeding effect of EDTA and glycerol has been observed earlier in the Polyomavirus as well [78].

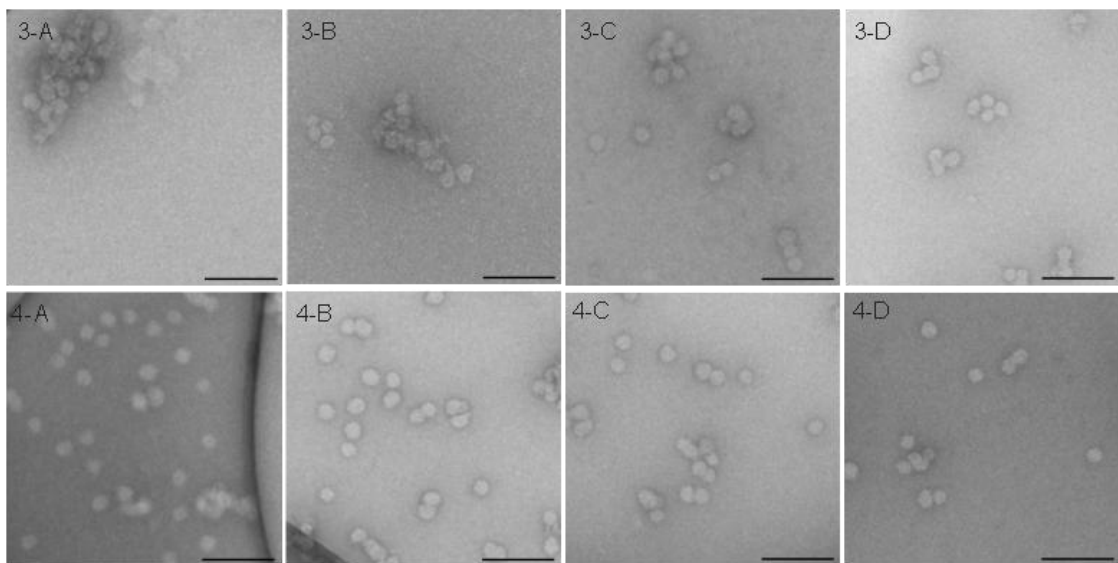


Figure 4.16. Effect of the buffer system on HBsAg VLP morphology. 3-A – 3-D are the micrographs from control-3 where purified VLPs were added to the purification buffers and allowed to stand for 24 h. The images shown here are of HBsAg VLPs in the lysis buffer (3-A), PEG precipitation buffer (3-B), Aerosil binding buffer (3-C) and Aerosil elution buffer (3-D). Samples 4-A – 4-D represent the corresponding protein contents in PBS, pH 7.2. Scale bar = 100 nm.

In human papillomavirus (HPV) VLPs, the presence of urea is reported to decrease the rate of assembly. This can be implied to explain the observation that during Aerosil elution, a low VLP count is observed despite the presence of significant concentration of HBsAg in lysate, as indicated by the gel densitometry (Figure 4.10).

There have been reports stating the effects of several environmental factors such as pH, Ca^+ ion and ionic strength on the assembly process of other VLPs [103]. The presence of bivalent cation has been claimed to be important in the *in vitro* assembly process. Studies have shown that calcium ion is required for the particle stabilization

[76]. Other studies have shown that in the case of HPV, Zn^{+2} influences the assembly negatively because of its involvement in aggregation [104].

The effect of pH on the fact that no VLP assemblage is observable in initial steps cannot be ruled out. It has been reported that the pH plays an important part in the *in vitro* formation of VLPs [78, 103]. It is shown that the Norwalk VLPs, for example, can withstand appropriately acidic pH but in alkaline condition (pH 8.0), the dissociation occurs [105]. However in the present study, the pH appears to be least decisive. During the lysis and PEG precipitation, the pH is kept at 8.0 whereas during Aerosil binding and washing it remains constant at pH 7.2. HBsAg is afterwards eluted from Aerosil using buffer system with pH 10.8 and later stages exhibit pH condition similar to initial steps. As HBsAg contents are rather high in initial steps, we should be able to see VLPs accordingly. But since it is not the case here, it may lead to the conclusion that effects due to detergent and HCCs are more influential than that of pH, if at all, in case of HBsAg VLPs.

The idea of denaturant-based solvent effect is indirectly supported by the *in vitro* assembly processes (of HBsAg as well as other VLP systems) where the subunits are produced and purified under the denaturing conditions. As soon as the purified product is added into the so called 'assembly buffer', the assembly process takes place resulting in the formation of VLPs. When the composition of 'assembly buffer' is closely inspected, it is simply a buffer with a particular ionic strength and suitable pH which allows subunits to acquire specific conformation [79, 104, 106]. Due to this switch in conformation, the subunits are spatially aligned with respect to each other so that they can bind together via their 'active-sites' [37].

Broadly speaking, the phenomenon of solvent influence on activity and conformation of proteins is not new. Since years, biologists have used certain salts and sugars as stabilizers to retain the activity of proteins. Concomitantly, the solvent constituents have also been manipulated to denature and renature the native protein structures. There are several principles involved in the stabilization of structure by solvent components. In short, the stabilization process can be considered as a reverse reaction of the defolding process, usually characterized by a two-state mechanism. In former case, the solvent additive tends to shift the equilibrium towards the native state, thus favoring the retention of native conformation and a stabilized system [107]. The effect

of solvent system on the VLP structure will be discussed in depth in the forthcoming pages.

4.2.6. VLP count during the downstream process and control experiments

The most obvious characteristic of HBsAg activity is the VLP formation itself. In order to scrutinize the influence of various factors quantitatively, the VLP count was determined during the routine downstream process as well as the control experiments (Figure 4.17). For control experiments, VLP count from control-4 (purified VLPs in PBS, pH 7.2) was considered as reference to calculate the percent VLP count. The samples in control experiments contain the same amount of HBsAg as in respective samples from routine downstream processing.

It can be observed that VLP appear for the first time during Aerosil elution step. The absence of VLPs before this step, despite the presence of high amount of HBsAg in the lysate, can be explained on the expense of rigorous buffer systems and HCCs. Further quantitative analysis of the HBsAg VLP count during the control experiments provides a deeper understanding into the effects of milieu factors, i.e. HCCs and buffer system, on the VLP assembly. In this analysis, the VLP count in control-4 i.e., purified VLPs in PBS, pH 7.2 is considered as a reference with which the rest of the results are compared to.

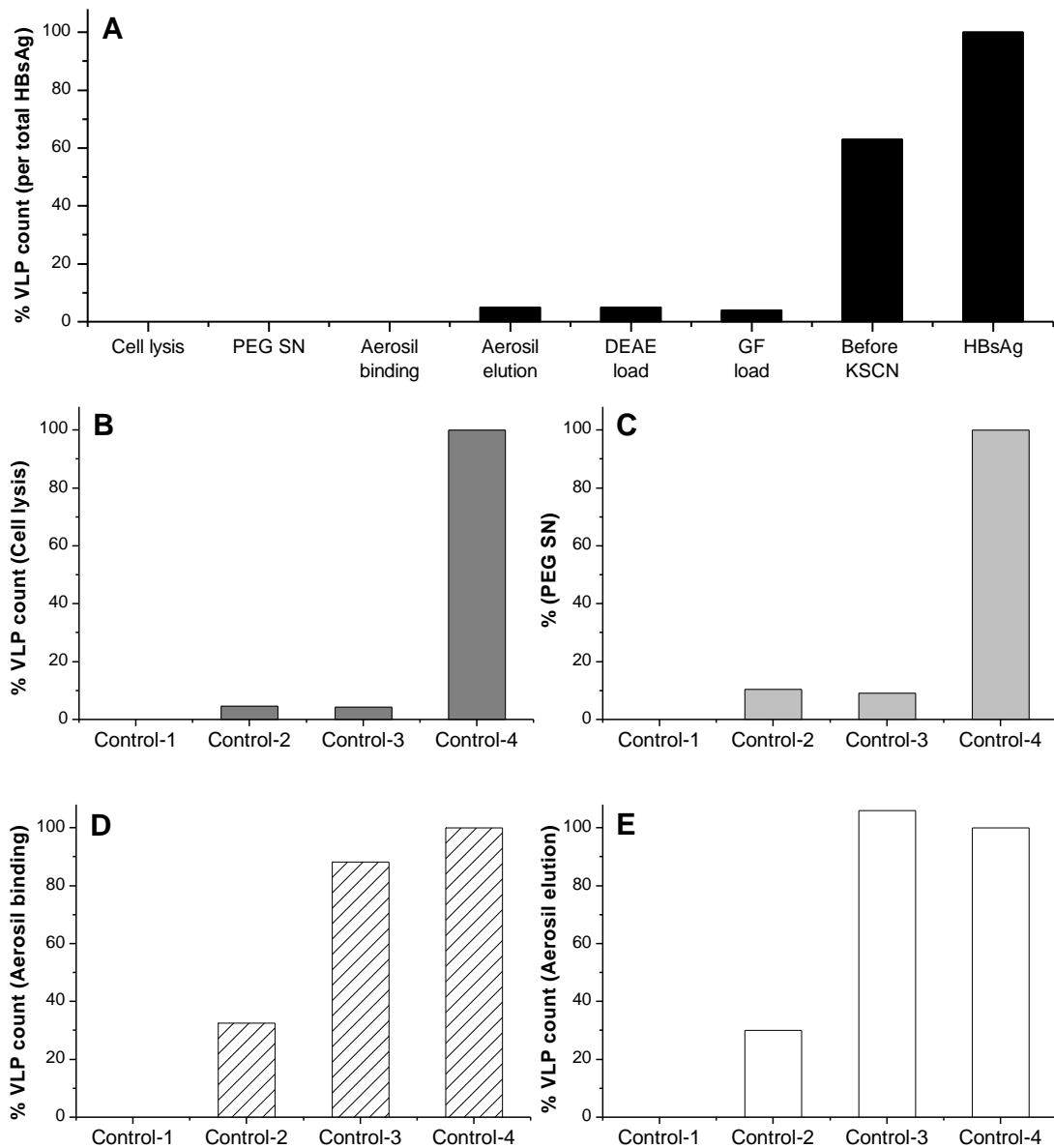


Figure 4.17. Quantitative survey of the VLP formation during routine and control experiments. The upper most panel (A) shows % VLP count (w.r.t. total HBsAg contents) of the samples during routine HBsAg purification process. The initial four steps were further investigated in the control experiments. Control-1 is the purification process of *P. pastoris* GS115 whereas in control-2, VLPs were added in their corresponding samples from control-1. Control-3 comprises purified VLPs in the buffer systems pertaining to the initial purification steps and control-4 contains VLPs in PBS, pH 7.2 as a reference. Middle left panel (B) represents the VLP count of *P. pastoris* GS115 lysate samples from the four control experiments whereas middle right panel (C) is for the second step i.e. PEG precipitation. Lower left (D) and right (E) panels show results from the Aerosil binding and elution steps, respectively. For each measurement, on average, 4-5 images were used and the counting was done via ImageJ.

The VLP count during the routine downstream processing suggests that VLP appear for the first time during the Aerosil elution step. At this step, only 7% of the total HBsAg is assembled into the VLPs (Figure 4.17, panel A). The similar trend is

observed during ion exchange chromatography. A 15-fold increase in the VLP count is observed at GF step i.e., from GF load to GF eluate. At this point, the HBsAg purity increases to almost 2-fold due to the removal of HCPs (Figure 4.11, panel A). This increase in the VLP count at this step is 13 fold higher than the increase in purity of HBsAg.

The 15-fold increase in the VLP count during GF can be explained on the expense of a favorable buffer system (PBS, pH 7.2), apart from the removal of host cell proteins. A further theoretical explanation can be presented by the assumption that VLPs are being formed on-column. This may be supported by the fact that the VLP assembly is promoted by the presence of relatively higher purity of the subunit protein i.e. HBsAg. Moreover, the presence of an optimal buffer system helps to expedite the assembly process.

It is observed that the VLP count decreases by 95% during their incubation in the samples comprising *P. pastoris* GS115 cell lysates (Figure 4.17, panel B). During the control experiment, investigating the PEG precipitation step, a decrease of about 10% was observed in control-2 and -3 samples. However during the later steps, Aerosil binding and elution, the loss decreases to 30-80 percent. This trend suggests that together the host cell contents and the purification buffer system have influence on the *in vitro* VLP assembly.

It can also be comprehended that the solvent system (control-3) has a stronger effect on the VLP dissociation as compared to the HCCs as the VLP number decreases to almost 5 percent after addition of VLPs in purification buffer for the lysis and the PEG precipitation. Nonetheless, the impact of HCCs cannot be ruled out altogether because the last two samples in control-2, i.e. Aerosil binding and elution, express 30 percent decrease in the VLP number whereas the solvent system does not contain very strong constituents like Tween 20 or EDTA. This decrease may be well explained by the presence of HCPs to a concentration of around 40% of the total protein contents in the sample (Figure 4.11).

4.2.7. Effect of Tween 20 and EDTA on VLPs

It has been observed from the previous experiments that VLPs do not appear suddenly en masse. The formation of VLPs is a gradual procedure which occurs step by step.

The first step to observe VLPs in the purification process is after the Aerosil elution. Results from the routine purification during initial two steps i.e. lysis and PEG precipitation do not show any particles whereas control experiment-2 and -3 suggest that the samples from these steps exhibit a decline in the count of purified VLP when added afterwards.

The above observation could be explained on the account of buffer composition during these purification steps which provide a hostile environment for the VLP structure. When these buffer systems are carefully scrutinized, there are two possible components which may be responsible for the instability of VLPs, namely Tween 20 and EDTA. Tween 20 is a nonionic polyoxyethylene surfactant used to facilitate the lysis and release of the protein from cellular compartments [108]. It has a critical micelle concentration (CMC) of 0.0074% (w/v) or 0.06 mM. EDTA, a polyamino carboxylic acid, is a chelating agent. It is used in the lysis buffer commonly to serve two purposes. Firstly, it chelates Ca^{+2} ions involved in the intercellular and intracellular adhesion (in lipid bilayer) to get a better break down of the cells. Secondly, it inhibits the divalent cations which are co-factors of certain enzymes involved in the degradation of proteins and DNA.

In order to verify conclusively the effect of Tween 20 and EDTA, the lysis was performed in absence of each constituent one by one. Control lysate-1 (CL-1) contains the routine lysis buffer. CL-2 and CL-3 are lysates in the absence of Tween 20 and EDTA, separately, whereas the CL-4 lacks both components, together. The typical lysate in lysis buffer [25 mM sodium phosphate buffer, pH 8, 5 mM EDTA, 0.6 % (v/v) Tween 20] is shown in the figure 4.18.

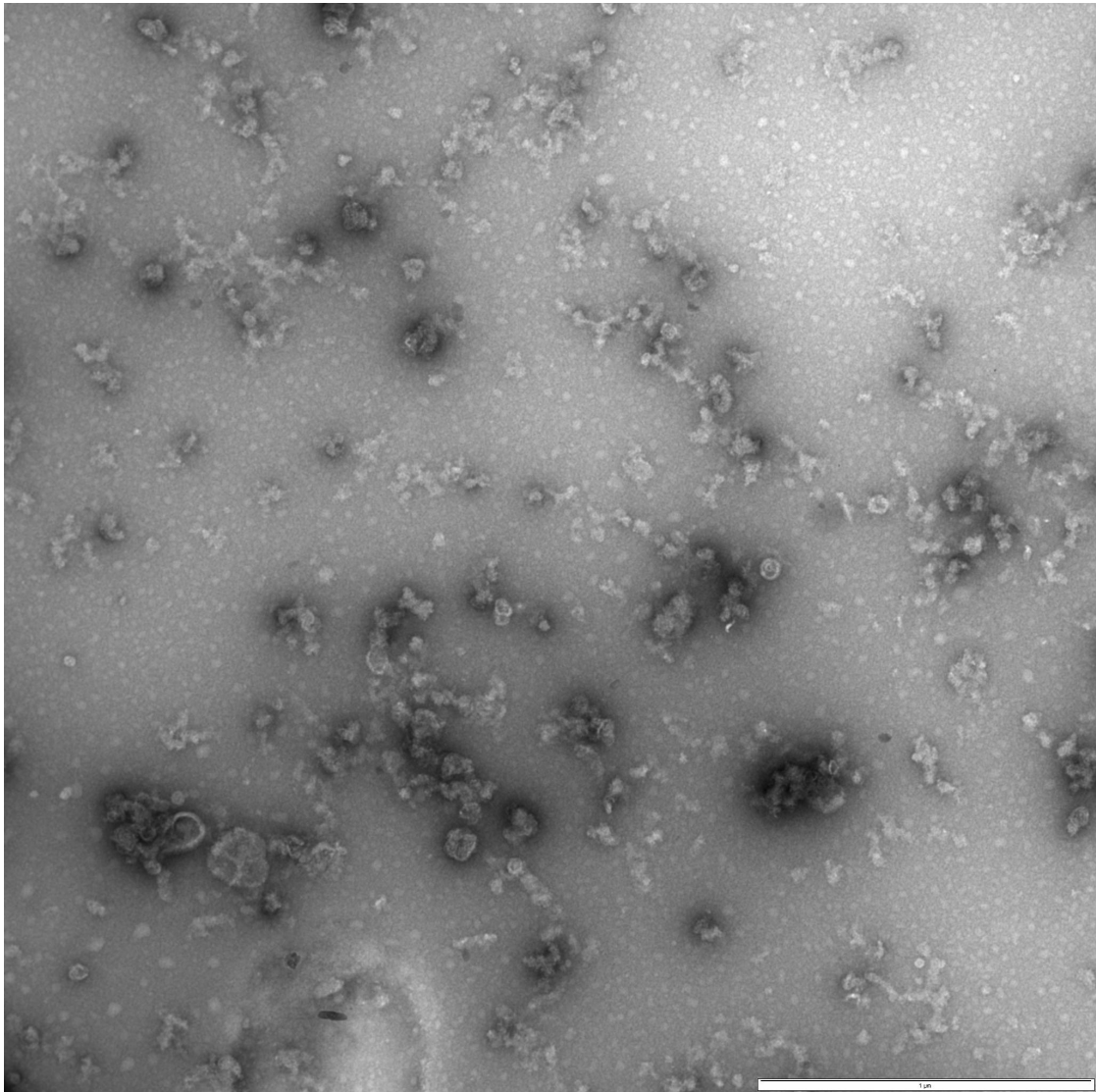


Figure 4.18. A survey view of the HBsAg producing *P. pastoris* cell lysate (CL-1) via TEM. Here the total protein concentration is 0.5 mg/mL. Scale bar = 1000 nm.

In general, cell lysates with Tween 20 are more homogeneously stained (e.g., figure 4.18). TEM survey indicates that in the sample with regular lysis buffer as well as without Tween, no intact VLPs are present. However some random VLP agglomerates in the form of well-packed clusters can be observed. The size of each particle in this cluster corresponds to an HBsAg VLP. Overall a significant amount of agglomerated structures are observed in all lysate samples, however their characteristic appearance varies.

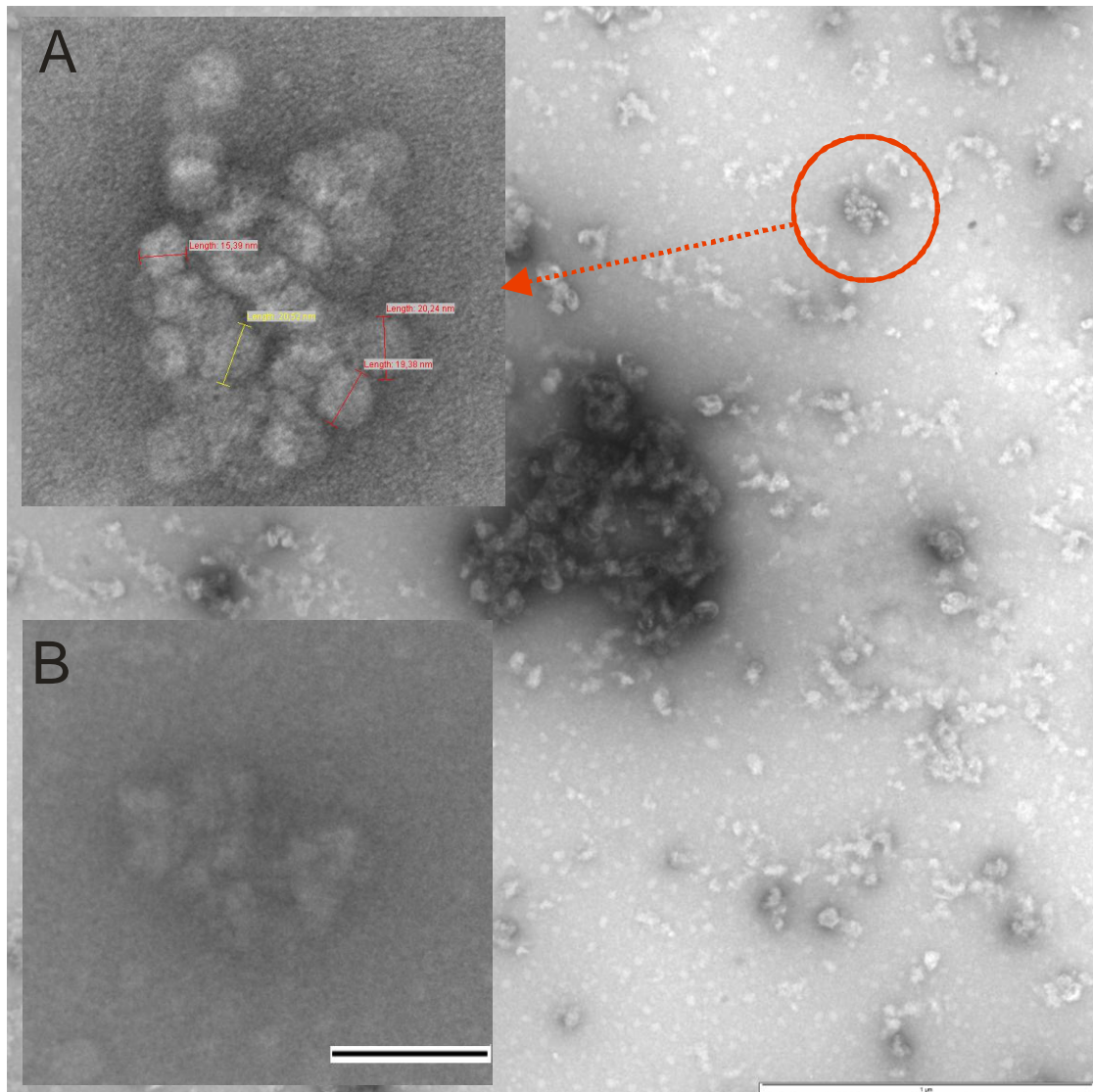


Figure 4.19. An example of VLP agglomerate present in the cell lysate. These VLP clusters were seen in the samples without Tween 20 (CL-2). The inset A shows close up of this agglomerate. Notice that the size of particle is similar to that of a mature intact VLP. In the inset B, an aggregate from *P. pastoris* GS115 cell lysate is shown (scale bar = 50 nm), for comparison purpose. The difference of this aggregate from VLP agglomerate can be well observed due to its random morphology. Scale bar (main image) = 1000 nm.

Due to its detergent properties, Tween 20 decreases the surface tension and renders the samples homogeneity. Therefore, most of the agglomerated VLP patches are observed in the samples lacking Tween 20. These densely-packed proteinaceous structures are easily distinguishable because of their thick stain. Due to their spatial geometry they soak more stain, because of the capillary effect, and hence appear darker in color. For better examination of such structures, the image intensity (and magnification) was adjusted appropriately in some cases.

In order to better comprehend the role of Tween 20, it is important to explain its mechanism of interaction with the proteins. Usually, the non-ionic surfactants can be used to increase the stability of stored proteins. There are many physical factors involved in the protein aggregation and a common believe to trigger the aggregation is the adsorption of hydrophobic regions of protein on the interfaces e.g. vessel and interfacial surfaces. Surfactants like Tween 20 may inhibit the aggregation process by binding to the hydrophobic regions, however their capacity is quite limited [109, 110]. Tween 20 has also been claimed to influence the release of HBsAg from the cellular compartments [111]. In this study, it was observed that Tween 20 disrupts the striated HBsAg membranes (Figure 4.23) by decreasing hydrophobic interaction and this may possibly help in the release of protein from ER.

More interesting structures were found in the lysate samples CL-3 and CL-4 (Figure 4.20, 4.21). In samples lacking EDTA, lamellar structures with definite membrane pattern were observed. Due to their thick stain, they are clearly distinguishable from rest of the structures. On first sight, they appear as a local aggregate of sample due to staining procedure. When observed closely, with adjusted brightness and contrast settings, they are found as stacks of membranous layers lying over each other. These stacks of lamellar membrane exhibit characteristic thickness as well as interlayer distance (Figure 4.20, 4.21).

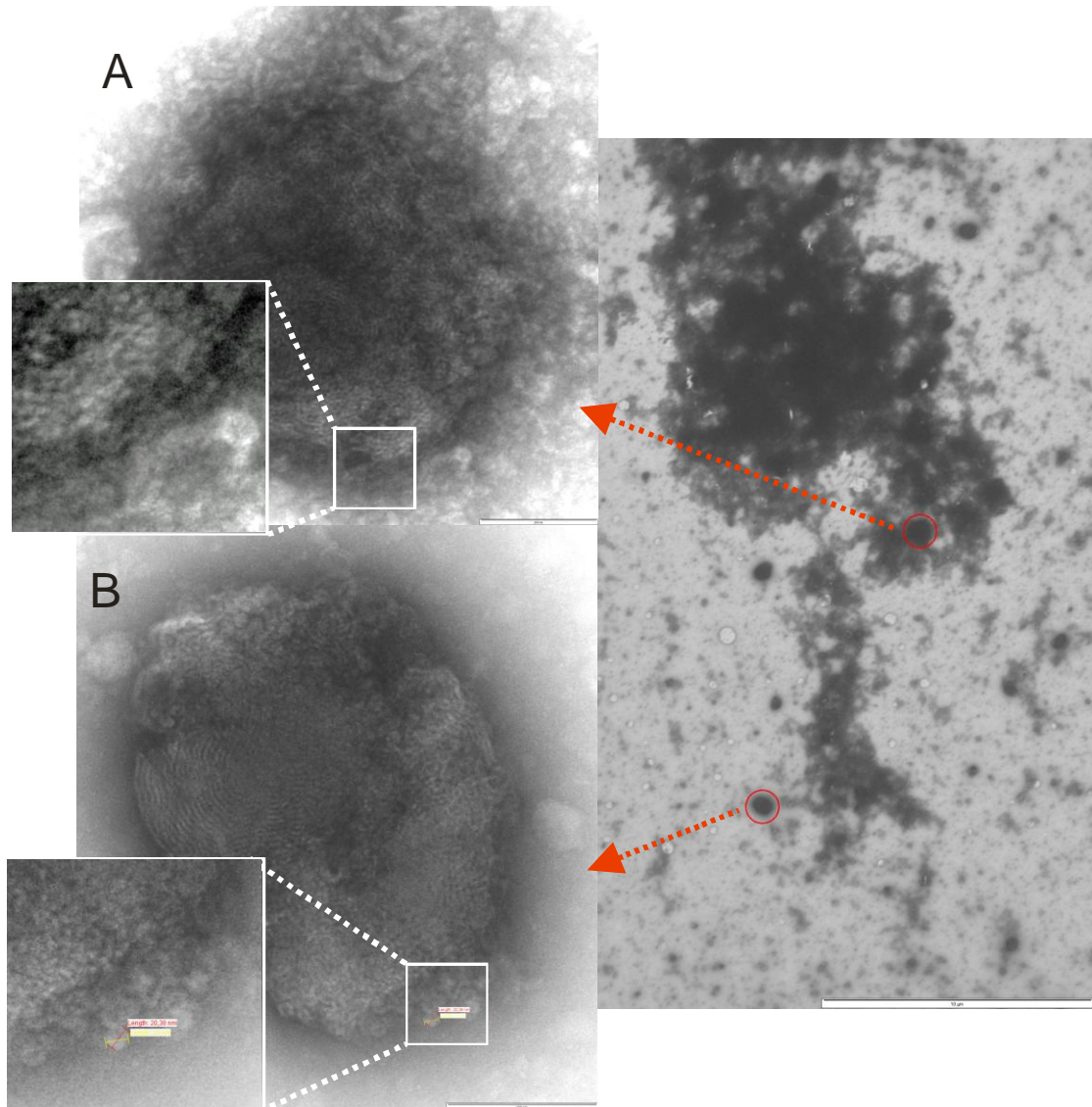


Figure 4.20. A close up of agglomerated protein patches in the lysate sample in absence of EDTA. The striated lamellar structure of HBsAg can be seen in close-up insets. In close-up B, few random VLPs are present on the edges of the aggregate. Scale bar for main image = 1000 nm, for image A and B = 200 nm

The structures found in the samples without EDTA resemble to those found in the endoplasmic reticulum (ER) of HBsAg-producing *P. pastoris* cells. This observation can be attributed to the chelating effect of EDTA. Being a chelating agent, EDTA binds with the bivalent ions (e.g. Ca^{+2} and Mg^{+2}) which are responsible for the membrane stability. It has been reported previously that EDTA helps to release the proteins bound to the cellular membranes in yeasts [112]. In Gram-negative bacteria, EDTA has been found to enhance the effect of antibiotics by destabilizing the cell walls [113]. This is done by chelating the bivalent ions in the outer membrane of bacteria, a phenomenon often referred as the permeabilization [114].

In the absence of EDTA, these structures retained their integrity, including the ER membrane where HBsAg accumulates. The fact that HBsAg remains localized in the ER has been used artfully by Kee *et al.* as exploitation of cellular compartments for the ease in purification process [115].

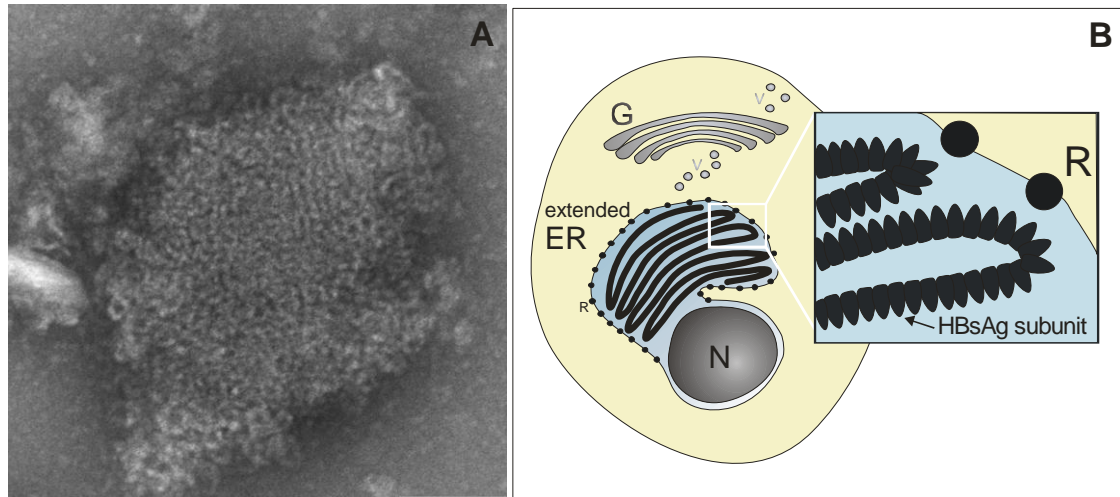


Figure 4.21. Striated lamella in lysate sample in the absence of EDTA (CL-3) with regular pattern (A). The similar membranous structures have been observed in the ER of HBsAg-producing *P. pastoris* cells (B- adapted from Lünsdorf *et al.* [75]). Scale bar = 100 nm.

In CL-3 (sample without EDTA), the thickness of a lamellar layers and the distance between them was measured via iTEM software. The average thickness of one single layer was found to be 6.38 nm (SD = 0.97 nm) whereas the interlayer distance was 4.2 nm (SD = 0.24 nm). The lamellar structures were sought also in lysate samples with regular lysis buffer as well as lysis buffer without Tween 20. The typical striated pattern could not be found as such, however on close examination, the agglomerates appear to be the distorted form of lamellar structures (Figure 4.22).

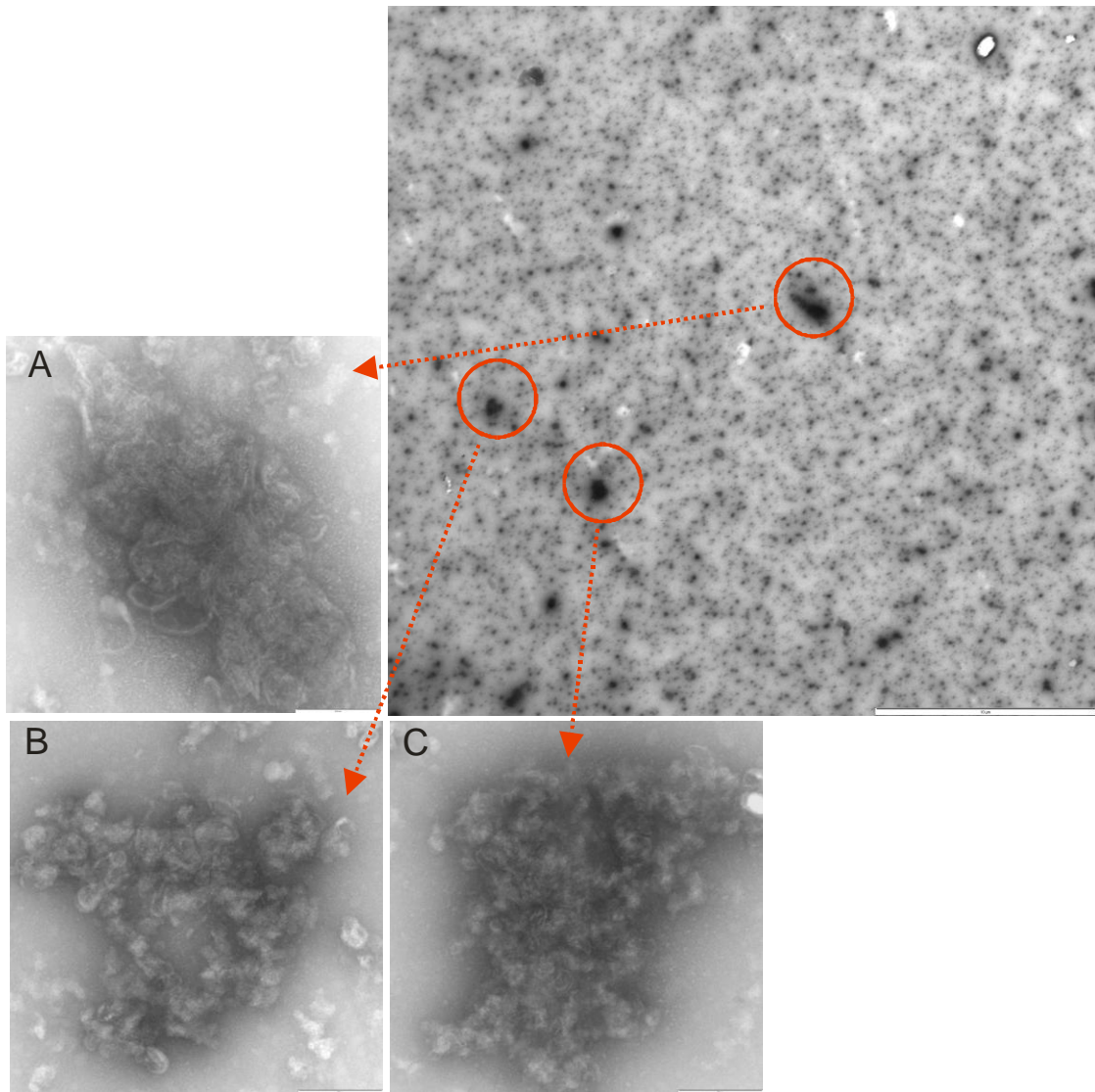


Figure 4.22. Close up of the agglomerated protein stacks in samples with lysis buffer (CL-1). These structures are distinctively different from those found in the absence of EDTA as the typical lamellar pattern is missing here. Scale bar for main image = 10 μm ; for close-ups = 200 nm.

In samples with EDTA, instead of lamellar membranes, the disrupted agglomerates of proteins were found (Figure 4.22). As mentioned earlier, EDTA helps to disrupt the cellular membranes by binding to the bivalent cations. In samples lacking EDTA, HBsAg remains attached to ER membrane, and as a result lamellar structures are observed (CL-3 and CL-4). In samples with EDTA, HBsAg is released from ER membrane but, due to the presence of Tween 20 and HCCs in the solution, forms disrupted lamellar membranes (Figure 4.22, panel A, B and C). These structures have not been observed in the non-producing *P. pastoris* lysate.

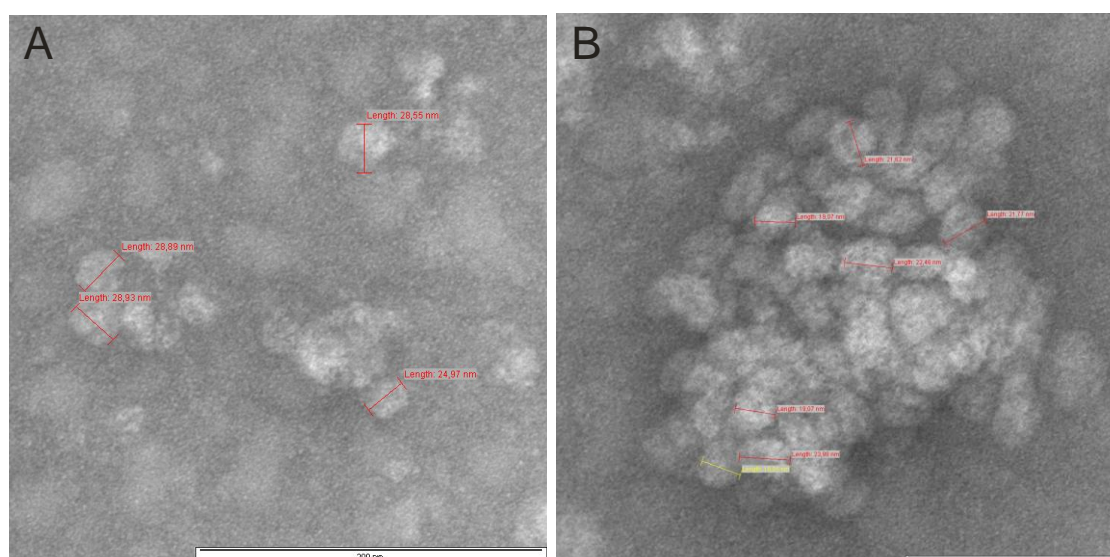


Figure 4.23. Single VLPs and VLP agglomerate in the sample CL-4 (cell lysate in phosphate buffer, pH 8.0). Scale bar = 200 nm for image A; 100 nm for image B

In sample without Tween 20 and EDTA, some single VLPs could be observed (Figure 4.23 A). The number of single VLPs is not very high as compared to the purified sample with same HBsAg contents. Moreover, the compactness of these VLPs is not well-defined and they do not seem to contain the typical octahedral geometry. This may be explained on the account of deterring effect of some host cell components on VLP assembly.

Sample	Solvent	Single VLPs	VLP agglomerate	Striated lamella	distorted lamella
CL-1	Lysis buffer	no	no	no	yes
CL-2	Lysis buffer without Tween 20	no	yes	no	yes
CL-3	Lysis buffer without EDTA	no	no	yes	no
CL-4	Lysis buffer without Tween 20 and EDTA	Yes*	yes	yes	no

Table 4.3. Summary of structures observed in the TEM analysis of samples examined for the effect of Tween 20 and EDTA (control-5)

* not seen very often (as compared to sample containing pure VLPs)

On the basis of above results, it may be inferred that the absence of VLPs in lysate during routine downstream processing is due to the influence of Tween 20 and EDTA. In the absence of both, HBsAg is present in form of striated lamellas (as present in ER of *P. pastoris* cells [75]) or clusters of closely-packed VLPs. However this cannot be

misinterpreted as an evidence for a stable particulate structure as the morphology of VLPs in these samples is not so well-defined when compared to the purified product.

4.2.8. Conclusion

In this study, the factors affecting the self-assembly of HBsAg VLPs during the downstream processing were identified. As standard, samples from the routine downstream process were examined via TEM. For background structure, GS115 cell lysate was treated in the same way as routine purification method, and the samples were collected from this process (control-1). These samples were introduced with purified HBsAg VLPs for 24 h at 4°C (control-2). The experiments pertaining to incubation of the purified VLPs in purification buffers (Table 4.2) and storage buffer (PBS, pH 7.2) were named as control-3 and control-4, respectively. Lysis test in various combination of the lysis buffer components were called control-5.

On the basis of micrographs from routine downstream process, it could be concluded that the VLPs start appearing after treatment with Aerosil 380 (fumed Silica), increase in number during the ion exchange chromatography and the tendency towards the formation of single and well-defined VLPs (from clump formation) enhances significantly after size exclusion chromatography where the non-VLP HBsAg (e.g., aggregated form) is removed. The partial defolding-refolding with KSCN helps to polish the loose ends in VLPs. It has been already established that KSCN treatment helps to increase the cross-linking due to disulfide bonds in HBsAg particles [86]. This gradual development of VLP quality is also illustrated by the trend from clump formation, in the beginning of downstream process, to the individual VLPs at the end. In general, the impurities decrease and the VLP count increase concurrently during the course of purification.

It was observed during control-2 experiment that VLPs lost their define structure as well as integrity when added to initial steps of downstream process. Hence it was deduced from the control purification experiments that the environmental factors play very crucial role in the VLP assembly as well as morphology. Two central factors were deduced to be HCCs and solvent system.

The later control experiments in presence of *P. pastoris* proteins and purification buffer systems (control-2 and -3) indicated that the morphology of VLPs is disturbed

and their number decreases, irrespective of presence or absence of HCP. Hence, it was concluded that components from host cell may not be as crucial as the buffer system. However, quantitatively, this effect is still influenced by the HCCs.

During the downstream processing, the morphology of VLPs improves gradually as well as the VLP count. It has been noted that the tendency of VLPs to stick together decreases over the whole process and later stages exhibit more stable and compact particles with more uniformity in shape and size.

The absence of VLPs in initial steps of purification is conceived to be partially due to the presence of Tween 20 and EDTA, in addition to the HCCs. In order to examine the effect of buffer system, the control experiment containing the constituents of lysis buffer in different combination was performed. The control lysis in the presence and absence of Tween 20 and EDTA, individually and together, gave a very useful insight into the VLP assembly during downstream processing. In samples with Tween 20 and EDTA (CL-1), no intact VLPs could be observed. The Patches of protein with distinct lamellar membranes are observed in the absence of EDTA where the membranes from yeast cells are not disrupted and HBsAg, due to its hydrophobic nature, remains associated with the remnant membrane of ER. In the presence of EDTA i.e. in CL-1 and CL-2 the distorted structures are observed, which are possibly the HBsAg lamella, disfigured by Tween 20 and HCCs. The clusters of agglomerated VLPs are observed in CL-2 and CL-4 i.e., only in the absence of Tween 20 as due of the detergent effect of Tween, these structures may get dissolved in the lysate solution

In the light of the above stated results, it can be stated that during assembly process, HCCs as well as denaturant-containing buffer play pivotal roles. The gradual removal of adverse buffer system and HCCs results in the occurrence of self-assembled HBsAg VLPs.

According to the present study, the decisive factor in the *in vitro* assembly of HBsAg VLP during the downstream process is chiefly the presence of components like Tween 20, EDTA and urea in the buffer system whereas the HCCs also seem to play a deterring role in this respect.

4.3. Monitoring of conformational changes in HBsAg VLPs in the presence of chaotropic agents via steady-state fluorescence spectroscopy

In previous section, the probing of downstream process of HBsAg via TEM was discussed. The assembly of HBsAg VLPs during the purification process was examined comprehensively and the factors involved in it were studied. Here, it is a matter of special interest to analyze the stability of VLPs via defolding studies. The defolding series serve double purpose; first, as the name suggests, they give an idea about the stability of VLP. Secondly, they help to better understand the assembly process, as the defolding is a reverse process of self-assembly. Therefore, in this part of work, purified HBsAg VLPs were put under the denaturing conditions and the changes occurring as a result of this were observed via fluorescence spectroscopy. Later the fluorescence spectroscopic observations were verified by other parallel techniques such as by virus counter which works on principle of flow cytometry and by dynamic light scattering measurements.

Fluorescence spectroscopy is one of the most accurate and handy optical techniques to investigate the structure of proteins. In the last two decades, a large number of applications involving fluorescence, steady-state as well as time-resolved, have emerged in discipline of biochemistry and biophysics. Being non-destructive it has an advantage over many other analytical techniques which render the sample unfit for further use.

The intrinsic fluorescence properties of a protein arise from the aromatic residues, tryptophan, tyrosine and phenylalanine [116]. This is mainly because of the indole ring, specifically determined by the electrical potential difference across the long axis of the indole ring [117]. On the other hand, extrinsic properties are rendered by the fluorescent probes. Most of the probes bind covalently to different amino acids in a protein, e.g. via the ϵ -amino group of lysine, the α -amino group of the N-terminus, or the thiol group of cysteine. Some fluorescent dyes attach noncovalently to the protein degradation products, e.g. via hydrophobic or electrostatic interactions [118]. In this study, both extrinsic and intrinsic fluorescent measurements were carried out to observe the effect of chaotropic reagents.

4.3.1. Fluorescence spectroscopic studies of HBsAg VLPs

In general, fluorescence properties of proteins can be used to observe the product formation online as well as offline. Moreover, fluorescence spectroscopy makes it possible to have a close look into the protein structure at molecular level because fluorescence properties are influenced by the local electrostatic environment. In this study, conformational changes of the HBsAg, after treating with chaotropic salts, were observed via steady state fluorescence spectroscopy.

4.3.1.1. HBsAg intrinsic fluorescence measurements

As mentioned previously, one HBsAg subunit comprises 226 amino acids. The fluorescence excitation spectrum shows maxima at 320 nm, which indicates that most of the intrinsic fluorescence is by virtue of its tryptophan residues while a small part comes from the tyrosine residues. This is in compliance with the previous reports [83, 119].

Amino acid	Number of residues
Tryptophan	13
Tyrosine	6
Phenylalanine	16

Table 4.4. Important amino acid residues in one subunit of HBsAg w.r.t. intrinsic fluorescence properties

4.3.1.2. Extrinsic fluorescence measurements

Fluorescent dyes are excellent tools for monitoring the change in microenvironment of proteins in solution. In general, the phenomenon of protein fluorescence on account of an extrinsic dye may occur via either of two main mechanisms. The first mechanism involves a shift of charge, as a result of excitation, in dye molecule and consequently in the solvent around it. This creates fluorescence on account of more suitable conformation of the molecule. The second mechanism involves exchange of electron/s leading to the intramolecular charge transfer (ICT) [120].

There are many probes available for the characterization of lipoproteins, most famous of them being ANS (8-anilino-1-naphthalenesulfonic acid) and bis-ANS (4,4'-Dianilino-1,1'-binaphthyl-5,5'-disulfonic acid). Bis-ANS is sensitive to change in the

environment with respect to polarity and viscosity hence giving idea about hydrophobicity of the protein. The binding equilibrium between protein and bis-ANS gives valuable information about the protein structure [118].

In present work, bis-ANS was used to monitor the structural changes in HBsAg induced by denaturants. The structural formula of bis-ANS is given in figure 4.24.

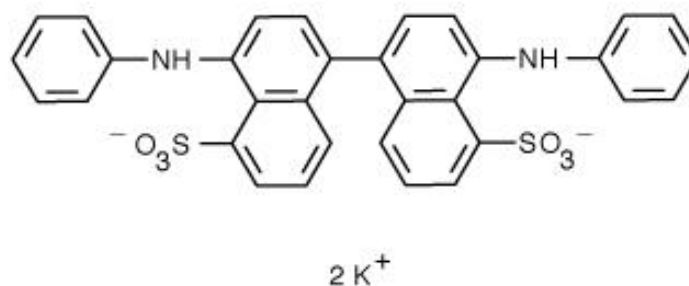


Figure 4.24. Structural formula of Bis-ANS, the fluorescent dye used for binding with the hydrophobic domains

Ostensibly bis-ANS binds with the protein on account of hydrophobic as well as ionic interactions. The major binding force between the protein and bis-ANS is reported to be hydrophobic interactions. However, the electrostatic interaction between anionic sulfonate groups from the dye and cationic amino acids also help to make the protein-dye complex [121]. Its monomeric form, ANS, is used to quantify the surface hydrophobicity of proteins [122].

The parameters for fluorescence measurements of HBsAg are summarized in table 4.5.

		Wavelength (nm)
Intrinsic fluorescence	excitation	280
	emission	300-450
Extrinsic fluorescence	excitation	400
	emission	430-550

Table 4.5. Summary of fluorescence parameters used for the stability studies of HBsAg VLPs.

4.3.2. Denaturation studies of HBsAg

In the field of biochemistry, unfolding studies in presence of denaturants has provided useful insight into protein conformation. The transition from native to unfolded state and reverse can occur via two-state kinetic or folding intermediates [123-125]. Either way, the equilibrium between folded and non-folded protein alters in the presence of denaturant. The ease (or difficulty) with which a protein undergoes these transitions is used to interpret its structural stability [126]. In general, both increase and decrease in fluorescence intensities can occur during the denaturation experiments.

In this experiment, the changes in fluorescence prosperities of HBsAg VLPs were studied by performing the denaturing experiments with different chaotropic agents. Chaotrope is a reagent which disrupts the structure of a macromolecule [127] and hence increases the entropy. Chaotropic reagents have the ability to interfere with hydrogen bonding and van der Waals forces in a substance. Denaturing (chaotropic) reagents induce quenching effect which can be used to measure the accessibility of fluorophores and hence indirectly the conformational changes in proteins. Such studies in VLP technology help to explain structural aspects as well as, indirectly, mechanism involved in cell entry and viral replication [128].

The chaotropes opted for this study are, GdnSCN, KSCN and GdnHCl. GdnSCN is a commonly used denaturant with, both anion and cation, as strong chaotropes. Similarly, GdnHCl is widely used to follow the unfolding curve of proteins [129]. It is known that unfolding induced by GdnHCl and urea mostly leads to randomly coiled conformation [130]. The main reason for using KSCN is that it is used in partial defolding step during downstream process of HBsAg. The purpose of using multiple denaturants is to understand the structure of VLPs from multiple prospects.

In this study, some preliminary tests were performed to see the scope of change in the fluorescence profile, intrinsic as well as extrinsic, under native and denatured conditions. The initial results indicate an obvious difference between fluorescence maxima of native protein in form of VLPs and the denatured one (Figure 4.25).

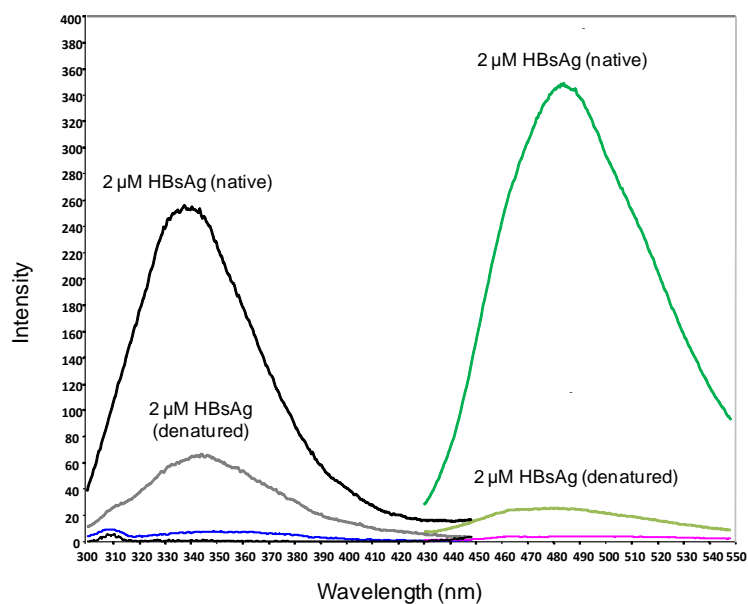


Figure 4.25. The emission spectra of HBsAg VLPs in native and denatured form (after treating with 6 M GdnSCN). Black and grey spectra correspond to intrinsic fluorescent properties of native and denatured forms of HBsAg VLPs. The extrinsic fluorescence profile is shown in dark and light green colored spectra for native and denatured VLPs respectively. The signals near the base belong to buffer in absence (blue) and presence (pink) of fluorescent dye.

This preliminary data indicates that intensity maximum exhibits a small red shift from about 340 nm to 350 nm. This shift in the emission maximum is because of change in vicinity of tryptophan residues. In later studies it was observed that throughout a transition curve, under the influence of all chaotropic salts used, the maxima showed a linear increase, from 340 nm to 350 nm i.e. a shift of 10 nm.

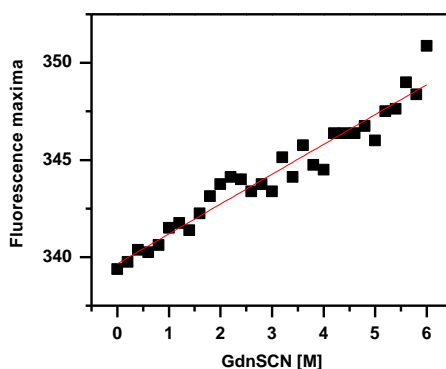


Figure 4.26. The Red shift in fluorescence maxima in the presence of chaotropic agent. In this case, 2 μ M HBsAg was treated with GdnSCN (0 – 6 M) and the trend in fluorescence maxima was observed.

The initial experiments showed that the effect of denaturant salts on the defolding curve was almost the same when the VLPs were incubated for 3 min or 24 h at 25°C

(Figure 4.27). The incubation after 48 h resulted in a linear trend showing no change in the fluorescence intensity between samples with and without GdnSCN. This may be because of loss of the VLP structure due to incubation at 25°C.

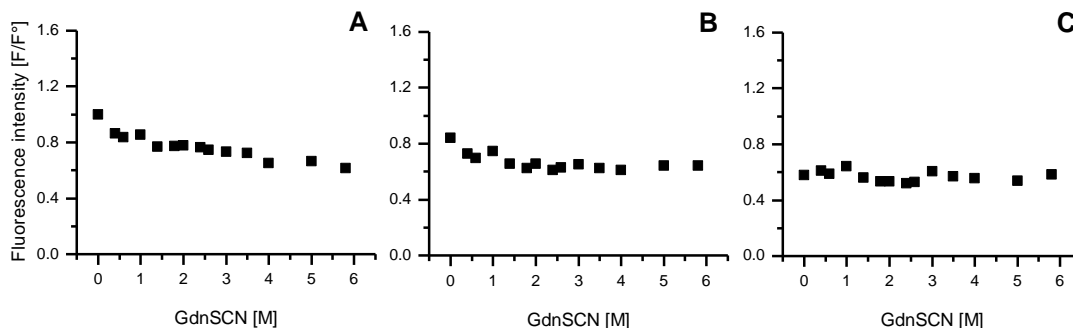


Figure 4.27. The trend in defolding curve of HBsAg VLP in the presence of GdnSCN. The sample containing 2 μ M HBsAg VLP were incubated with GdnSCN (0 – 6 M) at 25°C. The incubation time is 3 min (panel A), 24 h (panel B) and 48 h (panel C).

The transition curves under the effect of denaturants are represented in the figure 4.28. As it can be seen, the intrinsic fluorescence profile does not contain any drastic change in the transition curve. On the contrary, a meager and steep curve is observed in presence of GdnSCN and KSCN. GdnHCl does not show any significant change in intrinsic fluorescence intensity which appear to be due to inaccessibility of non-covalent interactions and/or disulfide bonds of VLP. It is known that solubilizing ability of GdnHCl is more leaned towards nonpolar groups, which are buried in the inner core of VLPs [130, 131].

The general modest profile of intrinsic fluorescence properties of HBsAg VLPs can be arguably supported by “molten globules” as folding intermediates. The partially folded conformation of protein, so called molten globule, is formed under mild denaturing conditions and is different from native protein by the fact that it does not contain the tertiary structure as do the native proteins [132, 133]. However these molten globular proteins are markedly stable under a wide range of environmental conditions such as acidic change, presence of denaturant etc [134]. Based on this fact, it may be deduced that VLPs, during initial stage of transition curve, acquire molten globular conformation which explains the observation that VLPs do not show a significant change in their intrinsic fluorescence properties. However, when bound to fluorescent dye, the change in micro environment becomes rather obvious.

As discussed earlier, no significant change was observed in the intrinsic fluorescence of HBsAg particles during chaotropic transition curves. However the extrinsic fluorescence data, in presence of bis-ANS, shows interesting results. Bis-ANS is an example of solvent relaxing probes used to characterize the micro viscosities and polarities of protein solutions. Interestingly, it is reported to hinder the viral assembly when bound to the dimer. The speculated reason for it is that bis-ANS binds to dimer interface which is a very suitable location for a molecular wedge [135].

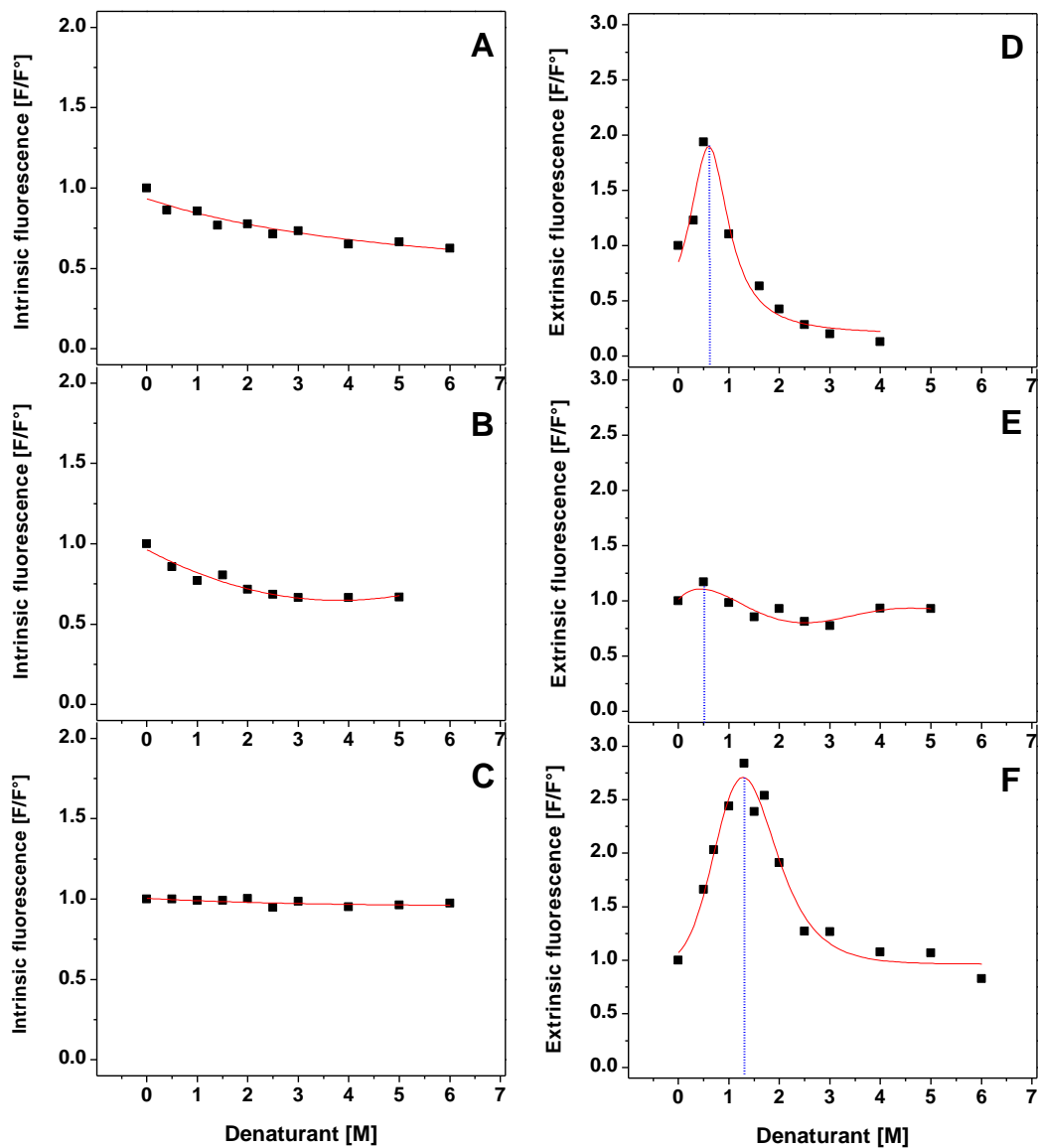


Figure 4.28. Denaturing curves of the HBsAg VLPs during treatment with chaotropic agents. The panels A, B and C on left hand side represent the intrinsic fluorescence curves in presence of GdnSCN, KSCN and GdnHCl respectively. Similarly panels D, E and F on the right hand side show changes in the extrinsic fluorescence after treating with same chaotropic agents. Bis-ANS (4,4'-Dianilino-1,1'-binaphthyl-5,5'-disulfonic acid), a dye which is sensitive to change in environment with respect to polarity and viscosity was used as the fluorescence probe.

No typical two-state unfolding kinetics could be observed, irrespective of sort of chaotrope used. A two-state kinetic is representative of unfolding of globular proteins, with which VLPs are frequently compared to. However this comparison is irrational due to the reason that VLP is an entity comprising of several subunits, unlike a globular protein. The inter-molecular interaction is, therefore, of prime importance in this structure.

During the extrinsic studies, transition trend with both GdnSCN and GdnHCl showed a peculiar curve, although with peak position at different concentration of the chaotrope salt. In transition curve, the initial thrust in extrinsic fluorescence is attributed to the formation of a molten globule-resembling partially folded form, which possesses a quasi-native structure (Figure 4.29). Due to loose structure, the molten-globular structure has increased solvent-exposed hydrophobic surface area as compared to the native state. This is why even the buried hydrophobic cavities become exposed to the solvent and a substantial increase in intensity is observed. On further increase of denaturant concentration, the secondary and tertiary structure is disturbed which leads to the loss of hydrophobic cavities and consequently a decrease in the fluorescence intensity (Figure 4.28).

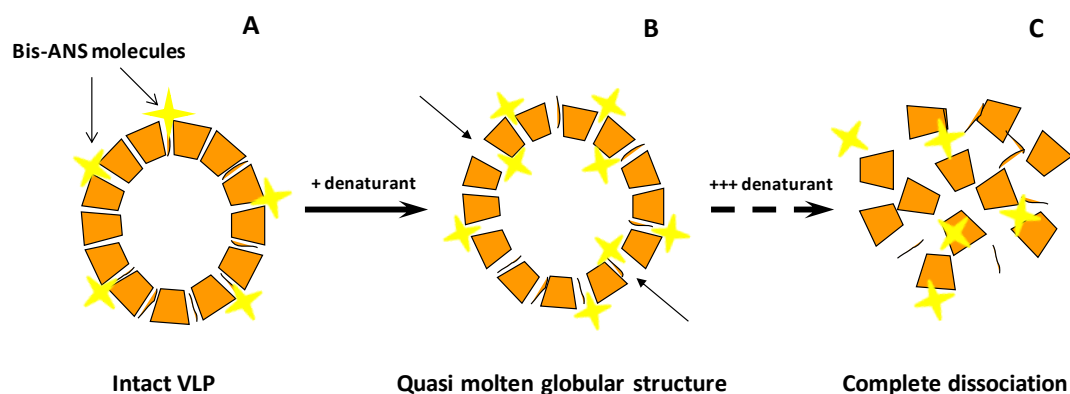


Figure 4.29. Supposed mechanism of the defolding process monitored via fluorescence measurements in the presence of bis-ANS. An initial increase in the (extrinsic) fluorescence intensity is due to access of more hydrophobic regions to the fluorescence dye, which suggests the presence of a quasi-molten globular structure in the defolding curve.

The fluorescence data shows that GdnSCN exposed the hydrophobic cavities around 0.5 M salt concentration. This has been suggested in a previous study by Zhao *et al.* as well [119]. In the presence of GdnHCl, this point is shifted to around 1.2 M. The specificity of GdnHCl for polar groups is higher than that for non-polar groups which

explains that GdnHCl is weaker chaotrope as compared to GdnSCN. A similar trend has been observed in the unfolding studies of papain in presence of GdnHCl [136].

The denaturation with KSCN did not show similar curve which can be explained by the fact that KSCN is a chaotropic reagent which also acts as destaining agent [137]. Apparently it dissociates the protein-dye complex which produces the fluorescent signal. Therefore the extrinsic fluorescence measurements are not as evident as in presence of other chaotropic agents.

4.3.3. Stern-Volmer relation

Stern-volmer equation is a very useful relation to analyze the condition of residues of a protein in a certain milieu [138].

$$F^{\circ} / F = 1 + KSV [Q]$$

Above equation was used to measure the stern-volmer plot of VLPs in presence of GdnSCN, KSCN and GdnHCl (Figure 4.30).

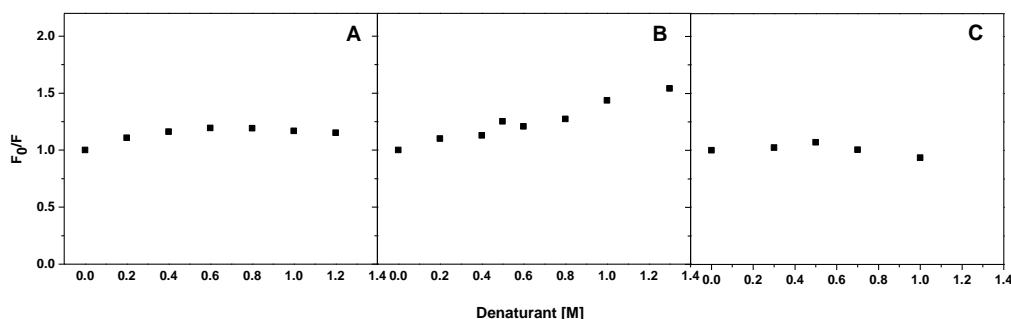


Figure 4.30. Stern-Volmer plot of HBsAg VLPs under the quenching effect of GdnSCN (A), KSCN (B) and GdnHCl (C).

The stern-Volmer plots reveal an exponential curve under the denaturing effect of KSCN, which suggests that the fluorescence is dominated by a single amino acid residue. The GdnSCN and GdnHCl plots show a linear trend which indicates that the residues display different degree of exposure to the denaturant and thus are not equally accessible. This behavior is because of the fact that tryptophan residues, which constitute the major source of fluorescence, are present in different environmental arrangement [139]. Keeping in view the VLP structure, it is implied that the HBsAg VLPs comprise of hydrophilic and hydrophobic regions in distinctive conformation.

The model of a lipoprotein with hydrophobic inner core surrounded by a compact lipid monolayer has been already suggested in *Hansenula polymorpha*-derived HBsAg [82].

4.3.4. HBsAg VP count determination using Virus counter

The results from denaturation studies were further ascertained by the measurements via Virus counter (ViroCyt 2100, InDevR Inc. USA). In this case, due to their more obvious transition in intrinsic fluorescence curve, GdnSCN and KSCN were selected to verify the results obtained from fluorescence measurements (Figure 4.28). Here the virus particle count (VP count) is estimated by the combined data of protein and nucleic acid signals. An example of PMT signal for a VLP sample is shown in figure 4.31.

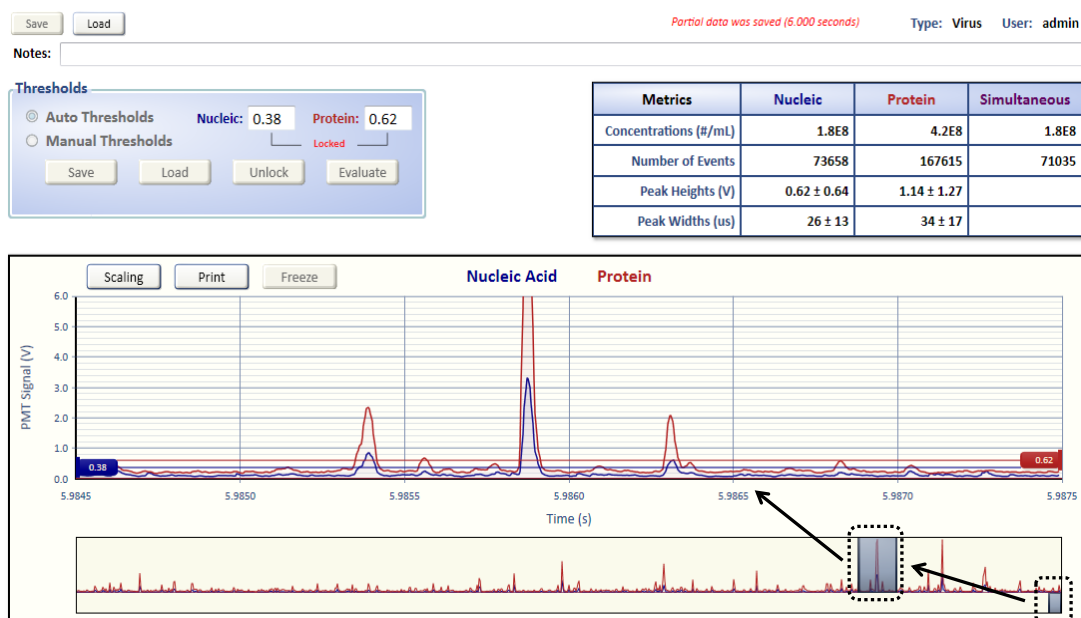


Figure 4.31. A Raw data screenshot of the VP count of purified HBsAg particles. The peak area is close up of only a part of one single measurement. Notice that the protein and nucleic acid signals appear simultaneously.

The results from GdnSCN defolding, represented in the figure 4.32, correlate to the fluorescence profile of HBsAg in presence of series of GdnSCN. Since it was observed that the obvious changes occurred at a concentration of 0-3 M, the measurements via ViroCyt were performed in presence of chaotrope within this range of GdnSCN molarity. The tendency of total VP count implies that increasing molarity of GdnSCN leads to gradual decline of intact particles. The initial increase of protein contents may be attributed to the exposure of residues in milder unfolding conditions which leads to a succeeding decrease due to the stronger denaturation effect.

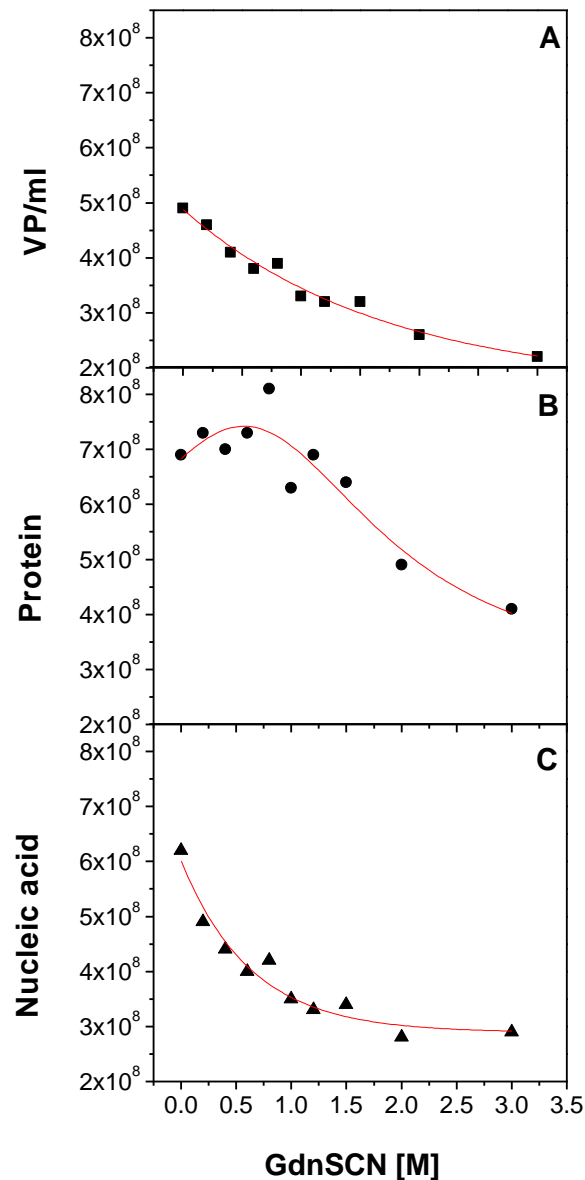


Figure 4.32. HBsAg VP count during the GdnSCN treatment. The upper box corresponds to total VP number ascertained via virus counter by combining the protein and nucleic acid quantitative results. The middle and lower box represents these results individually.

The samples with KSCN denaturation could not be measured due to its destaining effect. Thiocyanate ions in KSCN have dissociative property and therefore may have disturbed the protein-dye complex [137]. This results in the breaking of bonds between hydrophobic amino acid residues and dye molecule which ultimately results in no fluorescence signal, as fluorescence dye alone exhibits no fluorescence.

The instrument, by default, measures not only the collective VP count but also the protein- and nucleic acid contents individually. In case of HBsAg VLPs, the occurrence of nucleic acid signal is unexpected. Since the signal appears concurrently

with protein signal, it was considered that it does not belong to free nucleic acid present in the sample as contaminant. One plausible explanation which can be inferred in this case is that the dye (provided in kit from instrument's manufacturer) binds nonspecifically with the lipid contents of VLP and hence generates a synchronized signal. Second speculation is that this signal is observed due to the host cell genetic material trapped inside the HBsAg VLPs during the process of downstream. The encapsulation of host cell contents during self-assembly is a common problem encountered during VLP downstream processing [140, 141]. Since the contents of so-called Combo dye are confidential, it could not be ascertained that what the origin of nucleic acid PMT signal is.

4.3.5. Dynamic light scattering measurements

Light scattering provides information about the molecular mass and size of a protein in solution. It can nicely distinguish between the native and non-native biomolecules. In order to monitor the size of VLPs as a function of chaotropic molarity, experiments were carried out via dynamic light scattering (DLS) technique. Since the purpose was to confirm the trend observed in intrinsic fluorescence results, the conditions for the sample preparation were kept similar as those for the fluorescence studies.

4.3.5.1. Preliminary DLS studies

To begin with, HBsAg was treated with 6M of all three chaotropic salts and compared with native VLP scattering results. The initial results with DLS showed a similar trend in transition curve as that observed via intrinsic fluorescence. The gradual decrease in structural integrity and lack of a typical two-state mechanism are unanimously visible by both techniques. The VLP size by DLS measurement i.e. 12 nm (data not shown) was observed to be not in agreement with the TEM data. It was assumed that the discrepancy in size occurs because of a population in the solution other than VLP.

4.3.5.2. Discrepancy in VLP size via DLS

Since the production of VLP is a biosynthetic process, the presence of small molecular weight (SMW) species and aggregates cannot be rule out altogether. In principle, VLP self-assembly and aggregation exist simultaneously and in competition with each other [77]. Moreover storage of even a pure product in sterile conditions can still lead to the aggregation. Originally, it was not clear that whether this difference of size is because

of SMW species, mono-, di-, tri-, oligomer etc, or it is caused by the aggregates. In order to figure out these reasons, the sample was analyzed via electron microscopy. The TEM images showed the presence of a minor amount of aggregates, in addition to the VLPs still being the dominant population (data not shown).

4.3.5.3. Effect of SMW species

As TEM has arguably a size limitation of ~ 2 nm (depending on the staining procedure), it was not possible to verify the presence of monomer which has a theoretical size of 2.4 nm. The sample was filtered via spin column of cut-off size 300 kDa to remove the SMW species present, if any. The DLS measurements were repeated using the same protocol. Since no change in the trend and VLP size was observed (Figure 4.33), the presence of (substantial amount of) SMW species was ruled out. As a cross-check, the filtrate from the spin column was analyzed via DLS as well as SDS-PAGE. No significant amount of HBsAg or any other protein was observed in this fraction. The collective results of former experiment are shown in the figure 4.33.

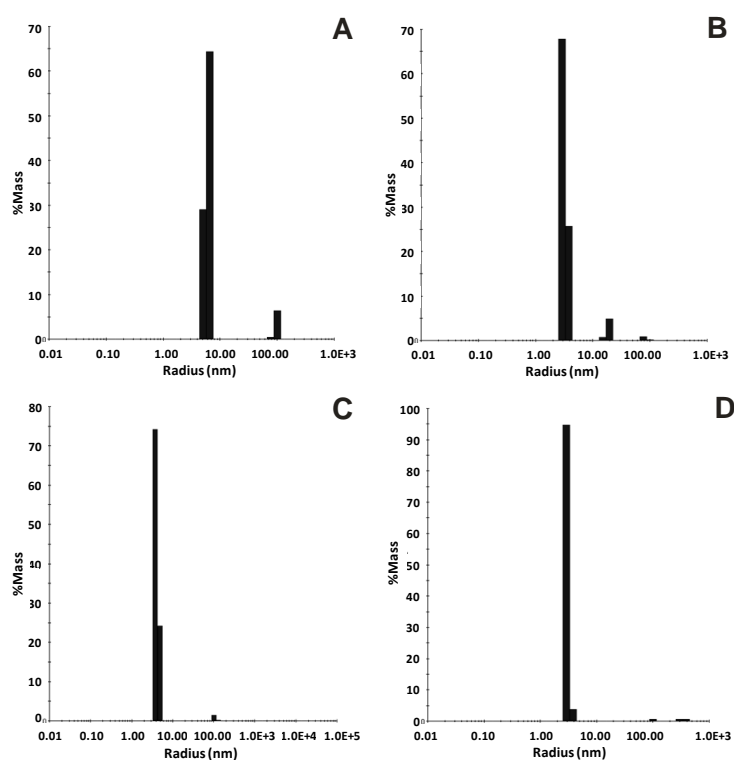


Figure 4.33. Histograms of the DLS measurements of native HBsAg VLPs (A) as well as in the presence of GdnSCN (B), KSCN (B) and GdnHCl (D). Note that in presence of denaturant, the size (diameter) has been shifted towards the left hand side of histogram. The results are presented in terms of scattering caused by the percentage mass.

It can be observed from the graph that the diameter of the VLPs is still smaller than the observed (as well as reported) diameter via EM techniques. Whereas, in case of HBsAg VLPs, it has been seen that diameter observed via DLS is bigger than that via TEM. The reason for this is probable dehydration of sample while the sample preparation [142].

4.3.5.4. Effect of aggregates

It has been proposed that the yeast-derived HBsAg in crude extract is highly prone to aggregation [143]. This is particularly because of the synthesis method of VLPs. The steps which involve concentration or removal of salts are usually performed via ultra filtration. Due to the protein-protein and protein-surface interactions during these steps, HBsAg tends to form aggregates. These aggregates still may retain the antigenicity; however during the aging the activity reduces to about 20 % [89, 102].

During DLS analysis of the sample devoid of SMW, the VLP size still does not coincide with the EM (as well as reported) data. DLS data indicates the presence of high molecular weight (HMW) specie (size ranging from 200 nm to 250 nm). The occurrence of this HMW specie is rather rare as compared to VLPs i.e. 1:20,000-30,000. The discrepancy in VLP size due to aggregation has been reported earlier by Kee *et al.* [108]

It is known that the presence of large aggregates causes strong scattering which presumably surpass the scattering caused by 22 nm particles. In DLS, the signal intensity is dominated by the size which may be the reason that the large size aggregate over-scatter the signal of smaller particles. This may mislead to the representation of size distribution, especially in case of a sample consisting of multiple populations. The variance in the HBsAg VLP size observed by DLS has been reported earlier by Kee *et al.* [108].

4.3.5.5. Optimized DLS measurement

DLS is a very convenient and useful technique but it provides more reliable and accurate results for samples consisting of a narrow size-distribution. Considering the previous observations, the purified product was filtered via a viva spin column of cut off 300 kDa to remove SMW species. Subsequently, this protein solution was filtered

via a membrane of cut-off $0.2\ \mu\text{m}$ to remove large size aggregates. DLS measurements were carried out according to the previously described protocol. The graph in figure 4.34 represents the observations found in optimized DLS evaluation. The fluorescence results from denaturation series are represented in figure 4.28.

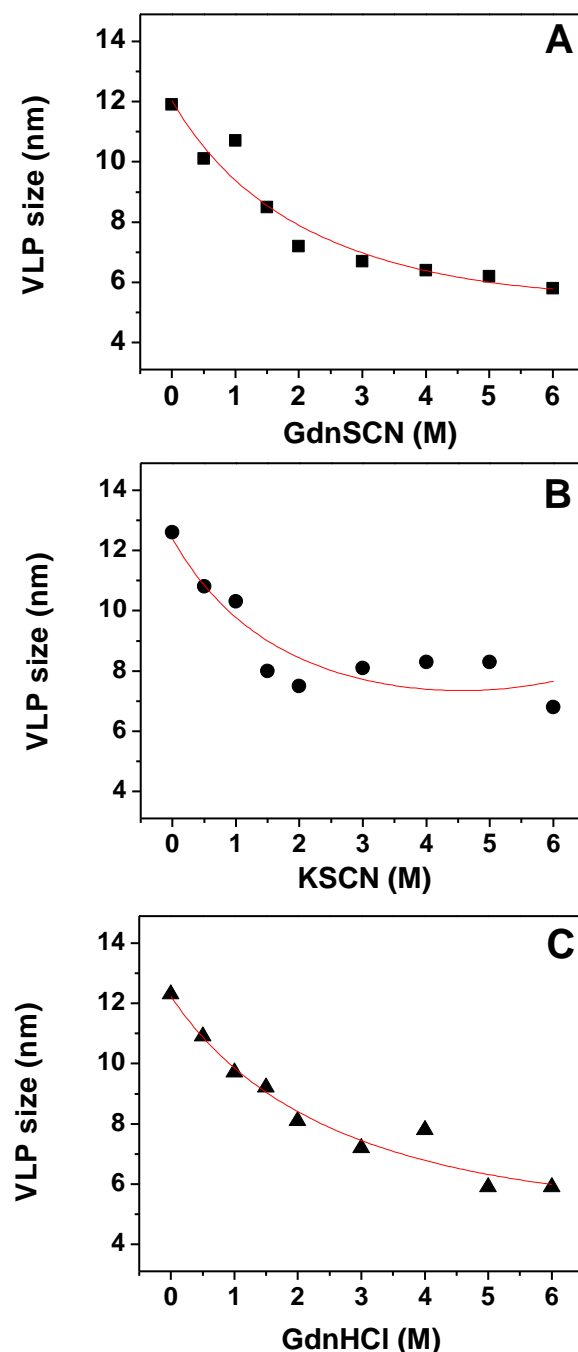


Figure 4.34. The effect of chaotropic salt on the VLP size (diameter) monitored via DLS. Three chaotropes were used for this study i.e., guanidine thiocyanate (panel A), potassium thiocyanate (panel B) and guanidine hydrochloride (panel C). The trend in each case is shown by a curve fitting.

In case of all three denaturants, a gradual decrease in the VLP size was observed. It can be seen that the curve here coincides with trend observed in the intrinsic fluorescence profile of HBsAg VLPs. Also here, no two-state mechanism could be observed. A hypothetical mechanism of defolding process, based on the denaturation curves, is presented in the figure 4.35.

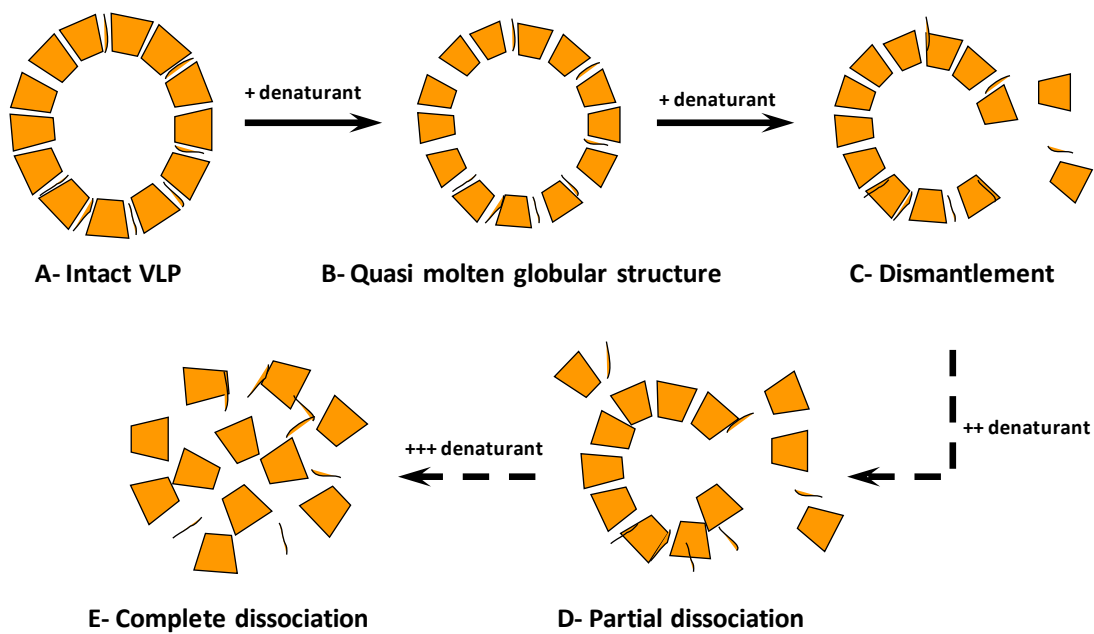


Figure 4.35. A pictorial explanation of the defolding process of VLPs in increasing concentration of denaturant. As a result of the defolding effect, the VLPs assume molten globular structure. As the concentration of denaturant increases, the subunits start to dismantle gradually, ultimately leading to denatured HBsAg subunits.

The general mechanism seems to be the gradual disruption of VLP structure, plausibly with several intermediates. Based on the intrinsic fluorescence data and above DLS measurements, it is suggested that under denaturing conditions, VLPs lose their structure slowly yet steadily. This may happen as a gradual detachment of subunits which results in complete disassembly of VLP and ultimately ends up in the presence of only randomly coiled structures.

4.3.6. Conclusion

Several spectral approaches were applied to monitor the structure of HBsAg VLPs. Initial fluorescence measurements suggest the dominance of tryptophan emission with less contributing signal from tyrosine residues. Time-resolved fluorescence spectroscopy measurements were used to calculate the Stern-Volmer relation. The Stern-Volmer plot connotes that most of fluorescing residues are present in

heterogeneous environment which is supported by the VLPs lipoprotein model in which phospholipids constitute a hydrophobic core and HBsAg subunit proteins are immersed in it.

The structural stability of VLPs was studied by adding a gradually increasing series of chaotrope. In this study three different chaotrope salts were used, namely GdnSCN, KSCN and GdnHCl. The changes in conformation and structure were observed via steady-state fluorescence microscopy. It was observed that the intrinsic fluorescence decrease gradually during the course of denaturing series with GdnSCN and KSCN. However, there was no evident change observed while treating with GdnHCl. Intrinsic properties did not show any considerable change during the treatment with GdnHCl. However, KSCN and GdnSCN transition curve showed a meager yet steady decrease in the fluorescence intensity.

In case of HBsAg VLPs, while treating with chaotropic reagents, no typical two-state unfolding curves were observed. A gradual decrease in intrinsic profile of fluorescence intensity suggests that the unfolding of HBsAg VLPs takes place via folding intermediate. On the basis of initial increase and further decrease in extrinsic fluorescence properties, it is suggested that a molten globular structure exists as folding intermediate.

The changes in VLP size during the denaturation curve were ascertained via DLS measurements as well. The data indicates a gradual decrease in the diameter, unlike a two-state mechanism as observed in most globular proteins. In this respect, DLS results verify the trend noticed in the intrinsic fluorescence properties of VLPs. It can be concluded that due to their distinctive structure, VLPs undergo denaturation process by several intermediates, which occur as a cascade of reactions involving gradual detachment of subunits. This is suggested on the basis of gradual decrease of VLP size as observed by the intrinsic fluorescence and the DLS measurements.

5. Summary and perspectives

Worldwide millions of people die and many more suffer from side effects of one or other disease. There is an old but still equally valid saying, “prevention is better than cure”. Vaccines play a major role in prevention of many illnesses every year. The concept of vaccination buds from 18th century by Edward Jenner whereafter it extended vastly. In traditional medication against a viral disease, mostly attenuated or inactivated vaccines have been used in the previous decade. In the last two to three decades, VLP vaccines have been in focus due to their better efficacy and safety aspects. VLP technology makes use of a particle which mimics the actual virus structurally, but lacks chiefly the genetic material. Therefore, VLP vaccines are much safer as well as equally effective. However, the self-assembly of VLPs has been a poorly discovered area.

It has been known that in bacterial and yeast-based systems, the VLPs do not occur inside the cell, which leads to the proposition that they may be formed during the purification process. In the work presented in this thesis, an effort has been made to figure out the stage(s) where VLP are formed during the downstream processing. Later the factors affecting the self-assembly have been scrutinized and structure-based stability studies have been scrutinized. Here HBsAg VLPs have been used as a model system.

The successful production and purification of HBsAg VLPs has been reported in this thesis. HBsAg was produced in *P. pastoris* GS115 cells with 8-copy cassette in a 10-L bioreactor using basal defined media. The cells were grown in batch mode with glycerol as sole carbon source. After the complete consumption of glycerol, methanol feed was started in fed-batch mode. The cultivation was harvested 136 h after induction at OD₆₀₀=330. During the cultivation, HBsAg production was confirmed by the Western blot and ELISA.

Multi-step downstream processing was applied to obtain the purified HBsAg. Cells were lysed using high-pressure homogenizer to release the intracellular contents. The lysate was subjected to PEG precipitation and the supernatant was proceeded with

adsorption on fumed silica (Aerosil® 380). The Aerosil eluate (supernatant) was bound on anionic exchange resin and the fractions containing HBsAg were pooled. The pooled HBsAg fraction was further purified by using size exclusion chromatography, to obtain only VLPs and remove non-VLP HBsAg. The main peak in 20% void volume indicates that large part consists of VLPs with a tailing consisting of non-VLP HBsAg as well as remaining HCPs. The fractions pertaining to VLPs were pooled and treated with KSCN to a final molarity of 1.2 M. The VLPs were dialyzed against PBS, pH 7.2 to remove the KSCN. The final product was examined via TEM to confirm the assembly of VLPs.

It is observed that a large amount of HBsAg is lost during the initial steps of purification, particularly, during PEG precipitation and adsorption and elution from the Aerosil. Further optimization is required to decrease the loss during these stages. It is recommended that PEG precipitation should be further optimized using various NaCl and PEG concentration to reduce the product loss. It might be interesting to try different sizes of PEG to get better recovery. Moreover different media for hydrophobic interactions should be tried out in order to achieve a higher yield of HBsAg.

Since the downstream process ensures formation of VLPs reproducibly, further step was to probe thoroughly the purification protocol. Samples were collected during purification procedure and analyzed via TEM. The TEM analysis showed that VLPs appear for the first time after the Aerosil elution (treatment based on hydrophobic interaction forces) and the morphology and the number improves drastically after the size exclusion chromatography where the non-VLP HBsAg is removed. A 12-fold increase in VLP count is observed from ion exchange chromatography to the gel filtration. The gradual development of VLP quality is also illustrated from the trend of clump formation to the individual VLPs at the end of downstream process. In general, the impurities decrease and the VLP count increase concurrently during the course of purification.

In order to pin point the crucial factors, several control experiments were performed in the presence and absence of purification buffers and HCCs. On the basis of quantitative examination of VLP morphology and count during these control experiments, it was concluded that although HBsAg is present in the lysate, the

rigorous buffer system and HCPs impede the self-assembly process. Moreover, the VLPs are dissociated more drastically in sample containing lysis buffer and crude lysate.

The lysis buffer contains two peculiar constituents i.e. Tween 20 and EDTA. The TEM control experiments with different combination of these both constituents show that Tween 20 and EDTA disturb the HBsAg arrangement existing in host cell ER. In absence of Tween 20 (CL-2), the clusters of agglomerated VLPs are frequently observed in the cell lysate. Moreover, some random distorted lamella are also seen which, due to their partially stacked structure, appear to be remnants of HBsAg lamella. It may be concluded that Tween 20, due to its detergent effect, helps to dissolve the agglomerates and therefore in its absence, these lamellar structures are present in the lysate.

It has been reported in the literature that HBsAg is present in form of striated lamellas intracellularly [75]. The TEM data indicates that in absence of EDTA, the typical HBsAg lamellas exist frequently in the lysate. EDTA, being a chelating agent, binds to the divalent cations stabilizing the ER membrane and helps in the release of HBsAg. However in the absence of EDTA, these lamellar structures retain their arrangement. The striated lamellar structures are not found in samples CL-1 and CL-2, i.e. in presence of EDTA. It may lead to the conclusion that Tween 20 as well as HCCs disrupt the lamellar arrangement.

Tween 20 or EDTA alone are not the decisive factors and hinder the assembly simultaneously. Additionally, the HCCs also execute negative effect on VLP assembly. However, further studies would be required to ascertain the specific effect of *P. pastoris* HCCs. It might be of interest to analyze the HBsAg VLPs in presence of certain groups of *P. pastoris* homologous proteins and enzymes to further ascertain the HCC effect. Moreover the production of HBsAg in other expression system and its comparison with HBsAg-producing *P. pastoris* lysate can provide advance insight.

The structural aspect of VLPs and their stability was monitored via defolding curves using GdnSCN, KSCN and GdnHCl. The changes were monitored via steady-state fluorescence spectroscopy. The intrinsic properties indicated that VLPs lack a two-state mechanism in defolding process. It was concluded that a quasi-molten-globule

structure exists as intermediate in VLP transition curve. The extrinsic fluorescence profile in presence of hydrophobic dye shows an initial increase and then decrease of intensity. This trend corresponds to first exposure of hydrophobic cavities to the dye and subsequent disruption thereof, as a function of chaotrope concentration. This transition trend was verified also via DLS measurements.

The DLS data affirms the absence of two-state kinetics which is quite plausible, keeping in view the intrinsic fluorescence data besides the characteristic structure of a VLP. It may be concluded that VLPs dissociate gradually in increasing molarity of denaturant till the whole structure is distorted. The size of HBsAg VLP via DLS shows as discrepancy of 8-10 nm. It has been proposed that presence of aggregated form leads to stronger scattering as compared to that caused by VLP which leads to an imprecise particle size. It is strongly recommended that further studies using multiangle light scattering (MALS) with field flow-fractionation (AF4) should be carried out. This system works on a similar principle as that of SEC except that the separation of different sized species is more accurate. The individual specie fractions should be monitored for defolding studies to obtain more authentic curve, devoid of any aggregate conflict.

6. References

1. World Health Organization, Hepatitis B Fact sheet N°204, 2008 August 2008 [cited 2012 June]; Available from: <http://www.who.int/mediacentre/factsheets/fs204/en/>.
2. Brooks, G.F., K.C. Carroll, J.S. Butel, and S.A. Morse, Medical Microbiology, 24th edition (Jawetz, Melnick, & Adelberg's Medical Microbiology). 24 ed. 2007: McGraw-Hill Medical.
3. Brunette, G.W., P.E. Kozarsky, A.J. Magill, D.R. Shlim, and A.D. Whatley, CDC Health information for international travel 2012. Chapter 3: Infectious diseases related to travel, ed. E.H. Teshale. 2012: Oxford University Press, Inc.,.
4. Lok, A.S.F. and B.J. McMahon, Chronic hepatitis B. *Hepatology*, 2001. **34**(6): p. 1225-1241.
5. Kudo, M., Viral hepatitis A to E: An update in 2010. *Intervirology*, 2010. **53**(1): p. 5-9.
6. Surveillance and prevention of hepatitis B and C in Europe. 2010, European Centre for Disease Prevention and Control (ECDC): Stockholm.
7. Lavanchy, D., Hepatitis B virus epidemiology, disease burden, treatment, and current and emerging prevention and control measures. *J Viral Hepatitis*, 2004. **11**(2): p. 97-107.
8. Lavanchy, D., Public health measures in the control of viral hepatitis: a World Health Organization perspective for the next millennium. *J Gastroenterol Hepatol*, 2002. **17 Suppl**: p. S452-9.
9. Qiao, Z.K., M.L. Halliday, J.G. Rankin, and R.A. Coates, Relationship between hepatitis B surface antigen prevalence, per capita alcohol consumption and primary liver cancer death rate in 30 countries. *J Clin Epidemiol*, 1988. **41**(8): p. 787-92.
10. Hepatitis B vaccines: WHO position paper--recommendations, in *Vaccine*. 2010. p. 589-90.
11. Michel, M.L. and P. Tiollais, Hepatitis B vaccines: Protective efficacy and therapeutic potential. *Pathol Biol*, 2010. **58**(4): p. 288-295.
12. Tiollais, P., P. Charnay, and G.N. Vyas, Biology of hepatitis B virus. *Science*, 1981. **213**(4506): p. 406-11.
13. Seeger, C. and W.S. Mason, Hepatitis B virus biology. *Microbiol Mol Biol R*, 2000. **64**(1): p. 51-+.
14. Robinson, W.S., Genome of hepatitis B virus. *Annu Rev Microbiol*, 1977. **31**: p. 357-377.
15. Cohen, B.J. and J.E. Richmond, Electron microscopy of hepatitis B core antigen synthesized in *Escherichia coli*. *Nature*, 1982. **296**(5858): p. 677-678.

16. Jilg, W., Novel hepatitis B vaccines. *Vaccine*, 1998. **16**: p. S65-S68.
17. Kabelitz, D. and S.H.E. Kaufmann, Immunology of infection. Third ed. *Methods in Microbiology*. Vol. 37. 2010: Elsevier Science.
18. Bertoletti, A. and A.J. Gehring, The immune response during hepatitis B virus infection. *J Gen Virol*, 2006. **87**: p. 1439-1449.
19. Alexopoulou, L., A.C. Holt, R. Medzhitov, and R.A. Flavell, Recognition of double-stranded RNA and activation of NF-kappa B by Toll-like receptor 3. *Nature*, 2001. **413**(6857): p. 732-738.
20. Huang, C.F., S.S. Lin, Y.C. Ho, F.L. Chen, and C.C. Yang, The immune response induced by hepatitis B virus principal antigens. *Cell Mol Immunol*, 2006. **3**(2): p. 97-106.
21. Neurath, A.R., S.B.H. Kent, N. Strick, and K. Parker, Identification and chemical synthesis of a host cell receptor binding site on hepatitis B virus. *Cell*, 1986. **46**(3): p. 429-436.
22. Cooper, A., N. Paran, and Y. Shaul, The earliest steps in hepatitis B virus infection. *BBA-Biomembranes*, 2003. **1614**(1): p. 89-96.
23. Urban, S., A. Schulze, M. Dandri, and J. Petersen, The replication cycle of hepatitis B virus. *J Hepatol*, 2010. **52**(2): p. 282-284.
24. Butel, J.S., T.H. Lee, and B.L. Slagle, Is the DNA repair system involved in hepatitis B virus-mediated hepatocellular carcinogenesis? *Trends Microbiol*, 1996. **4**(7): p. 285-285.
25. Blumberg, B.S., H.J. Alter, and S. Visnich, A new antigen in leukemia sera. *JAMA-J Am Med Assoc*, 1965. **191**(7): p. 541-&.
26. Zuckerman, A.J., The development of novel hepatitis B vaccines. *B World Health Organ*, 1987. **65**(3): p. 265-275.
27. Paran, N., B. Geiger, and Y. Shaul, HBV infection of cell culture: evidence for multivalent and cooperative attachment. *EMBO J*, 2001. **20**(16): p. 4443-4453.
28. Guha, C., S. Mohan, N. Roy-Chowdhury, and J. Roy-Chowdhury, Cell culture and animal models of viral hepatitis. Part I: Hepatitis B. *Lab Animal*, 2004. **33**(7): p. 37-46.
29. Zuckerman, A.J., Novel hepatitis B vaccines. *J Infection*, 1986. **13**: p. 61-71.
30. Peterson, D.L., The structure of hepatitis B surface antigen and its antigenic sites. *Bioessays*, 1987. **6**(6): p. 258-262.
31. Kutzler, M.A. and D.B. Weiner, DNA vaccines: ready for prime time? *Nat Rev Genet*, 2008. **9**(10): p. 776-88.
32. Bhowmik, T., B. D'Souza, M.N. Uddin, and M.J. D'Souza, Oral delivery of microparticles containing plasmid DNA encoding hepatitis-B surface antigen. *J Drug Target*, 2012. **20**(4): p. 364-371.
33. Itoh, Y., E. Takai, H. Ohnuma, K. Kitajima, F. Tsuda, A. Machida, S. Mishiro, T. Nakamura, Y. Miyakawa, and M. Mayumi, A synthetic peptide vaccine involving the product of the pre-S(2) region of hepatitis B virus DNA - protective efficacy in chimpanzees. *P Natl Acad Sci USA*, 1986. **83**(23): p. 9174-9178.

34. Choi, Y.C., J. Kim, M.-H. Yu, and M.H. Han, Expression of hepatitis B virus surface antigen gene in *E. coli*. *Korean J Biochem*, 1986. **19**(4): p. 377-382.
35. Fujisawa, Y., Y. Ito, R. Sasada, Y. Ono, K. Igarashi, R. Marumoto, M. Kikuchi, and Y. Sugino, Direct expression of hepatitis B surface antigen gene in *E. coli*. *Nucleic Acids Res*, 1983. **11**(11): p. 3581-91.
36. Roldao, A., M.C. Mellado, L.R. Castilho, M.J. Carrondo, and P.M. Alves, Virus-like particles in vaccine development. *Expert Rev Vaccines*, 2010. **9**(10): p. 1149-76.
37. Gilbert, R.J.C., L. Beales, D. Blond, M.N. Simon, B.Y. Lin, F.V. Chisari, D.I. Stuart, and D.J. Rowlands, Hepatitis B small surface antigen particles are octahedral. *P Natl Acad Sci USA*, 2005. **102**(41): p. 14783-14788.
38. Pasek, M., T. Goto, W. Gilbert, B. Zink, H. Schaller, P. MacKay, G. Leadbetter, and K. Murray, Hepatitis B virus genes and their expression in *E. coli*. *Nature*, 1979. **282**(5739): p. 575-9.
39. Burrell, C.J., P. Mackay, P.J. Greenaway, P.H. Hofschneider, and K. Murray, Expression in *Escherichia coli* of hepatitis B virus DNA sequences cloned in plasmid-Pbr322. *Nature*, 1979. **279**(5708): p. 43-47.
40. McAleer, W.J., E.B. Buynak, R.Z. Maigetter, D.E. Wampler, W.J. Miller, and M.R. Hilleman, Human hepatitis B vaccine from recombinant yeast. *Nature*, 1984. **307**(5947): p. 178-180.
41. Valenzuela, P., A. Medina, and W.J. Rutter, Synthesis and assembly of hepatitis B virus surface antigen particles in yeast. *Nature*, 1982. **298**(5872): p. 347-350.
42. Miyanojara, A., A. Tohe, C. Nozaki, F. Hamada, N. Ohtomo, and K. Matsubara, Expression of hepatitis B surface-antigen gene in yeast. *P Natl Acad Sci USA*, 1983. **80**(1): p. 1-5.
43. Heijntink, R.A., P. Bergen, K. Melber, Z.A. Janowicz, and A.D. Osterhaus, Hepatitis B surface antigen (HBsAg) derived from yeast cells (*Hansenula polymorpha*) used to establish an influence of antigenic subtype (*adw2*, *adr*, *ayw3*) in measuring the immune response after vaccination. *Vaccine*, 2002. **20**(17-18): p. 2191-6.
44. Pluddemann, A. and W.H. Van Zyl, Evaluation of *Aspergillus niger* as host for virus-like particle production, using the hepatitis B surface antigen as a model. *Curr Genet*, 2003. **43**(6): p. 439-46.
45. Gellissen, G., Heterologous protein production in methylotrophic yeasts. *Appl Microbiol Biot*, 2000. **54**(6): p. 741-50.
46. Schuster, E., N. Dunn-Coleman, J.C. Frisvad, and P.W.M. van Dijck, On the safety of *Aspergillus niger* - a review. *Appl Microbiol Biot*, 2002. **59**(4-5): p. 426-435.
47. Kunke, D., J. Broucek, L. Kutinova, S. Nemeckova, V. Ludvikova, I. Strnad, J. Kramosil, J. Nemcova, J. Schramlova, V. Simonova, and V. Vonka, Vaccinia virus recombinants coexpressing hepatitis B virus surface and core antigens. *Virology*, 1993. **195**(1): p. 132-139.

48. Smith, M.L., H.S. Mason, and M.L. Shuler, Hepatitis B surface antigen (HBsAg) expression in plant cell culture: Kinetics of antigen accumulation in batch culture and its intracellular form. *Biotechnol Bioeng*, 2002. **80**(7): p. 812-22.
49. Huang, Z., G. Elkin, B.J. Maloney, N. Beuhner, C.J. Arntzen, Y. Thanavala, and H.S. Mason, Virus-like particle expression and assembly in plants: hepatitis B and Norwalk viruses. *Vaccine*, 2005. **23**(15): p. 1851-8.
50. Gomez, E., S.C. Zoth, and A. Berinstein, Plant-based vaccines for potential human application: a review. *Hum Vaccin*, 2009. **5**(11): p. 738-44.
51. Shouval, D., Y. Ilan, R. Adler, R. Deepen, A. Panet, Z. Evenchen, M. Gorecki, and W.H. Gerlich, Improved immunogenicity in mice of a mammalian cell-derived recombinant hepatitis B vaccine containing Pre-S1 and Pre-S2 antigens as compared with conventional yeast-derived vaccines. *Vaccine*, 1994. **12**(15): p. 1453-1459.
52. Diminsky, D., R. Schirmbeck, J. Reimann, and Y. Barenholz, Comparison between hepatitis B surface antigen (HBsAg) particles derived from mammalian cells (CHO) and yeast cells (*Hansenula polymorpha*): composition, structure and immunogenicity. *Vaccine*, 1997. **15**(6-7): p. 637-47.
53. Deml, L., R. Schirmbeck, J. Reimann, H. Wolf, and R. Wagner, Purification and characterization of hepatitis B virus surface antigen particles produced in *Drosophila Schneider*-2 cells. *J Virol Methods*, 1999. **79**(2): p. 205-17.
54. Hitzeman, R.A., C.Y. Chen, F.E. Hagie, E.J. Patzer, C.C. Liu, D.A. Estell, J.V. Miller, A. Yaffe, D.G. Kleid, A.D. Levinson, and H. Oppermann, Expression of hepatitis B virus surface antigen in yeast. *Nucleic Acids Res*, 1983. **11**(9): p. 2745-63.
55. Ogata, K., Nishikaw.H, and M. Ohsugi, A yeast capable of utilizing methanol. *Agr Biol Chem Tokyo*, 1969. **33**(10): p. 1519-&.
56. Cregg, J.M. and J.L. Cereghino, Heterologous protein expression in the methylotrophic yeast *Pichia pastoris*. *Fems Microbiol Rev*, 2000. **24**(1): p. 45-66.
57. Cereghino, G.P.L., J.L. Cereghino, C. Ilgen, and J.M. Cregg, Production of recombinant proteins in fermenter cultures of the yeast *Pichia pastoris*. *Curr Opin Biotech*, 2002. **13**(4): p. 329-332.
58. Daly, R. and M.T.W. Hearn, Expression of heterologous proteins in *Pichia pastoris*: a useful experimental tool in protein engineering and production. *J Mol Recognit*, 2005. **18**(2): p. 119-138.
59. Macauley-Patrick, S., M.L. Fazenda, B. McNeil, and L.M. Harvey, Heterologous protein production using the *Pichia pastoris* expression system. *Yeast*, 2005. **22**(4): p. 249-270.
60. Vassileva, A., D.A. Chugh, S. Swaminathan, and N. Khanna, Expression of hepatitis B surface antigen in the methylotrophic yeast *Pichia pastoris* using the GAP promoter. *J Biotechnol*, 2001. **88**(1): p. 21-35.

61. Norden, K., M. Agemark, J.A. Danielson, E. Alexandersson, P. Kjellbom, and U. Johanson, Increasing gene dosage greatly enhances recombinant expression of aquaporins in *Pichia pastoris*. *Bmc Biotechnology*, 2011. **11**.
62. Mattanovich, D., H. Hohenblum, B. Gasser, M. Maurer, and N. Borth, Effects of gene dosage, promoters, and substrates on unfolded protein stress of recombinant *Pichia pastoris*. *Biotechnol Bioeng*, 2004. **85**(4): p. 367-375.
63. Guo, M.J., T.C. Zhu, Y.P. Zhuang, J. Chu, and S.L. Zhang, Understanding the effect of foreign gene dosage on the physiology of *Pichia pastoris* by transcriptional analysis of key genes. *Appl Microbiol Biot*, 2011. **89**(4): p. 1127-1135.
64. Palucha, A., A. Loniewska, S. Satheshkumar, A.M. Boguszewska-Chachulska, M. Umashankar, M. Milner, A.L. Haenni, and H.S. Savithri, Virus-like particles: Models for assembly studies and foreign epitope carriers. *Prog Nucleic Acid Re*, 2005. **80**: p. 135-168.
65. Shang, W.L., J. Liu, J. Yang, Z. Hu, and X.C. Rao, Dengue virus-like particles: construction and application. *Appl Microbiol Biot*, 2012. **94**(1): p. 39-46.
66. Kadish, A.S., Recombinant virus-like particles retain conformational epitopes of native human papillomaviruses and may be useful for vaccine development. *Gynecol Oncol*, 1994. **55**(1): p. 10-2.
67. Yao, Q., F.M. Kuhlmann, R. Eller, R.W. Compans, and C. Chen, Production and characterization of simian--human immunodeficiency virus-like particles. *AIDS Res Hum Retroviruses*, 2000. **16**(3): p. 227-36.
68. Roy, P. and R. Noad, Virus-like particles as immunogens. *Trends Microbiol*, 2003. **11**(9): p. 438-444.
69. Grgacic, E.V. and D.A. Anderson, Virus-like particles: passport to immune recognition. *Methods*, 2006. **40**(1): p. 60-5.
70. Jennings, G.T. and M.F. Bachmann, The coming of age of virus-like particle vaccines. *Biol Chem*, 2008. **389**(5): p. 521-36.
71. Ludwig, C. and R. Wagner, Virus-like particles-universal molecular toolboxes. *Curr Opin Biotechnol*, 2007. **18**(6): p. 537-45.
72. Patzer, E.J., G.R. Nakamura, and A. Yaffe, Intracellular transport and secretion of hepatitis B surface antigen in mammalian cells. *J Virol*, 1984. **51**(2): p. 346-353.
73. Kamimura, T., A. Yoshikawa, F. Ichida, and H. Sasaki, Electron microscopic studies of Dane particles in hepatocytes with special reference to intracellular development of Dane particles and their relation with Hbeag in serum. *Hepatology*, 1981. **1**(5): p. 392-397.
74. Patzer, E.J., G.R. Nakamura, C.C. Simonsen, A.D. Levinson, and R. Brands, Intracellular assembly and packaging of hepatitis B surface antigen particles occur in the endoplasmic reticulum. *J Virol*, 1986. **58**(3): p. 884-892.
75. Lunsdorf, H., C. Gurrnkonda, A. Adnan, N. Khanna, and U. Rinas, Virus-like particle production with yeast: ultrastructural and immunocytochemical insights into *Pichia pastoris* producing high levels of the Hepatitis B surface antigen. *Microb Cell Fact*, 2011. **10**(1): p. 48.

76. Mellado, M.C.M., J.A. Mena, A. Lopes, O.T. Ramirez, M.J.T. Carrondo, L.A. Palomares, and P.M. Alves, Impact of physicochemical parameters on *in vitro* assembly and disassembly kinetics of recombinant triple-layered rotavirus-like particles. *Biotechnol Bioeng*, 2009. **104**(4): p. 674-686.
77. Ding, Y., Y.P. Chuan, L.Z. He, and A.P.J. Middelberg, Modeling the competition between aggregation and self-assembly during virus-like particle processing. *Biotechnol Bioeng*, 2010. **107**(3): p. 550-560.
78. Salunke, D.M., D.L.D. Caspar, and R.L. Garcea, Polymorphism in the assembly of polyomavirus capsid protein Vp1. *Biophys J*, 1989. **56**(5): p. 887-900.
79. Katen, S.P., S.R. Chirapu, M.G. Finn, and A. Zlotnick, Trapping of hepatitis B virus capsid assembly intermediates by phenylpropenamide assembly accelerators. *ACS Chem Biol*, 2010. **5**(12): p. 1125-1136.
80. Moisant, P., H. Neeman, and A. Zlotnick, Exploring the paths of (virus) assembly. *Biophys J*, 2010. **99**(5): p. 1350-1357.
81. Gavilanes, F., J.M. Gonzalezros, and D.L. Peterson, Structure of hepatitis B surface antigen - characterization of the lipid components and their association with the viral proteins. *J Biol Chem*, 1982. **257**(13): p. 7770-7777.
82. Greiner, V.J., C. Egele, S. Oncul, F. Ronzon, C. Manin, A. Klymchenko, and Y. Mely, Characterization of the lipid and protein organization in HBsAg viral particles by steady-state and time-resolved fluorescence spectroscopy. *Biochimie*, 2010. **92**(8): p. 994-1002.
83. Gavilanes, F., J. Gomez-Gutierrez, M. Aracil, J.M. Gonzalez-Ros, J.A. Ferragut, E. Guerrero, and D.L. Peterson, Hepatitis B surface antigen. Role of lipids in maintaining the structural and antigenic properties of protein components. *Biochem J*, 1990. **265**(3): p. 857-64.
84. Zhou, W., J. Bi, J.C. Janson, Y. Li, Y. Huang, Y. Zhang, and Z. Su, Molecular characterization of recombinant hepatitis B surface antigen from Chinese hamster ovary and *Hansenula polymorpha* cells by high-performance size exclusion chromatography and multi-angle laser light scattering. *J Chromatogr B Analyt Technol Biomed Life Sci*, 2006. **838**(2): p. 71-7.
85. Peterson, D.L., N. Nath, and F. Gavilanes, Structure of hepatitis B surface antigen - Correlation of subtype with amino acid sequence and location of the carbohydrate moiety. *J Biol Chem*, 1982. **257**(17): p. 414-420.
86. Zhao, Q.J., Y. Wang, D. Abraham, V. Towne, R. Kennedy, and R.D. Sitrin, Real time monitoring of antigenicity development of HBsAg virus-like particles (VLPs) during heat- and redox-treatment. *Biochem Bioph Res Co*, 2011. **408**(3): p. 447-453.
87. Carman, W.F., The clinical significance of surface antigen variants of hepatitis B virus. *J Viral Hepatitis*, 1997. **4**: p. 11-20.
88. Wynne, S.A., R.A. Crowther, and A.G.W. Leslie, The crystal structure of the human hepatitis B virus capsid. *Mol Cell*, 1999. **3**(6): p. 771-780.
89. Li, Y., J.X. Bi, W.B. Zhou, Y.D. Huang, L.J. Sun, A.P. Zeng, G.H. Ma, and Z.G. Su, Characterization of the large size aggregation of Hepatitis B virus

- surface antigen (HBsAg) formed in ultrafiltration process. *Process Biochem*, 2007. **42**(3): p. 315-319.
90. Vassileva, A., D.A. Chugh, S. Swaminathan, and N. Khanna, Effect of copy number on the expression levels of hepatitis B surface antigen in the methylotrophic yeast *Pichia pastoris*. *Protein Expres Purif*, 2001. **21**(1): p. 71-80.
91. Vanz, A.L., H. Lünsdorf, A. Adnan, M. Nimtz, C. Gurramkonda, N. Khanna, and U. Rinas, Physiological response of *Pichia pastoris* GS115 to methanol-induced high level production of the Hepatitis B surface antigen: catabolic adaptation, stress responses, and autophagic processes. *Microb Cell Fact*. **11**(1): p. 103.
92. Cregg, J.M., J.F. Tschopp, C. Stillman, R. Siegel, M. Akong, W.S. Craig, R.G. Buckholz, K.R. Madden, P.A. Kellaris, G.R. Davis, B.L. Smiley, J. Cruze, R. Torregrossa, G. Velicelebi, and G.P. Thill, High-level expression and efficient assembly of hepatitis B surface antigen in the methylotrophic yeast, *Pichia pastoris*. *Bio-Technol*, 1987. **5**(5): p. 479-485.
93. Gurramkonda, C., A. Adnan, T. Gabel, H. Lunsdorf, A. Ross, S.K. Nemani, S. Swaminathan, N. Khanna, and U. Rinas, Simple high-cell density fed-batch technique for high-level recombinant protein production with *Pichia pastoris*: Application to intracellular production of Hepatitis B surface antigen. *Microb Cell Fact*, 2009. **8**.
94. Pointek, M. and M. Weniger, Method for obtaining recombinant HBsAg. Aug 6, 2002. **US 6,428,984 B1**(09/701,197).
95. Candiano, G., M. Bruschi, L. Musante, L. Santucci, G.M. Ghiggeri, B. Carnemolla, P. Orecchia, L. Zardi, and P.G. Righetti, Blue silver: A very sensitive colloidal Coomassie G-250 staining for proteome analysis. *Electrophoresis*, 2004. **25**(9): p. 1327-1333.
96. Paulij, W.P., P.L. de Wit, C.M. Sunnen, M.H. van Roosmalen, A. Petersen-van Ettehoven, M.P. Cooreman, and R.A. Heijntink, Localization of a unique hepatitis B virus epitope sheds new light on the structure of hepatitis B virus surface antigen. *J Gen Virol*, 1999. **80**: p. 2121-6.
97. O'Keefe, D.O. and A.M. Paiva, Assay for recombinant hepatitis B surface antigen using reversed-phase high-performance liquid chromatography. *Anal Biochem*, 1995. **230**(1): p. 48-54.
98. Rasband, W., ImageJ. 1997-2005, U.S. National Institutes of Health, Bethesda, MD.
99. Yamamoto, K.R., B.M. Alberts, R. Benzinger, L. Lawhorne, and G. Treiber, Rapid bacteriophage sedimentation in the presence of polyethylene glycol and its application to large-scale virus purification. *Virology*, 1970. **40**(3): p. 734-744.
100. Polson, A., A theory for the displacement of proteins and viruses with polyethylene glycol. *Prep Biochem*, 1977. **7**(2): p. 129-154.
101. Wampler, D.E., E.D. Lehman, J. Boger, W.J. McAleer, and E.M. Scolnick, Multiple chemical forms of hepatitis B surface antigen produced in yeast. *P Natl Acad Sci USA*, 1985. **82**(20): p. 6830-4.

102. Tleugabulova, D., V. Falcon, M. Sewer, and E. Penton, Aggregation of recombinant hepatitis B surface antigen in *Pichia pastoris*. *J Chromatogr B*, 1998. **716**(1-2): p. 209-219.
103. Mukherjee, S., M.V. Thorsteinsson, L.B. Johnston, P.A. DePhillips, and A. Ziotnick, A quantitative description of *in vitro* assembly of human papillomavirus 16 virus-like particles. *J Mol Biol*, 2008. **381**(1): p. 229-237.
104. Hanslip, S.J., N.R. Zaccai, A.P. Middelberg, and R.J. Falconer, Assembly of human papillomavirus type-16 virus-like particles: multifactorial study of assembly and competing aggregation. *Biotechnol Prog*, 2006. **22**(2): p. 554-60.
105. Ausar, S.F., T.R. Foubert, M.H. Hudson, T.S. Vedvick, and C.R. Middaugh, Conformational stability and disassembly of Norwalk virus-like particles - Effect of pH and temperature. *J Biol Chem*, 2006. **281**(28): p. 19478-19488.
106. Chuan, Y.P., L.H.L. Lua, and A.P.J. Middelberg, High-level expression of soluble viral structural protein in *Escherichia coli*. *J Biotechnol*, 2008. **134**(1-2): p. 64-71.
107. Creighton, T.E., *Protein Structure: A Practical Approach*. The practical approach series, ed. D. Rickwood. 1997, Oxford, England: IRL Press at Oxford University Press.
108. Kee, G.S., N.S. Pujar, and N.J. Titchener-Hooker, Study of detergent-mediated liberation of hepatitis B virus-like particles from *S. cerevisiae* homogenate: identifying a framework for the design of future generation lipoprotein vaccine processes. *Biotechnol Progr*, 2008. **24**(3): p. 623-31.
109. Sarciaux, J.M., S. Mansour, M.J. Hageman, and S.L. Nail, Effects of buffer composition and processing conditions on aggregation of bovine IgG during freeze-drying. *J Pharm Sci*, 1999. **88**(12): p. 1354-1361.
110. Jones, L.S., T.W. Randolph, U. Kohnert, A. Papadimitriou, G. Winter, M.L. Hagmann, M.C. Manning, and J.F. Carpenter, The effects of tween 20 and sucrose on the stability of anti-L-selectin during lyophilization and reconstitution. *J Pharm Sci*, 2001. **90**(10): p. 1466-1477.
111. Patil, A. and N. Khanna, Novel membrane extraction procedure for the purification of hepatitis B surface antigen from *Pichia pastoris*. *J Chromatogr B*, 2012. **898**: p. 7-14.
112. Elferink, J.G., The effect of ethylenediaminetetraacetic acid on yeast cell membranes. *Protoplasma*, 1974. **80**(1): p. 261-8.
113. Jackson, C., M. Adedokun, E. Etim, A. Agboke, I. Jackson, and E. Ibezim, Effect of EDTA on the activity of ciprofloxacin against *Shigella sonnei*. *Res Pharm Biotech*, 2011. **3** (2): p. 22-24.
114. Vaara, M., Agents that increase the permeability of the outer membrane. *Microbiol Rev*, 1992. **56**(3): p. 395-411.
115. Kee, G.S., J. Jin, B. Balasundaram, D.G. Bracewell, N.S. Pujar, and N.J. Titchener-Hooker, Exploiting the Intracellular compartmentalization characteristics of the *S. cerevisiae* host cell for enhancing primary purification of lipid-envelope virus-like particles. *Biotechnol Progr*, 2010. **26**(1): p. 26-33.
116. Lakowicz, J.R., *Principles of fluorescence spectroscopy*. 3 ed. 2006: Springer.

117. Vivian, J.T. and P.R. Callis, Mechanisms of tryptophan fluorescence shifts in proteins. *Biophys J*, 2001. **80**(5): p. 2093-2109.
118. Hawe, A., M. Sutter, and W. Jiskoot, Extrinsic fluorescent dyes as tools for protein characterization. *Pharmaceut Res*, 2008. **25**(7): p. 1487-1499.
119. Zhao, Q., Y. Wang, D. Freed, T.M. Fu, J.A. Gimenez, R.D. Sitrin, and M.W. Washabaugh, Maturation of recombinant hepatitis B virus surface antigen particles. *Hum Vaccin*, 2006. **2**(4): p. 174-80.
120. Hof, M., R. Hutterer, and V. Fidler, Fluorescence spectroscopy in biology: advanced methods and their applications to membranes, proteins, DNA, and cells, ed. **O.S. Wolfbeis**. 2005: Springer.
121. Stryer, L., The interaction of a naphthalene dye with apomyoglobin and apohemoglobin. A fluorescent probe of non-polar binding sites. *J Mol Biol*, 1965. **13**(2): p. 482-95.
122. Cardamone, M. and N.K. Puri, Spectrofluorimetric assessment of the surface hydrophobicity of proteins. *Biochem J*, 1992. **282** (Pt 2): p. 589-93.
123. Pande, M., V.K. Dubey, V. Sahu, and M.V. Jagannadham, Conformational plasticity of cryptolepain: Accumulation of partially unfolded states in denaturants induced equilibrium unfolding. *J Biotechnol*, 2007. **131**(4): p. 404-417.
124. Ptitsyn, O.B., R.H. Pain, G.V. Semisotnov, E. Zerovnik, and O.I. Razgulyaev, Evidence for a molten globule state as a general intermediate in protein folding. *FEBS Lett*, 1990. **262**(1): p. 20-24.
125. Baldwin, R.L. and G.D. Rose, Is protein folding hierarchic? I. Local structure and peptide folding. *Trends Biochem Sci*, 1999. **24**(1): p. 26-33.
126. Bechtel, W.J. and J.A. Schellman, Protein stability curves. *Biopolymers*, 1987. **26**(11): p. 1859-1877.
127. Collins, K.D., Charge density-dependent strength of hydration and biological structure. *Biophys J*, 1997. **72**(1): p. 65-76.
128. Mach, H., D.B. Volkin, R.D. Troutman, B. Wang, Z. Luo, K.U. Jansen, and L. Shi, Disassembly and reassembly of yeast-derived recombinant human papillomavirus virus-like particles (HPV VLPs). *J Pharm Sci*, 2006. **95**(10): p. 2195-2206.
129. Ahmad, F., S. Yadav, and S. Taneja, Determining stability of proteins from guanidinium chloride transition curves. *Biochem J*, 1992. **287**: p. 481-485.
130. Greene, R.F. and C.N. Pace, Urea and guanidine hydrochloride denaturation of ribonuclease, lysozyme, alpha-chymotrypsin, and beta-lactoglobulin. *J Biol Chem*, 1974. **249**(17): p. 5388-5393.
131. Myers, J.K., C.N. Pace, and J.M. Scholtz, Denaturant M-values and heat-capacity changes - relation to changes in accessible surface-areas of protein unfolding. *Protein Sci*, 1995. **4**(10): p. 2138-2148.
132. Creighton, T.E., How important is the molten globule for correct protein folding? *Trends Biochem Sci*, 1997. **22**(1): p. 6-10.

133. Kuwajima, K., Protein folding *in vitro*. *Curr Opin Biotech*, 1992. **3**(5): p. 462-467.
134. Dill, K.A. and D. Shortle, Denatured states of proteins. *Annu Rev Biochem*, 1991. **60**: p. 795-825.
135. Zlotnick, A., P. Ceres, S. Singh, and J.M. Johnson, A small molecule inhibits and misdirects assembly of hepatitis B virus capsids. *J Virol*, 2002. **76**(10): p. 4848-4854.
136. Edwin, F. and M.V. Jagannadham, Sequential unfolding of papain in molten globule state. *Biochem Biophys Res Co*, 1998. **252**(3): p. 654-660.
137. Greenham, L.W. and E.O. Caul, Application of potassium thiocyanate as a destaining agent for confirming the specificity of viral immunofluorescence. *J Clin Microbiol*, 1982. **16**(5): p. 803-7.
138. Albani, J.R., Principles and applications of fluorescence spectroscopy. 2007: Blackwell Science.
139. Eftink, M.R. and C.A. Ghiron, Exposure of tryptophanyl residues in proteins - quantitative-determination by fluorescence quenching studies. *Biochemistry*, 1976. **15**(3): p. 672-680.
140. Pattenden, L.K., A.P.J. Middelberg, M. Niebert, and D.I. Lipin, Towards the preparative and large-scale precision manufacture of virus-like particles. *Trends Biotechnol*, 2005. **23**(10): p. 523-529.
141. Bundy, B.C., M.J. Franciszkowicz, and J.R. Swartz, Escherichia coli-based cell-free synthesis of virus-like particles. *Biotechnol Bioeng*, 2008. **100**(1): p. 28-37.
142. Kanno, T., T. Yamada, H. Iwabuki, H. Tanaka, S. Kuroda, K. Tanizawa, and T. Kawai, Size distribution measurement of vesicles by atomic force microscopy. *Anal Biochem*, 2002. **309**(2): p. 196-199.
143. Tleugabulova, D., V. Falcon, E. Penton, M. Sewer, and Y. Fleitas, Aggregation of recombinant hepatitis B surface antigen induced *in vitro* by oxidative stress. *J Chromatogr B*, 1999. **736**(1-2): p. 153-166.

7. Appendix

Abbreviation	Augmentation
<i>A. niger</i>	<i>Aspegillus niger</i>
BCA	Bicinchoninic acid
Bis-ANS	4,4'-Dianilino-1,1'-Binaphthyl-5,5'-Disulfonic Acid, dipotassium Salt
BMG	Buffered minimum glycerol
BMGY	Buffered glycerol-complex medium
BMM	Buffered minimal methanol
BMMY	Buffered methanol-complex medium
cccDNA	covalently-closed circular DNA
CHO cells	Chinese hamster ovary cells
DCs	Dendritic cells
DEAE	Diethylethanolamine
DLS	Dynamic light scattering
DM	Defined media
DO	Dissolved oxygen
<i>E. coli</i>	<i>Escherichia coli</i>
EDTA	Ethylenediaminetetraacetic acid
ELISA	Enzyme-linked immunosorbent assay
ER	Endoplasmic reticulum
FPLC	Fast protein liquid chromatography
GdnHCl	Guanidine hydrochloride
GdnSCN	Guanidine thiocyanate
GF	Gel filtration
HBcAg	Hepatitis B core antigen
HBsAg	Hepatitis B surface antigen
HBV	Hepatitis B virus
HCC	Host cell component
HCP	Host cell protein
HI	Hydrophobic interactions

HIS ⁴	Histidine (requiring auxotroph)
HMW	High molecular weight
IEX	Ion exchange chromatography
IgM	Immunoglobulin M
KDa	Kilo dalton
KSCN	Potassium thiocyanate
LHBs	Large Hepatitis B protein
MeOH	Methanol
MHBs	Middle Hepatitis B protein
Mut ⁺	Methanol utilization plus (phenotype)
Mut ^S	Methanol utilization slow (phenotype)
MWCO	Molecular weight cut off
OD	Optical density
<i>P. pastoris</i>	<i>Pichia pastoris</i>
PB	Phosphate buffer
PBS	Phosphate buffered saline
PEG	Polyethylene glycol
RP-HPLC	Reverse phase-high performance liquid chromatography
rpm	Revolutions per minute
RT	Room temperature
SDS-PAGE	Sodium dodecyl sulfate polyacrylamide gel electrophoresis
SEC	Size exclusion chromatography
SEM	Scanning electron microscopy
Semi-DM	Semi defined medium
SMW	Small molecular weight
TEM	Transmission electron microscopy
VLP	virus-like particle
VP	Viral particle
WHO	World health organization
YNB	Yeast nitrogen base
YTM	Yeast trace metal elements

Chemicals**Manufacturer**

All common lab reagents used were purchased Sigma-Aldrich unless stated otherwise. Here only some specific reagents are mentioned.

Histidine	Sigma-Aldrich Chemie GmbH, Germany
TEGO® Antifoam KS911	Evonik Industries AG, Germany
Tween 20 (for synthesis)	Merck Schuchardt OHD, Germany
EDTA (disodium salt)	Sigma-Aldrich Chemie GmbH, Germany
Bis-ANS	Sigma-Aldrich Chemie GmbH, Germany
Guanidine thiocyanate	Sigma-Aldrich Chemie GmbH, Germany
Guanidine hydrochloride	Sigma-Aldrich Chemie GmbH, Germany
Potassium thiocyanate	Carl Roth GmbH, Germany
YNB, without amino acids and ammonium sulfate	BD Difco, MD USA

Reagents**Manufacturer**

<i>PageRuler</i> (unstained) SM0661	Fermentas
<i>PageRuler</i> (prestained) SM0671	Fermentas
NovagenYeastBuster™ Protein extraction reagent	Merck KGa, Darmstadt, Germany
Pierce BCA protein Assay kit	Thermo Fisher Scientific
AP conjugate substrate kit	Bio-rad, München, Germany
HBsAg ELISA kit	bioMérieux, France

Antibodies**Manufacturer**

Goat anti-mouse polyclonal	Acris antibodies GmbH, Germany
----------------------------	--------------------------------

FPLC resin**Manufacture**

Aerosil ® 380	Evonik Degussa GmbH, Rheinfelden, Germany
DEAE Sepharose FF	Amersham Pharmacia Biotech, Sweden
HiPrep 26/60 Sephacryl S-300 High Resolution	GE healthcare

Equipments**Manufacturer**

UV-vis Spectrophotometer	Uvikon, Kontron Instruments
--------------------------	-----------------------------

(OD600 measurement)	
Autoclave	Systec V-150, Systec GmbH Wettenberg
Incubator (Shaker)	Certomat ® BS-1, B.Braun Biotech International
Bioreactor	Biostat C, B.Braun Biotech International
Gas analyzer	Modular System, S710, SICK MAIHAK GmbH, Reute
Centrifuge	Centrifuge Stratos, Continuous flow rotors, Heraeus
Centrifuge	Megafuge, Heraeus Instruments
Cell lyser	Microfluidizer M110L, Microfluidics, Newton, MA
Light microscope	Axiopot, Carl Zeiss AG, Oberkochen
Gel electrophoresis system	Mini Protean Tetra Cell, Bio-rad, München
Spectrophotometer	Cary, Multiskan Spectrum, Thermo Labsystems
(Absorbance measurement)	
HPLC	Merch-Hitachi La Chrome, Darmstadt
FPLC	BioLogic Duo-Flow, Bio-Rad, München
Luminescence spectrometer	Hitachi
Luminescence spectrometer	PerkinElmer Ltd., United Kingdom
Virus counter	ViroCyt 2100, InDevR Inc. USA
Dynamic light scattering	DynaPro Titan, Wyatt Technology Corporation
Software	Manufacturer
<i>RISP software</i>	Institute of technical chemistry, University of
(Bioreactor on-line data collection)	Hannover
<i>BioLogic DuoFlowV.5</i>	Bio-Rad Laboratories, Inc.
(FPLC)	
<i>OriginPro 8</i>	OriginLab Corporation, MA
<i>ImageJ</i>	U.S. National Institutes of Health, Bethesda, MD
(TEM Image processing)	
<i>Graphic Analyzer</i>	Institute of Technical Chemistry, University of
(TEM Image processing)	Hannover
<i>CRISP ver. 2.1</i>	Calidris, Sollentuna, Sweden
(TEM Image processing)	

FL WinLab Software

PerkinElmer Ltd., United Kingdom

(Fluorescence analysis)

Dynamics Version 6.10

Wyatt Technology Corporation

(DLS measurements)

Nucleotide and amino acid sequence of the PCR amplified HBsAg gene

GAATTCAAGCTTGGATAAAAAGA ATG	GAG AAC ATC ACA TCA GGA TTC CTA GGA CCC CTG	51
	<i>Met Glu Asn Ile Thr Ser Gly Phe Leu Gly Pro Leu</i>	12
CTC GTG TTA CAG GCG GGG TTT TTC TTG TTG ACA AGA ATC CTC ACA ATA		99
<i>Leu Val Leu Gln Ala Gly Phe Phe Leu Leu Thr Arg Ile Leu Thr Ile</i>		28
CCG CAG AGT CTA GAC TCG TGG TGG GCT TCT CTC AAT TTT CTA GGG GGA		147
<i>Pro Gln Ser Leu Asp Ser Trp Trp Ala Ser Leu Asn Phe Leu Gly Gly</i>		44
TCA CCC GTG TGT CTT GGC CAA AAT TCG CAG TCC CCA ACC TCC AAT CAC		195
<i>Ser Pro Val Cys Leu Gly Gln Asn Ser Gln Ser Pro Thr Ser Asn His</i>		60
TCA CCA ACC TCC TGT CCT CCA ATT TGT CCT GGT TAT CGC TGG ATG TGT		243
<i>Ser Pro Thr Ser Cys Pro Pro Ile Cys Pro Gly Tyr Arg Trp Met Cys</i>		76
CTG CGG CGT TTT ATC ATA TTC CTC TTC ATC CTG CTG CTA TGC CTC ATC		291
<i>Leu Arg Arg Phe Ile Ile Phe Leu Phe Ile Leu Leu Leu Cys Leu Ile</i>		92
TTC TTA TTG GTT CTT CTG GAT TAT CAA GGT ATG TTG CCC GTT TGT TCT		339
<i>Phe Leu Leu Val Leu Leu Asp Tyr Gln Gly Met Leu Pro Val Cys Ser</i>		108
CTA ATT CCA GGA TCA ACA ACA ACC AGT ACG GGA CCA TGC AAA ACC TGC		387
<i>Leu Ile Pro Gly Ser Thr Thr Thr Ser Thr Gly Pro Cys Lys Thr Cys</i>		124
ACG ACT CCT GCT CAA GGC AAC TCT ATG TTT CCC TCA TGT TGC TGT ACA		435
<i>Thr Thr Pro Ala Gln Gly Asn Ser Met Phe Pro Ser Cys Cys Cys Thr</i>		140
AAA CCT ACG GAT GGA AAT TGC ACC TGT ATT CCC ATC CCA TCG TCC TGG		483
<i>Lys Pro Thr Asp Gly Asn Cys Thr Cys Ile Pro Ile Pro Ser Ser Trp</i>		156
GCT TTC GCA AAA TAC CTA TGG GAG TGG GCC TCA GTC CGT TTC TCT TGG		531
<i>Ala Phe Ala Lys Tyr Leu Trp Glu Trp Ala Ser Val Arg Phe Ser Trp</i>		172
CTC AGT TTA CTA GTG CCA TTT GTT CAG TGG TTC GTA GGG CTT TCC CCC		579
<i>Leu Ser Leu Leu Val Pro Phe Val Gln Trp Phe Val Gly Leu Ser Pro</i>		188
ACT GTT TGG CTT TCA GCT ATA TGG ATG ATG TGG TAT TGG GGG CCA AGT		627
<i>Thr Val Trp Leu Ser Ala Ile Trp Met Met Trp Tyr Trp Gly Pro Ser</i>		204
CTG TAC AGC ATC GTG AGT CCC TTT ATA CCG CTG TTA CCA ATT TTC TTT		675
<i>Leu Tyr Ser Ile Val Ser Pro Phe Ile Pro Leu Leu Pro Ile Phe Phe</i>		220
TGT CTC TGG GTA TAC ATT TAA TAGG TCGACAAGCTTGAATTC		724
<i>Cys Leu Trp Val Tyr Ile</i>		226

The HBsAg gene was PCR amplified from hepatitis B virus DNA (subtype *adw*) using primers containing Eco RI site to facilitate subsequent cloning of the gene into Pichia expression vectors. The start (in blue) and stop (in red) codons are italicized. The corresponding HBsAg amino acid sequence is shown in italic.

Media

Table 7.1. Recipe of media for shake flask cultivation

	Buffered minimal glycerol (BMG)	Buffered minimal methanol (BMM)	Buffered glycerol-complex medium (BMGY)	Buffered methanol-complex medium (BMMY)	Defined medium A (DM A)	Defined medium B (DM B)	Semi-defined medium A (SM A)	Semi-defined medium B (SM B)
Glycerol (g/l)	10		10		95.2	60	60	60
*Methanol (% volume per litre)		0.5		0.5	0.5	0.5	0.5	0.5
Potassium phosphate (g/L)	13.6	13.6	13.6	13.6	9.4	9.4	4.3	4.3
YNB (% w/v)	1.34	1.34	1.34	1.34				
Biotin (mg/L)	0.4	0.4	0.4	0.4	0.4	0.4	0.4	
Yeast extract (g/L)			10	10				
Peptone (g/L)			20	20				
**Histidine (g/L)	0.04	0.04	0.04	0.04	0.04	0.04	0.04	0.04
Casein hydrolysate (g/l)							10	10
(NH ₄) ₂ SO ₄ (g/L)					15.7	15.7	15.7	9
KH ₂ PO ₄ (g/L)					9.4	9.4	9.4	4.3

o-Phosphoric acid(85%) (mL/L)	for pH adjustment	for pH adjustment	for pH adjustment	for pH adjustment	for pH adjustment	for pH adjustment	for pH adjustment	for pH adjustment
KOH (g/L)					for pH adjustment	for pH adjustment	for pH adjustment	for pH adjustment
MgSO ₄ ·7H ₂ O (g/L)					1.83	1.83	4.6	3.2
CaCl ₂ ·2H ₂ O (g/L)					0.28	0.28	0.28	0.22
CaSO ₄ ·2H ₂ O (g/L)								
YTM soln (g/L)					1.14	1.14	4.56	
PTM 1 (mL/L)								5

* MeOH was used in after-induction phase.

** Histidine was added for the growth of *his4* strains only.

Recipe of Media for bioreactor cultivation

Component	Amount in 1L	Amount in 9L	Make the vol. up to	Sterilization
Glycerin [99.5%]	105.71 g	951.39 g	n.a.	Autoclave
KH ₂ PO ₄	10.28 g	92.52 g	771.30 g w/ H ₂ O (≈750 mL H ₂ O)	Autoclave
(NH ₄) ₂ SO ₄	17.14 g	154.26 g	771.30 g w/ H ₂ O (≈750 mL H ₂ O)	Autoclave
MgSO ₄ ·7H ₂ O	1.83 g	16.47 g	(≈150 mL H ₂ O)	Autoclave

CaCl ₂ ·2H ₂ O	0.309 g	2.78 g	771.30 g w/ H ₂ O (≈750 mL H ₂ O)	Autoclave
Biotin	0.45 mg	4.1 mg	20.55 g w/ H ₂ O	Filter sterilize
Anti-foam		100 g		Autoclave
NH ₃ -H ₂ O		512.30 g	n.a.	
MeOH			n.a.	Filter sterilize
YTM			n.a.	Filter sterilize

Yeast trace metal solution (YTM)

Component	For 1000 g	For 100 g
KI	207.50 mg	20.75 mg
MnSO ₄ ·H ₂ O	760.59 mg	76.059 mg
Na ₂ MoO ₄	483.9 mg	48.39 mg
H ₃ BO ₃	46.37 mg	4.637 mg
ZnSO ₄ ·7H ₂ O	5031.95 mg	503.195 mg
FeCl ₃ ·6H ₂ O	12.03 mg	1.203 mg
H ₂ SO ₄ [98 %]	9.20 mg	0.920 mg

Weigh and make up the volume accordingly with ddH₂O.

Buffers

Buffers for HBsAg downstream process

Step	Buffer	pH
lysis	25 mM PB, 8.0 + 5 mM EDTA + 0.6% Tween 20	8.0
PEGylation / PEG precipitation (O/N)	lysis buffer + 500 mM NaCl + 5% PEG 6000	8.0
Aerosil binding	25 mM PB + 500 mM NaCl	7.2
Aerosil washing	25 mM PB	7.2
Aerosil elution	50 mM CBB + 1.2 M Urea	10.8
Aging	50 mM CBB	10.8
IEX binding	50 mM CBB	8.0
IEX washing	50 mM Tris-HCl	8.0
IEX elution	Tris-HCl + 500 mM NaCl	8.0
Concentration via vivaspin column	50 mM Tris-HCl + 500 mM NaCl	8.0
SEC	PBS, 7.2	7.2
KSCN	PBS, 7.2 + 1.2 M KSCN	7.2
Dialysis	PBS, 7.2	7.2

PB: (Sodium) phosphate buffer
CCB: Sodium carbonate-bicarbonate buffer
PBS: Phosphate buffered saline

Phosphate buffered saline, pH 7.2

Compoundt	Concentration [M]	Concentration [g/L] 1X	Concentration [g/L]10X
NaCl	137	8.00	80.0
KCl	2.7	0.20	2.0
Na ₂ HPO ₄	10.0	1.44	14.4
KH ₂ PO ₄	1.76	0.24	2.4
pH	7.2	7.2	7.2

Dissolve all the salts in ddH₂O and mix together. Adjust the pH with conc.HCL or NaOH, if required.

Glycerol stock Glycerol stock was used as pre Pre-culture for shake flask and bioreactor cultivations of HBsAg producing and non-producing clones. In order to prepare glycerol stock, pick an isolated single colony of HBsAg producing *Pichia pastoris* GS115 cells and grow in YPD till OD₆₀₀=12-14. Resuspend in YPD containing 15% glycerol to obtain a final OD₆₀₀=50-52 ($\approx 2.6 \times 10^9$ cells/mL). Aliquot and shock freeze in liquid N₂. Store at -80°C .

OD_{600nm} Measurement Throughout the cultivations (in shake flasks as well as bioreactor), cell optical density (OD) was measured via spectrophotometer. At different stages during cultivation, time point samples were collected and OD was measured at 600nm. The instrument was calibrated for zero-adjustment with 0.9% (w/v) saline solution before all the measurements. Wherever necessary, dilutions were made with calibration solution. The dilutions were made, in a proportion of 1:5, 1:10, 1:20, 1:50 etc, in order to obtain the observed absorbance value in a range of 0.1 – 0.8.

Cell lysis

Cell Lysis using glass beads Wash cell pellet with 25 mM PB, pH 8.0 and resuspend in lysis buffer. Add glass beads [0.45 mm; Sigma G-8772] of roughly equal weight to cell pellet. Vortex for 40 sec at maximum speed and keep at ice for next 40 sec. Repeat the cycle of vortexing and chilling 8-10 times. Centrifuge for 10 min at 13,000 rpm ($17,000 \times g$). Collect the supernatant and store at -20°C . (-80°C for longer term)

Cell lysis via Microfluidizer Resuspend the cell pellet in lysis buffer and pass through the Microfluidizer. During this process, the cells are pushed through the interaction chamber at high pressure, and passed through a cooling coil. Tighten the screws on the pressure compartment of machine. Fill the tray with ice-water slush for cooling. Turn on

the air supply, open valve to create pressure (5-8 bar). Add 100 mL water; slowly turn on the red handle counter clock wise. Let it run for some passages to get isopropanol out. Repeat the water wash. Wash once with 20 mL lysis buffer. Pass cells at 12,000 psi (38 psi at inlet) through Microfluidizer for 12-14 times. Confirm the complete lysis by viewing the sample under microscope.

After lysis, wash out with buffer until it runs clear. Wash with 100 mL 1 M NaOH and then with 500 mL water. Wash and fill with 70 % isopropanol for storage.

SDS-PAGE recipe

Following solutions are required for casting the gel,

- i. Acrylamid-bisacrylamid mixture, 37.5:1
- ii. 1.5 M Tris (pH 8.8)
- iii. 1.5 M Tris (pH 6.8)
- iv. 1% SDS solution
- v. Temed (N,N,N',N''Tetramethylethylenediamine)
- vi. 25 % APS (ammonium persulphate)

For 2 gels,

Sr. nr.	Separating gel (6 %)	Volume	Collecting gel (12 %)	Volume
1	Acryl-Bisacryl mixture	3.0 mL	Acryl-Bisacryl mixture	0.75 mL
2	Tris (pH 8.8)	2.5 mL	Tris (pH 6.8)	1.25 mL
3	SDS (1%)	1.0 mL	SDS (1%)	0.52 mL
4	dd H ₂ O	1.76 mL	dd H ₂ O	2.46 mL
5	Temed	20 µL	Temed	10 µL
6	APS	20 µL	APS	10 µL

SDS sample buffer	20 mM Tris-HCl
	2 mM EDTA
	5 % SDS (w/v)
	0.02 % Bromophenol blue

Modified Laemmli	50 % SDS sample buffer
Sample buffer	45 % β -ME
	5 % Glycerol

Mix equal volume of Laemmli buffer and sample, boil at 95°C for 10 min and spin for 1min to get all the contents down.

Running buffer	25 mM Tris-Base
	192 mM Glycin
	0.1 % SDS (w/v)
	pH 8.3

Load the gel and run at 60 V for 15 min and at 120 V for 60 min (or until the end).

Afterwards, stain the gel with colloidal coomassie or silver staining.

Colloidal coomassie staining

Reagents	a- For fixing solution EtOH, 50%; O-H ₃ PO ₄ , 20% and ddH ₂ O 30%
	b- For staining solution ddH ₂ O, 270 mL; 85% O-H ₃ PO ₄ , 35.3 mL; (NH ₄) ₂ SO ₄ , 30g; Coomassie G-250, 0.36g; MeOH, 60 mL. Take 30 mL of ddH ₂ O in a flask and add 30 mL H ₃ PO ₄ . Also add (NH ₄) ₂ SO ₄ and Coomassie G-250. Shake and add the remaining 240 mL ddH ₂ O. Lastly add MeOH slowly and dissolve using magnetic stirrer.
Fixing	After finishing the electrophoresis, rinse the gel briefly with ddH ₂ O. To fix the gel, rinse it in the fixing solution for 2 times, 20 min each.
Staining	Put the gel along with staining solution on the shaker and stain overnight.
Destaining	Rinse the gel with ddH ₂ O until the background is clear and bands are visible.

Storage This coomassie staining solution is reusable for nearly 6 months. Keep in amber bottle at 4°C.

Silver staining

Reagents Fixing solution: 5 parts ddH₂O, 5 parts EtOH and 1 part AcOH (eg., 400 mL H₂O + 400 mL EtOH + 80 mL AcOH)
Farmer reducer: 0.1 g Potassium hexacyanoferrate (II) and 0.1g Sodium thiosulphate in 100 mL ddH₂O
0.1% AgNO₃ solution: 1 small pinch in 100 mL ddH₂O
2.5 % Na₂CO₃ solution: 50 g Na₂CO₃ (dehydrated) in 1000 mL ddH₂O
Formaldehyde: 300-500 µL per 100 mL Na₂CO₃

Fixing and reduction Incubate the gel for 20 min in destaining/fixing solution. Wash quickly twice with ddH₂O. Incubate in Farmer reducer solution for 2.5 min. Wash with ddH₂O for 5 min. (wash till the yellow color is gone and the gel is again transparent)

Staining Incubate in AgNO₃ solution for 30 min. Wash for 30 sec with ddH₂O twice. Wash swiftly with Na₂CO₃ solution. Add 400 µl formaldehyde in 100 mL Na₂CO₃ solution and incubate the gel in this solution until the bands are nicely visible. Stop the band development by adding the gel in 5% AcOH solution for 10 min. Keep the gel in ddH₂O.

Western Blot

Reagents Transfer Buffer: 25 mM Tris, 192 mM Glycin, 10% Ethanol, pH 8.3

1. TBS: 25 mM Tris, 150 mM NaCl, pH 7.5
2. TBS-T: 25 mM Tris, 150 mM NaCl, 0.5% Tween 20, pH 7.5
3. BSA-TBS (Blocking buffer): 25 mM Tris, 150 mM NaCl, 0.5% Tween 20, 2% BSA, pH 7.5
4. AP-Buffer: 100 mM Tris-HCl, 100 mM NaCl, 5 mM MgCl₂·7H₂O, pH 9.5
5. 1° Ab Solution
6. TMB substrate

SDS-PAGE	Run an SDS-PAGE using previously described conditions and at end, wash the gel with ddH ₂ O.
Preparation of membrane	Cut the PVDF membrane of apt size and soak in MeOH/EtOH for a minute or two and then immerse in ddH ₂ O. Equilibrate the fibre pad, blotting paper, membrane and gel in transfer buffer for 15 min. Make the setup in the sequence such that it follows to make a sandwich as → fibre pad – blotting paper – gel – PVDF membrane – filter paper – fibre pad. Make sure to evacuate all trapped air bubbles underneath the gel with a roller. Place the sandwich fittingly onto cassette and close the clamp. Insert the cassette into blotter tank with red side facing red electrode. Fill up the blotter tank with transfer buffer till level n also put a magnetic stirrer and ice block. Put this tank in a tub filled with ice and onto a magnetic plate.
Electro-transfer	Put on lid, plug in the cables and start electro-blotting at a constant voltage for 30 min. At the end of the run, rinse the membrane with ddH ₂ O for 5 min. Cross-check the gel for proper electrophoretic transfer (electroelution).
Immunodetection	Wash the membrane in ddH ₂ O for 5 min. Wash the membrane in BSA-TBS (blocking buffer) for 1 h. Incubate the membrane with 1° Ab solution for 1 h. Incubate the membrane with BSA-TBS (3 X 5 min). Incubate the membrane with 2° Ab for 1hr. Wash 3 times with TBST (3 X 5min). Wash 2 times with TBS (2 X 1 min). Develop the signal by introducing membrane to the substrate solution. Stop the developing by adding ddH ₂ O.

Protein estimation

BCA Protein Assay

For protein estimation via BCA assay, BSA is used as a standard protein. The concentration of stock solution is 2 mg/mL. Prepare a series of standard from stock solution; 2000, 1500, 1000, 750, 500, 250, 125, 75, 25 and 0 µg/mL.

Working Reagent	[WR]: Reagent A	+	Reagent B [50:1]
	3 mL	+	60 µL
Sample + WR	[1:8 ratio]: 25 µL	+	200 µL
	(Microplate Procedure)		

Mix well and incubate for 30 min at 37°C. Read the plate at 562 nm.

Absorption method Measure absorbance of the protein solution at 280 nm. Calculate the concentration by using the formula,

$$\text{Concentration} = \frac{\text{Absorbance at 280 nm}}{\text{absorbance coefficient} \times \text{cell path length}}$$

In all assays, the samples were diluted to appropriate concentrations to get results in the middle of assay range.

HPLC protocol

Column:	Supercosil LC-18 5 cm x 4.6 mm, 5 µm
Detection:	UV 280 nm
Solvent system:	A: 0.15% TFA in ddH ₂ O; B: 2-propanol:ACN in 80:20 ratio
Flow rate:	1 mL/min

Time (min)	A (%)	B (%)	C (%)
0	55.0	45.0	0
4	55.0	45.0	0
10	5.0	95.0	0
13	5.0	95.0	0
14	55.0	45.0	0
18	55.0	45.0	0

TFA: Trifluoroacetic acid (Sigma-Aldrich Chemie GmbH, Germany)

ACN: Acetonitrile (Sigma-Aldrich Chemie GmbH, Germany)

FPLC protocol for Ion exchange chromatography*

	Volume	Description	Parameters		
1	0.00	Collection Fractions within 2 time window(s) ending at 400.00 mL			
2	0.00	Lamp (UV Detector)	Turn ON		
3	0.00	Zero Baseline	UV Detector		
4	0.00	Isocratic Flow	A: A-Buffer 1	100%	Volume: 100.00 mL
			B: Buffer B	0%	Flow: 1.00 mL/min
5	100.00	Isocratic Flow	A: A-Buffer 2	100%	Volume: 200.00 mL
			B: Buffer B	0%	Flow: 1.00 mL/min
6	300.00	Isocratic Flow	A: A-Buffer 3	100%	Volume: 100.00 mL
			B: Buffer B	0%	Flow: 0.50 mL/min
7	400.00	Lamp (UV Detector)	Turn OFF		
	400.00	End of Protocol			

* The FPLC system (connected with column) was calibrated with first buffer system with at least 2 column volume (CV) before starting the run. All the buffers were filtered and degassed before use.

Buffer 1: 50 mM Na-Carb-bicarb buffer

Buffer 2: 50 mM Tris-HCl

Buffer 3: Tris-HCl + 500 mM NaCl

FPLC protocol for size exclusion chromatography*

	Volume	Description	Parameters		
1	0.00	Collection Fractions of size 5.0 mL within 1 time window(s) ending at 450.00 mL			
2	0.00	Lamp (UV Detector)	Turn ON		
3	0.00	Zero Baseline	UV Detector		
4	0.00	Isocratic Flow	A: A-Buffer 1	100%	Volume: 50.00 mL
			B: Buffer B	0%	Flow: 1.00 mL/min
5	50.00	Isocratic Flow	A: A-Buffer 2	100%	Volume: 10.00 mL
			B: Buffer B	0%	Flow: 1.00 mL/min
6	60.00	Isocratic Flow	A: A-Buffer 1	100%	Volume: 360.00 mL
			B: Buffer B	0%	Flow: 0.50 mL/min
7	420.00	Lamp (UV Detector)	Turn OFF		
	420.00	End of Protocol			

* The FPLC system (connected with column) was calibrated with first buffer system with at least 2 column volume (CV) before starting the run. All the buffers were filtered and degassed before use.

Buffer 1: Ion exchange eluate

Buffer 2: PBS, pH 7.2

Estimation of protein contents using ImageJ

For SDS-PAGE densitometry

- 1- Open ImageJ; drag and drop the image of gel.
- 2- → Analyze → Gels → Select first lane [strg+1]. For next lane, use [strg+2] n keep selecting until last desired lane.
- 3- Once finished with selection, → Plot lane [strg+3].
- 4- Plot of image will pop up. Select the base line manually by drawing a horizontal line using 'straight line' selection tool. Draw vertical lines to define the peak/s.
- 5- Before separating the peaks vertically, calculate the peak area by clicking inside using wand tool.
- 6- Save the results separately for each lane; Results → File → Save as.
- 7- Alternatively, label the peaks Analyze → Gels → label peaks. It gives peak area in percentage.

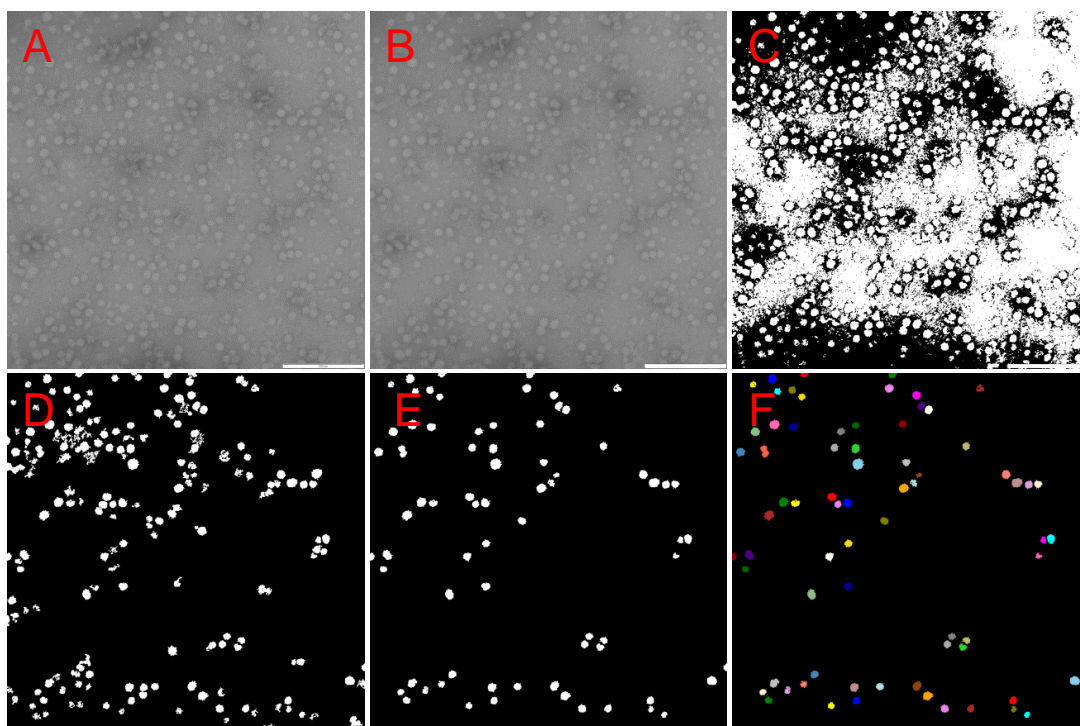
For VLP count

- 1- Open ImageJ; drag and drop the TEM image.
- 2- Calibrate the pixels in terms of size by using the scale bar in the image (Analyze → set scale).
- 3- Select the circle option in the shape tool.
- 4- Select all the VLPs as ROI (Analyze → tool → ROI manager).
- 5- Measure the selected data and export as CSV format.

Step by step method of using Graphic Analyzer

- 1- Open the image in Graphic Analyzer (A).
- 2- Adjust Median Functions → Grey filters → Median[7-9] (B)
- 3- Adjust threshold from grey filters [≈80-160] (C).
- 4- Functions → Morphology → eliminate by size [≈600-3500] (D).
- 5- Functions → Morphology → eliminate by compactness [1-2] (E)
- 6- Get 8-connected objects (F) and save as CSV data.
- 7- Get average of the diameter and convert into nm.

E.g. if the scale bar ranges from 1582 to 2037 pixels, the difference 455 pixel equals 200 nm, and 1 pixel is roughly equal to 0.44 nm.



Acknowledgements

I would like to extend my gratitude to,

- **Prof. Dr. Thomas Scheper** and **Prof. Dr. Ursula Rinas**; much appreciation is expressed to both supervisors for their insight, for providing infinite amount of guidance and help. Being Doktormutter and Doktorvater (as they say in German), they always supported me to pursue my research work in all possible ways. Danke Uschi und Thomas!

- **HEC** (Higher education commission, Pakistan) and **DAAD** (German academic exchange service) for providing continuous support, monetary and otherwise.

- **Dr. Heinrich Lünsdorf** (HZI, Braunschweig) for an enormous assistance in TEM studies of VLPs and for his intellectual guidance!

- **Dr. Thorsten Lührs** (HZI, Braunschweig); I owe a huge thanks to him for providing DLS facilities in his lab and also for the useful suggestions.

- **Dr. Patrick Lindner** for helping in the image processing and for programming the Graphic Analyzer.

- **Dr. Öznur Kökpınar** and **Dr. Johanna G. Walter**; a heartfelt thanks to both ladies for meticulously proof reading this thesis and for their fair criticism.

- **Dr. Chandrasekhar Gurramkonda** (ICGEB, India) for his thorough help in optimization of the downstream processing.

- **Dr. Ivo Havlik** and **Dr. Michael Dors** for all the IT-support.

- **Martina Weiss** and **Martin Pähler** for their valuable technical assistance. Things could have been quite baffling without their management in the labs.

- **Electrical** and **Mechanical workshop** for helping out with the instruments when they refused to run any further.

- Colleagues from **TCI**; a great deal of thanks goes to all the TCIIer colleagues for providing such a nice, cozy and friendly atmosphere. It's been a real pleasure working with you guys!

- above all, my **Family** for the colossal backup and having trust in me all the way, specially my **Amma**. I'm what I'm because of you!

Curriculum Vitae

Name Maria Zahid
Date of birth 04.01.1984 (Lahore, Pakistan)

Professional activities

Apr 2009 – Oct 2012 Ph.D. candidate at Institute of Technical Chemistry,
Leibniz University of Hannover

Oct 2008 – Mar 2009 Equivalence exams for M. Sc. (Hannover)

Jun 2008 – Sep 2008 German language course, A2 (Lahore), B2 (Frankfurt)

Jan 2008 – May 2008 Scientific officer at Applied Chemistry Research Centre,
PCSIR Laboratories Complex, Lahore

May 2007 – Dec 2007 Internship at Pathology Department, Allama Iqbal
Medical College, Lahore

Educational career

2004 – 2006 M. Sc. (Organic Chemistry) at Department of Chemistry,
Government College University, Lahore
Title of thesis: Isolation and characterization of
biologically active flavonoids from *Grewia asiatica*

2002 – 2004 B. Sc. (with Chemistry, Zoology and Botany as major
subjects), Government College University, Lahore

1999 – 2002 Intermediate (Pre-medical group), Queen Mary College,
Lahore

1989 – 1999 High School (Science group), F.G. Model High School,
Lahore Cantt, Lahore

Posters and presentations

Maria Zahid, Chandrasekhar Gurramkonda, Heinrich Lünsdorf, Satish Kumar, Sathyamangalam Swaminathan, Navin Khanna, Ursula Rinas: Production and characterisation of recombinant hepatitis B surface antigen VLPs derived from recombinant methylotrophic yeast, *Pichia pastoris*, Recombinant protein production 6 (RPP 6) 2011, Vienna, Austria

Maria Zahid, Chandrasekhar Gurramkonda, Heinrich Lünsdorf, Satish Kumar, Sathyamangalam Swaminathan, Navin Khanna, Ursula Rinas: Production and characterisation of recombinant hepatitis B surface antigen VLPs derived from recombinant methylotrophic yeast, *Pichia pastoris*, 1st European Congress of Applied Biotechnology 2011, Berlin, Germany